CATHETER LOCALIZATION UTILIZNG A SENSOR-ENABLED GUIDEWIRE

DESIGN OF A PROOF-OF-CONCEPT SYSTEM

A Thesis

presented to

the Faculty of California Polytechnic State University,

San Luis Obispo

In Partial Fulfillment

of the Requirements for the Degree

Master of Science in Biomedical Engineering

by

Adam Edward Evard

June 2018

COMMITTEE MEMBERSHIP

TITLE:	Catheter Localization Utilizing a Sensor-Enabled Guidewire: Design of a Proof-of-Concept System
AUTHOR:	Adam Edward Evard
DATE SUBMITTED:	June 14, 2018
COMMITTEE CHAIR:	Kristen O'Halloran Cardinal, Ph.D. Professor of Biomedical Engineering
COMMITTEE MEMBER:	Lily Laiho, Ph.D. Professor of Biomedical Engineering
COMMITTEE MEMBER:	Louis-Philippe Richer, Ph.D. Staff Scientist, Applied Research Abbott
COMMITTEE MEMBER	Stuart P. Rosenberg, M.S. Senior Manager, Applied Research Abbott

ABSTRACT

Catheter Localization Utilizing a Sensor-Enabled Guidewire:

Design of a Proof-of-Concept System

Adam Edward Evard

The purpose of this thesis project was to develop a proof-of-concept system for tracking the tip of a catheter without an embedded electromagnetic sensor by utilizing a sensor enabled guidewire. The motivation for the project was a reduction fluoroscopy radiation dose for clinicians in the interventional cardiology lab and the extension of navigation technology to be used with a wider variety of interventional devices through the implementation of expanded capabilities of the Abbott MediGuide system. The focus of the project was on the development of a proof-of-concept system capable of using an external device to track relative guidewire and catheter motion and apply that to a calculated position in the vasculature.

The research conducted covered multiple disciplines from mechanical design to software algorithms. A prototype system was developed that functions alongside the MediGuide system to provide a three dimensional depiction of catheter location and a measurement of the relative linear displacement separating the distal tip of the guidewire and the distal tip of the catheter. The system consists of an electromechanical device to measure relative motion and software to communicate with the device, interpret recorded guidewire position data into a representative trajectory, and display the results to the user.

The hardware and software components of the project were evaluated to determine accuracy and precision. The prototype device was determined to be accurate to 0.7±0.03% of total displacement. In a simulated use procedure the device was determined to be accurate to 1.4±0.53mm. The software algorithms to generate a simulated guidewire path were evaluated and tuned to generate the best response to the data sets available.

In summary, the work performed here shows the possibility of implementing a device and software system that can provide localization information to the operator about the catheters used in an interventional procedure without the need for a sensor in the catheter.

Keywords: Abbott, catheter, guidewire, localization, MediGuide

ACKNOWLEDGMENTS

Dr. Kristen Cardinal, thank you for your advice, guidance and support over the past three years of my college experience since I met you. Giving me the opportunity to join a project working in your lab at the start of my junior year set me on the path towards pursuing engineering in the medical device field. Your assistance with navigating the challenges of this thesis and the graduate program as a whole has been invaluable.

Louis-Philippe Richer, Stuart Rosenberg, and Abbott Inc., thank you for giving me the opportunity to work in collaboration with you on this project. Through the development of this thesis I have learned an incredible amount about the current state of interventional imaging, navigation, and device localization and have gotten a glimpse of the future. You have been vital in supporting my inquires for technical information and answering all the questions I could come up with.

To my friends and roommates who have supported me throughout this process, thank you. Throughout the completion of this thesis you supported me through tolerance of my frustrations, providing distractions to stress through bicycle rides, events, conversations, beers, and all around good times. To my roommates over the last year and a half specifically: Anthony Fryer, Brent Taylor, Ethan Fedor, Liam McDonnell; living in a house with like-minded people to convince me to get outside on a bike and pedal and forget about anything except the present moment was central to my success. BKE4Life. Thank you.

I am thankful for my family and their incredible support of my five years of education here in San Luis Obispo. To my parents, you have been supportive and encouraging of everything I have achieved. I would not be on the path I am now without your support of my studies and connections that got me a foot in the door in industry. To Aunt Trudy and Uncle Jim, your support of my education through undergrad was invaluable and made extending my graduation to get the Master’s degree all the more possible. Thank you.

TABLE OF CONTENTS

LIST OF TABLES

Table Page

LIST OF FIGURES

Chapter 1: Introduction

1.1 Overview

The purpose of this thesis project was to develop a proof-of-concept system for tracking the tip of a catheter without an electromagnetic sensor with the use of a sensor enabled guidewire. The motivation for the project is a reduction fluoroscopy radiation dose for clinicians in the interventional cardiology lab with the implementation of expanded capabilities of the Abbott MediGuide system. The MediGuide system uses sensor enabled guidewires and catheters to overlay the live position of the tool on pre-recorded fluoroscopy video “cine loops”. However, this system is only applicable to interventional tools that are compatible with the MediGuide system, containing an embedded electromagnetic sensor. [1] This limits the versatility of the system by restricting the library of possible tools that can be tracked. This could possibly prevent clinicians from utilizing their preferred tools. To address the challenge, the goal of this project was to develop technology that can, with the use of a sensor-enabled guidewire, acquire the necessary information to display real-time position information of a catheter tip, to the operator, as if it contained a sensor. The project covered multiple design challenge dimensions to develop the hardware, electrical, and software components to produce the proof-of-concept system.

This chapter will cover the problem in more detail, give background on electromagnetic localization of interventional tools, and then introduce the proposed solution. The thesis will then continue through an analysis of the current state of technologies related to the problem. These include current patents and hardware available for determining the relative motion between catheters and guidewires. Additionally the technologies that have been developed to simulate guidewire paths contained within the vasculature are evaluated. These technologies are categorized into image-based systems and sensor-based systems. Prior to the initiation of this project as a thesis project, work was completed during the 2015 – 2016 academic year by the Cal Poly Society of Women Engineers Team Tech to develop an early proof-of-concept prototype.

The work of this team is briefly covered in Chapter 3. In Chapter 4 the design of the prototype hardware is covered from the initial concepts to the final prototype iteration. Chapter 5 covers the electrical and sensor system and how those components interface with the software aspects of the project. A significant aspect of the project was the processing of data acquired from the guidewire to develop a simulation of the guidewire path in the vasculature. Chapter 6 covers the algorithm developed to handle this project component. Chapter 7 covers the use of all of these components in an integrated system to provide a proof-of-concept demonstration of the technology application. Chapter 8 summarizes the evaluation of the prototype system components for accuracy, precision, and feasibility of the system. The thesis concludes with a discussion of the results and consideration of future work directions the project could take in Chapter 9.

1.2 Clinical Problem

Traditional interventional cardiology procedures consist of a physician utilizing fluoroscopy to visualize the target vasculature, evaluate tool location, and assess the disease location and severity. The physician will gain access to the body through a minimally invasive access to the vasculature through the groin or arm. They will then use various guidewires, catheters, and other tools to access and treat the disease. Typically they first advance a guidewire near the target location in the vasculature and then use that guidewire as a rail to guide a catheter to the target location. Once in position, the catheter can be used to treat the disease.

Procedures conducted in electrophysiology and catheter laboratories utilize ionizing radiation to image patient anatomy and visualize the positions and orientations of tools inside the body. The patient is placed on an adjustable operating table and the imaging technology is attached to a rotatable “c-arm”. The imaging utilizes an x-ray emitter and receiver that can digitally record an image of the patient's anatomy and display it to operators in the room on a monitor. A typical catheterization laboratory set up is shown in Figure 1. The radiation dosage received from the imaging system presents a health risk to both patients and the staff in the operating room. Guidelines and recommendations for operating procedures are put into place to minimize this risk and achieve as low as reasonably achievable (ALARA) radiation dosage. [2]

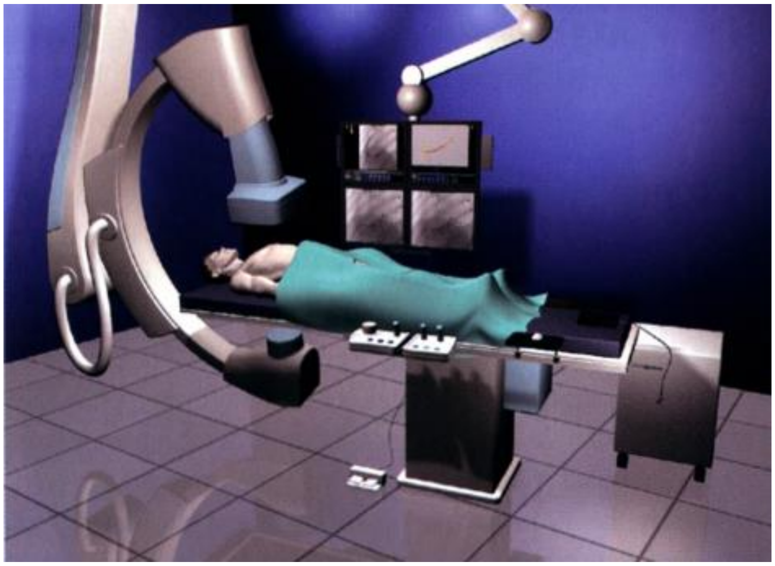

Figure 1. A typical cardiac catheterization laboratory setup.
[1]

The use of fluoroscopy and the resulting radiation exposure and use of toxic contrast medium [3] has become a concern in the medical community. Figure 2 shows the images typical from a fluoroscopy procedure and the effect on the image of contrast injection into the vasculature. As a result of the risks, other imaging and tool tracking technologies have been developed to reduce the fluoroscopy time and improve the visualization and tool tracking capabilities to assist physicians.

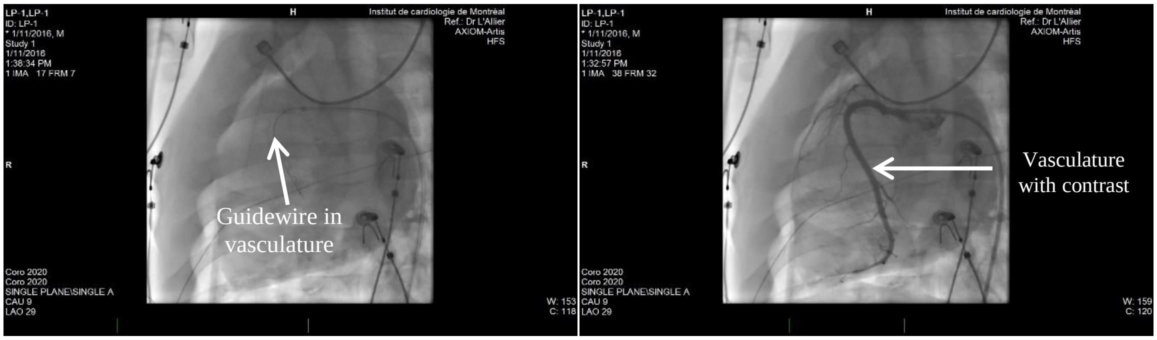

Figure 2. Fluoroscopy view of the catheterization of the right coronary artery. On the left is the image without a contrast injection, guidewire shown by the arrow. On the right the vasculature, shown by the arrow is visible when radiopaque contrast is delivered through the catheter. [4]

There are a large variety of catheter shapes and functions made by numerous manufacturers. Additionally, there are multiple tool tracking and navigation systems on the market that utilize different technologies. These technologies are not necessarily compatible between manufacturers. It may be that only tools made by a specific vendor can be used with that vendor's navigation system. The restrictions imposed by the limited combinations of navigation systems and compatible tools results in limited versatility and general utility of the systems. Another aspect worth considering is the additional costs associated with the development and construction of catheters and tools with an embedded sensor that will only be compatible with a single navigation system. These factors drive the development of this project to allow design a proof-of-concept system to track a catheter tip without an embedded sensor with the use of a sensor enabled guidewire that can be tracked in a navigation system.

1.3 Electromagnetic Tracking Systems

The Abbott MediGuide technology allows for the navigation of devices using pre-recorded or live x-ray fluoroscopic images. The system allows for the reduction in radiation dose to meet the principle of As Low As Reasonably Achievable (ALARA) and provides additional information and capabilities for the physician. The system facilitates the completion of cardiac resynchronization therapies and electrophysiology procedures by combining fluoroscopic imaging with real-time catheter tracking [5]. When used for implanting the leads in cardiac resynchronization therapy the MediGuide system has been shown to reduce radiation exposure by 82% and procedure time by 20 minutes. [6] A transmitter generating a dynamic electric field is used with miniature coil sensors embedded in the intracardiac tools that are tracked in the field by evaluating the voltage generated in the sensor. [7] A patient reference sensor (PRS) placed on the chest of the patient allows the system to track the spatial relationship of the imaging system and the patient. The tracking system is combined with conventional fluoroscopy imaging to project real-time position of tool position onto pre-acquired 2D cine loops. The system can compensate for respiration, cardiac motion, patient and table movement, and C-Arm angulation. [8]. An example of the image output and overlay of catheter position is shown in Figure 3.

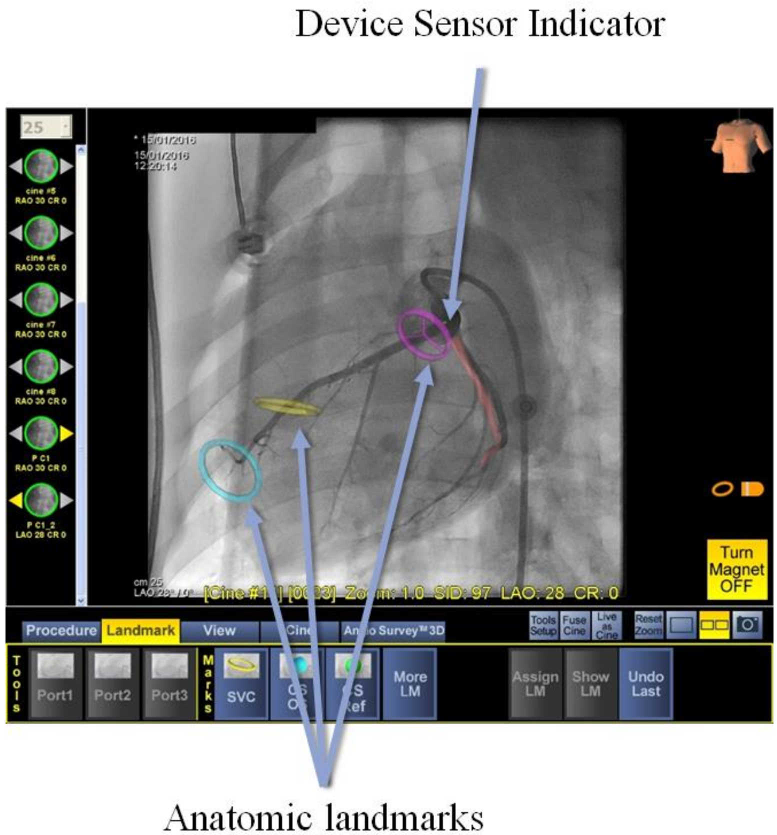

Figure 3. MediGuide system output example. The catheter tip is represented as the green dot overlaid onto the fluoroscopy image. The colored rings represent the "Landmark" locations that have been marked in the system.

Evaluation of the Medtronic StealthStation electromagnetic tracking system in a simulated left subclavian artery cannulation has shown positive results [9]. The study showed a reduction in fluoroscopy time for all experience groups. Total procedure time and contact with vessel walls was not significantly different between the methods. The system was able to track the guidewire with a sub-millimeter precision with a mean error of 0.56 millimeters. StealthStation provides a method of tracking interventional tools that is similar to MediGuide. Overall the study shows that electromagnetic navigation is a viable option to reduce fluoroscopy time for operators and patients.

Schwein et al studied the use of robotic catheter manipulation using the Aurora system and a 9F Magellan robotic catheter modified with sensors for the study. Six operators, two experts and four novices with the system, navigated the catheter to cannulate two targets in an aortic aneurysm phantom. The procedure was conducted with traditional fluoroscopy, fluoroscopy with real time catheter position, a 3D rendering technique (anteroposterier view) of the phantom showing catheter position and orientation, and a second 3D rendering technique (anteroposterier view and lateral view). The results of the study indicate that the use of EM tracking results in reduced fluoroscopy time and cannulation time along with improved motion consistency metrics of the catheter. [10] The literature demonstrates measureable benefits in radiation dose reduction through the use of electromagnetic imaging. The MediGuide system, with the proposed device in this thesis, allows for the display of information similar to the tracking of a sensor enabled device, without the need for a sensor in the device.

1.4 Guidewire Path Construction

There are multiple mathematical and image processing techniques that can be used to reconstruct a guidewire path and utilize that information for device tracking. Information about the 3D position and shape of a guidewire can help to address the issues of foreshortening and information loss with the single plane views of tradition x-ray fluoroscopy used in procedures.

Methods to determine guidewire position fall into the broad categories of either image-based tracking or sensor-based tracking systems. These systems attempt to determine the location of a guidewire or interventional tool through various sensors and algorithms. Chapter 2 covers the technologies and methods more thoroughly. The overall goal of the systems are either to provide a simulation of guidewire motion in order to train physicians in virtual reality environment or to generate additional information about the location of the guidewire and display that to the physician conducting a procedure.

1.5 Problem and Proposed Solution

The current function of the MediGuide system is dependent on the sensors embedded in the interventional tools in order to determine their spatial localization. The goal of this project was to evaluate the feasibility of a method to track catheter position by utilizing the information acquired from a sensor enabled guidewire and another device. The intended device would be small and simple enough to be able to integrate smoothly into the standard workflow of a physician. In order for the device to be clinically relevant it was necessary to work within the constraints outlined in Table 1. For the purpose of this project it was expected that the software prototype would provide a display of the information without the need to integrate into the commercial system software.

Table 1. Specifications for the prototype system

Spec No.	Specification	Description	Target	Tolerance
1	Resolution	Output resolution of the device	± 0.5 mm	Max
2	Precision	Consistent reliability of the device data output must be better than this value	± 0.5 mm	Max
3	Output Speed	The device must output live data within this range of frequencies	30 – 60 Hz	Nominal
4	Ease of use	The device must minimally interfere with the current procedure used for cardiac intervention. Specified as additional procedure time	< 5 min	Max
5	Cost	Typical budget for a Cal Poly/SJM MediTech Project	$5000	Max
6	Safety	No injury or damage to equipment, physicians, or patients.	Pass	Pass/Fail

Beyond the proof-of-concept prototype a finished product would need to adhere to additional requirements. Additional considerations for a finished product include reusability, sterility, size, electrical constraints, handling, and user experience. These additional requirements are outlined in Table 2.

Table 2. Additional specifications for a finished product concept.

Spec No.	Specification	Description	Target
1	Reusable	Is the device a single use product or can it be used multiple times?	Yes
2	Sterility	How is the device sterilized and can it be cleaned and sterilized for repeat usage.	Repeatable sterilization
3	Size	The shape and form of the device.	Ergonomic. As small as possible without limiting function.
4	Electrical Constraints	How the device would be powered if needed.	Low voltage from MediGuide plug
5	Handling	How does the use of the device affect the pushabiltiy, torqueability, and feel of the catheters and guidewires?	Minimal effect on handling
6	User Experience	How does the device limit or restrict the ability of the clinician to interact and treat the disease as they would normally.	Minimal change in experience from traditional procedure

1.6 Introduction Summary

The intended outcome of this project was to develop and evaluate the feasibility of extending the capability of the MediGuide system. Introduction of technology that provides relative location information to the clinicians of the placement of catheter and guidewire locations could be a valuable addition to the function of the system. Additionally it was desirable that the expansion of the system capabilities be applicable to a multitude of catheter and guidewire devices from multiple manufacturers. The scope of the project implementation required that there would be no modification of the devices it will be used with. The tasks necessary to evaluate the feasibility of such a technology were multidisciplinary consisting of mechanical device design, electrical signal transduction to measure a relative displacement, software to analyze transduced signals, the use of recorded position data to determine guidewire trajectory and placement, and the implementation of a graphical user interface to assist the clinicians in understanding the data. The completion of a prototype then necessitated evaluation of the device capabilities for which a series of tests were conducted. This thesis presents the culmination of work on all aspects of the project.

Chapter 2: Review of Current State of Technology

This chapter covers the current state of technologies related to the goal of catheter localization and is divided into two sections. The first section, “2.1 Devices”, covers the hardware and existing patents and technologies for locating an interventional device. The second section, “2.2 Guidewire and Catheter Tracking and Localization Technology”, covers the work that has been done to evaluate guidewire position in the body and develop methods to track and locate guidewires in patients and within simulated environments.

2.1 Devices

2.1.1 Existing Patents

The development of devices to provide more extensive information about the relative position of a catheter and a guidewire is an ongoing area of innovation. To evaluate the current state of development, patents on relevant and related areas were researched.

In patent application US20030187369, Optical Pullback Sensor for Measuring Linear Displacement of A Catheter or Other Elongate Member, priority date March 28, 2002, an optical pullback sensor is detailed for tracking displacement. The patent describes the concept of using a device that grips a catheter or tool and as that grip is moved, the displacement of the grip is tracked relative to another surface. The displacement of the grip is assumed to match the resulting displacement length at the tip of the tool inside the patient. [11] Figure 4 shows the diagram of this device.

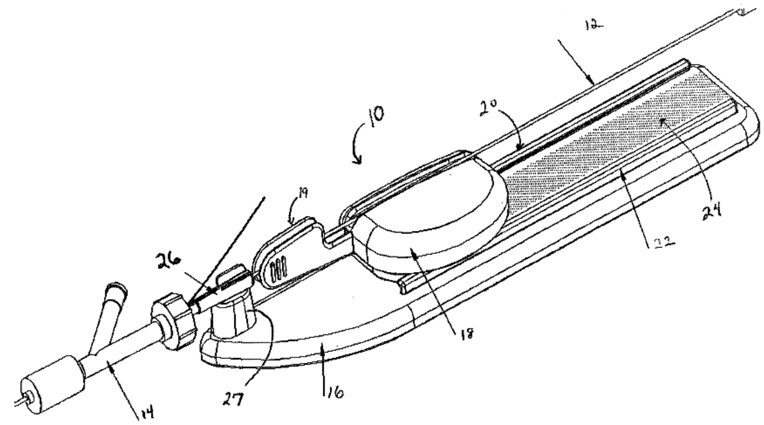

Figure 4. Diagram depicting an embodiment of the optical pullback sensor from US20030187369. [11]

Patent application US20080262473, Locating A Catheter Tip Using A Tracked Guide, priority date October 19, 2005, describes utilizing a known position of a first object along which a second travels to determine the position of the second object based on linear displacement between the two objects. [12] Examples of the technology are shown in Figure 5.

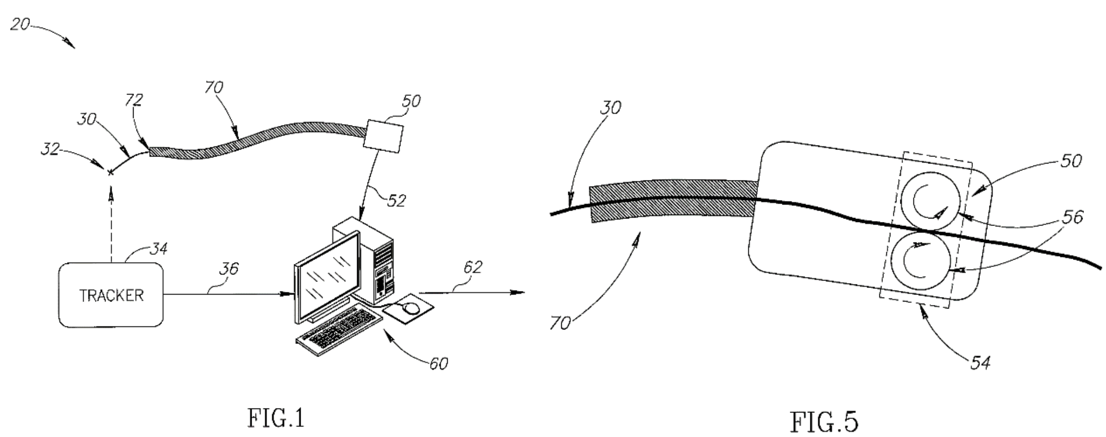

Figure 5. Diagrams of tracked guide device from US2008026473. [12]

Patent application US20090062739, Catheter Guidewire Tracking System and Method, priority date August 31, 2007, details a catheter and guidewire tracking system utilizing coils placed around each device and measuring inductance as one passes through the other [13]. This patent provides for a plausible method to determine relative motion between a guidewire and a catheter but requires two custom designed and developed devices. A depiction of the device concept is shown in Figure 6.

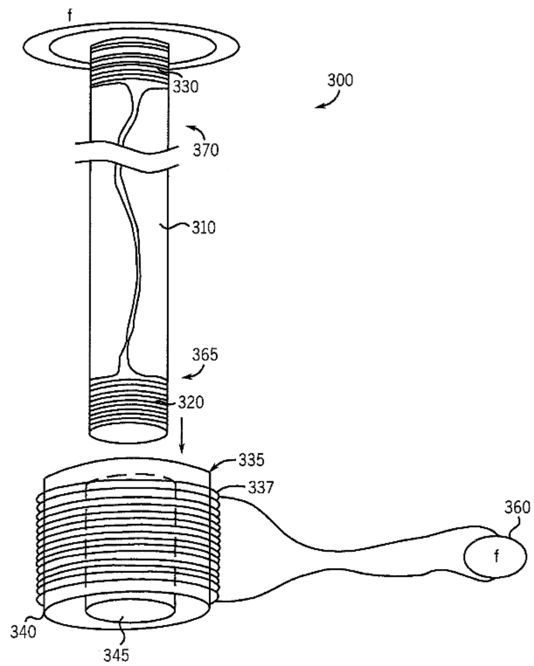

Figure 6. Diagram of measurement device depicted in US20090062739. [13]

In the expired US Patent US5437290, System and Method for Monitoring Intraluminal Device Position, published August 1, 1995, several methods of measuring the motion of luminal device positons are detailed. It uses both indexing on the device that is measured optically or a roller that contacts the device [14]. Several aspects of this patent cover device tracking concepts similar to the designs that SWE TeamTech developed over the course to the 2015-2016 year. The patent focuses on tracking of a single device and its displacement from a datum outside the body to an intraluminal positon instead of tracking of relative motion.

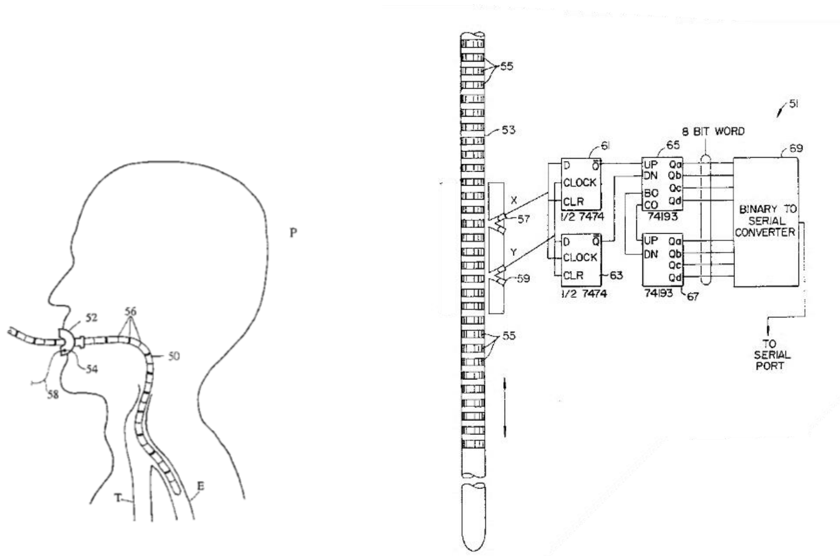

Figure 7. Diagram of device in US5437290. [14]

The expired US Patent US5709661, Electronic Catheter Displacement Sensor, published January 20th, 1998, covers the use of an electronic catheter tracking device that uses a sensing and idler roller to generate a signal that can be processed into displacement and visually displayed [15]. This patent closely resembles the design concept of the rotary encoder box developed by SWE Team Tech. It tracks a single device instead of the relative motion between two separate devices. The device is shown in Figure 8.

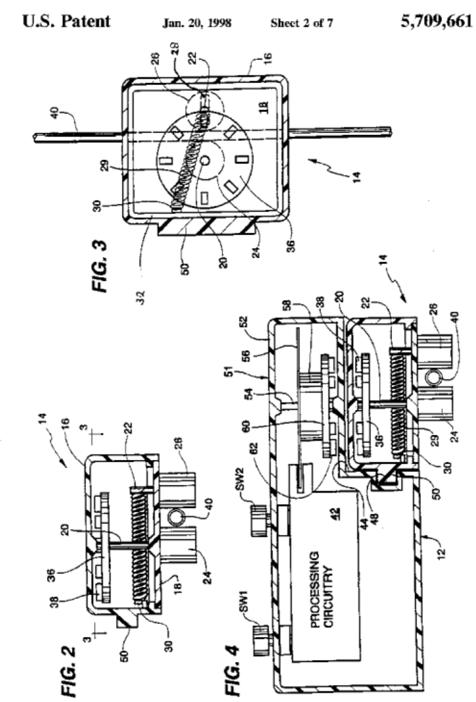

Figure 8. Diagram of device in US5709661. The catheter is indicated by #40 in this diagram. [15]

<u>2.1.2 Vascular Simulators</u>

A significant area of development in catheter and guidewire tracking is for the creation of surgical simulators. These devices allow physicians to train on procedures in a virtual environment. [16] Haptic feedback devices track catheters and provide force feedback during the simulation. Mintice Inc. develops vascular interventional procedure simulators, one example is shown in Figure 9. The device uses two optical sensors to track the displacement and rotation of catheters and guidewires; however it is limited in catheter tracking length. Feedback is supplied by motors that clamp on the surgical tools. [17]

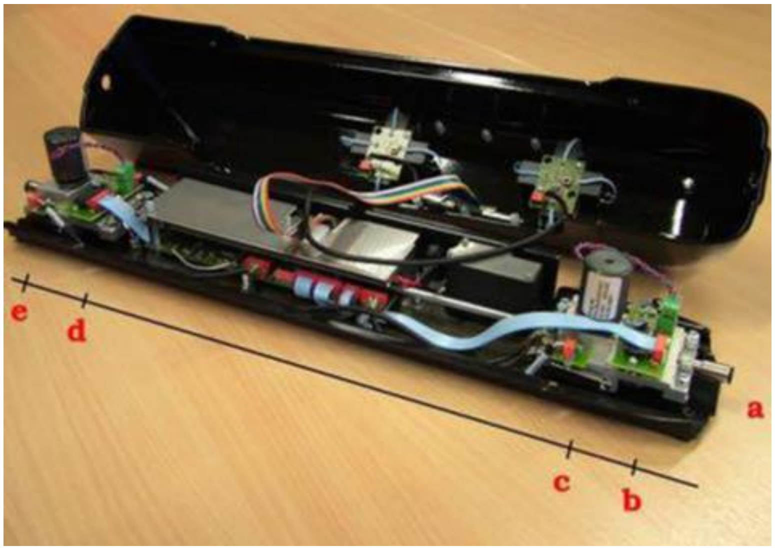

Figure 9. Haptic feedback tracking device with chassis cover removed. [17]

Figure 10 shows another example of a device developed by Luo et al to interact with their guidewire simulation. The simulation developed an algorithm and software to be able to run at 75 frames per second. [16]

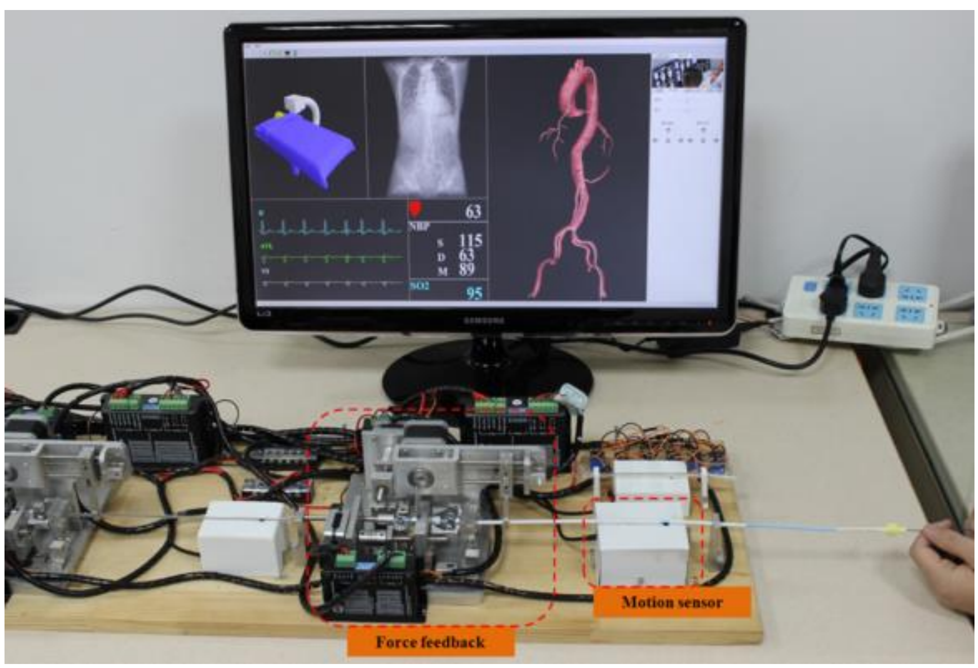

Figure 10. Virtual intervention simulator device. [16]

2.2 Guidewire and Catheter Tracking and Localization Technology

Technologies and techniques used to locate the placement of a catheter or guidewire placed in a patient anatomy fall into two main categories. The first is the use and extension of image based systems to calculate a guidewire location. These systems use the images recorded through various means such as fluoroscopy, x-ray, and echocardiography in combination with algorithms to process and calculate a representative path of the guidewire or catheter. These systems provide information about the guidewire location but still require the use of ionizing radiation for imaging. The second technique is to use sensors placed on the tools with an external system to track the position of the tools. These systems typically utilize electromagnetic field or resistance measurements.

2.2.1 Imaging Based Tracking Systems

Through improved visualization of the guidewire, such as enhancing the contrast of guidewire-like features, radiation dose can be reduced. [18] Imaging based tracking systems utilize processing of x-ray images to develop predicted paths for guidewire and catheter localization. The systems complement current imaging techniques to provide more information about the interventional devices in use.

Baert et. al. proposed enhancing line like structures in sequences of images and then finding the path of the guidewire from the enhanced images by fitting a spline. Figure 11 shows typical results of the algorithm. The results from the algorithm were compared to tracings generated by human operators. Difficulties in this method are determining the difference between features such as stitches, arteries, and structures that appear line-like similar to the guidewire. The parameters and methods of the algorithm were investigated to determine the algorithm with the highest tracking success. Localization of the tip of the guidewire was approximately 2mm. [18]

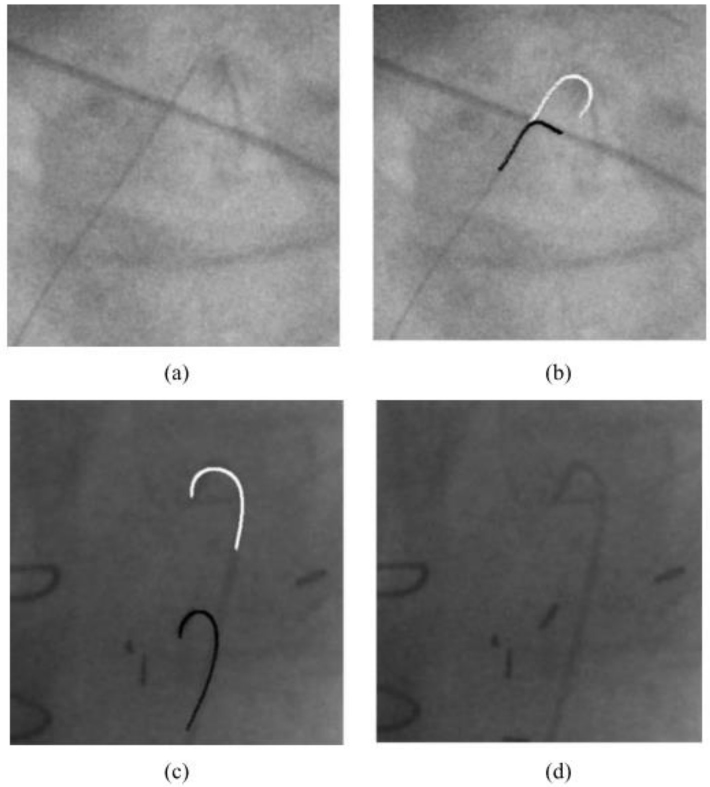

Figure 11. Example of guidewire tracking algorithm results. Two examples of misplacement of the spline, (a) The original image, (b) The guide wire can be detected using the subtraction images (white spline), but using the Hessian image, the method failed (black spline), (c) An example (white), but the method failed using different settings (black). The spline is then more attracted to a stitch. (d) The original image in this case. [18]

Ma et al developed a method to track multiple electrophysiology catheters in the same image. The algorithm uses the electrodes present on the electrophysiology catheters to detect high contrast blobs. The method developed is able to track the location of an ablation catheter, CS catheter, and lasso catheter simultaneously and in real time. They found that a 2D accuracy of less than 1mm was achievable. [19]

Challenges presented to catheter localization through C-Arm imaging systems is assumption of a fixed shape for the catheter and the effects of foreshortening due to projection of a 3D shape into a 2D image. Milletari et al developed a method through which the tip of the catheter is detected and the position is determined through detection of electrodes proximal to the tip. The catheter path is formed through the minimization of a cost function. The algorithm works around l1-sparse coding, a machine learning algorithm technique. [20] The technique is limited to catheters with multiple electrodes or radiopaque markers.

Petkovic et al proposed a method of monoplane guidewire tracking because of the complications introduced by 3D reconstruction of the guidewire from images. The problems with 3D reconstruction include the C-Arm must be repositioned to obtain biplane images and the guidewire must be stationary in both images to generate an accurate reconstruction. The method proposed uses a segmentation of blood vessels from a pre-operative scan to generate a restrictive volume. The 2D images during the procedure are used to generate an unordered set of pixels representing the guidewire location. The 2D pixels are backprojected into 3D with knowledge of the imaging arm location in combination with the pre-obtained restrictive volume to generate a 3D reconstruction. The restrictive volume and resulting calculation are shown in Figure 12. The solution is not unique so all solutions fitting the required parameters are presented to the operator. They conclude that the method is useful for guidewire localization accurate to one width of the vessel. [21] An example of implementing the algorithm on data from a patient procedure is shown in Figure 13.

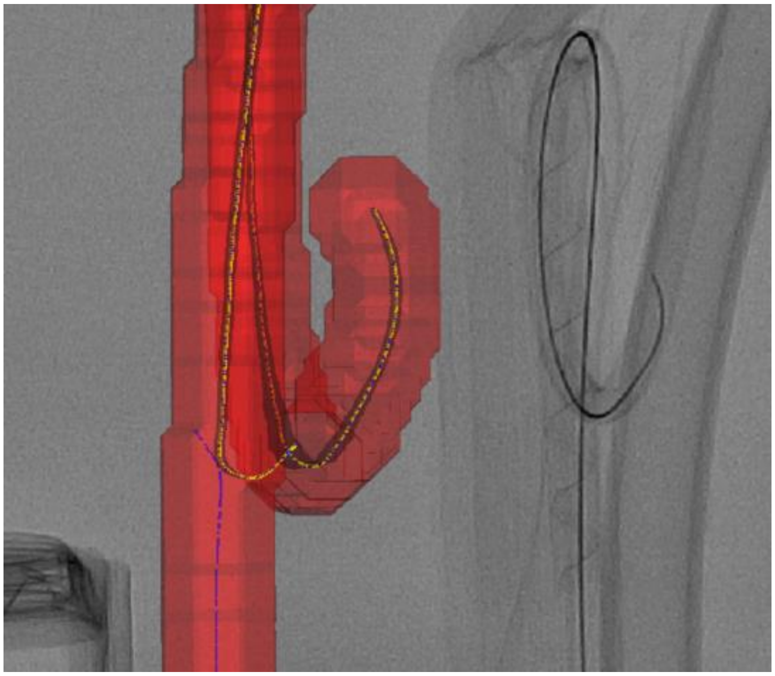

Figure 12. Representation of guidewire path reconstruction contained within a 3D restrictive volume. At a self-intersection the guidewire can continue either way. Two of several possible solutions are shown. The volume and 2D image are misaligned to make the self-intersection in 2D visible. [21]

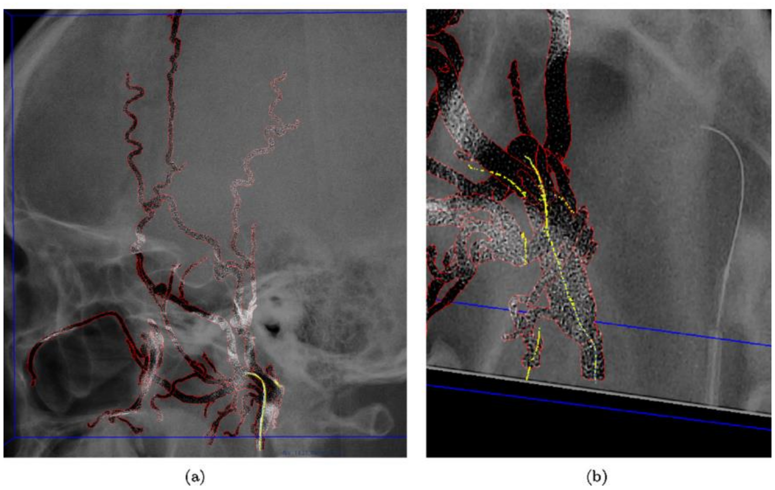

Figure 13. An example reconstruction for a patient case: (a) the 3D reconstruction of the guidewire overlaid over the X-ray image and (b) a 3D view where all possible curve reconstructions are visible. [21]

2.2.2 Sensor Based Tracking Systems

Sensor based tracking systems utilize sensors placed on interventional tools to provide the method of device localization. The systems are designed to either augment traditional fluoroscopy based navigation, or to replace it entirely. Often a model of the vasculature or 3D geometry of the area of interest is obtained prior to use of the localization system.

Condino et al focused on the reconstruction of catheter location with two sensors that allow for the reconstruction of the distal curvature of the catheter. The system allows for the tracking of a sensor enabled guidewire tip, a sensor enabled catheter tip, and the reconstruction of the distal curvature of the catheter.[22] Sensor enabled catheters were tracked in the NDI Auroroa system with two sensors, one placed on the tip of the catheter and one placed a few centimeters proximal to the tip sensor as shown in Figure 14. A tracking accuracy of 1.2±0.3mm was achieved with the system and no difference was observed between use of the system and traditional fluoroscopy [3], [22].

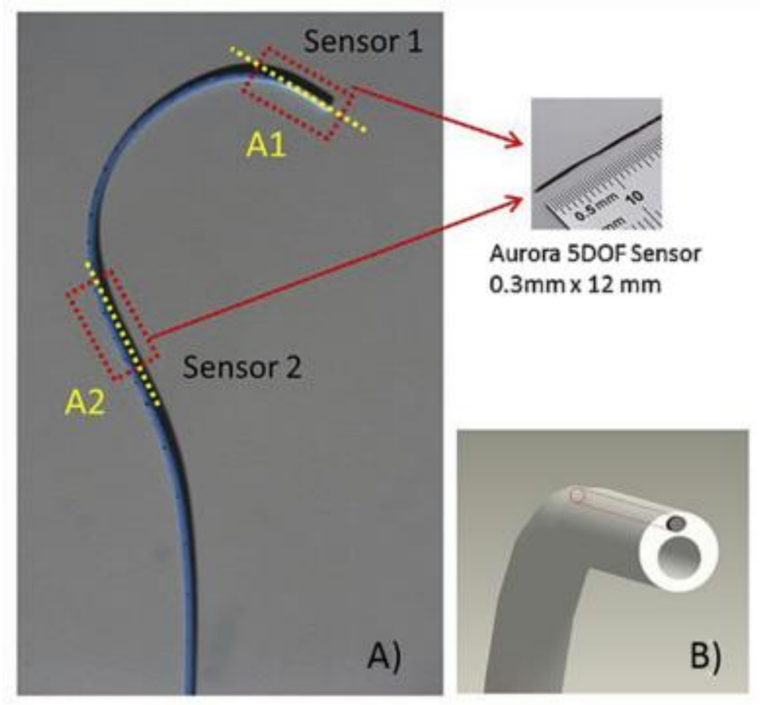

Figure 14. A sensor enabled 5-F cobra catheter. The catheter is made modifying a steerable angiographic catheter, the Orienter from Angiologica. (A). Sensors positions are highlighted in red: the axes of the coils are aligned with that of the catheter operative lumen. More particularly, one sensor is positioned at the catheter tip (B), while the other, which provides the sixth degree of freedom, is positioned a few centimeters below the first coil to acquire information about the curvature of the catheter distal part. [3]

Gepstein proposed an early implementation of a 3D mapping system using a magnetic field. A transmitter pad contains three emitters that decay at varying rates. From the information contained in these fields the position of the electrode can be determined as shown in Figure 15. The tools were used to build electrical and special maps of the heart. [23]

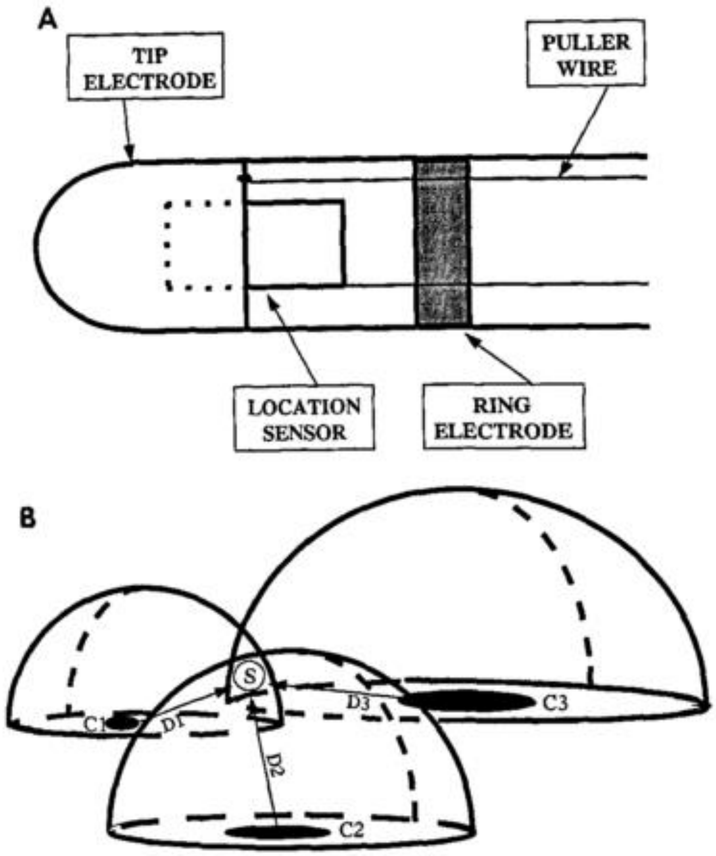

Figure 15. Diagram of the locatable catheter device (A), and method of location determination (B). [23]

Lam et al evaluated the use of an electromagnetic microsensor placed on a guidewire inside the lumen of a balloon catheter. The device was used to provide location information about the placement of the balloon catheter in the patient sinuses correlated to preoperative computed tomography imaging. The study qualitatively evaluated the utility of the microsensor information provided and found to be successful in assisting placement in 17 of 18 balloon dilations. [24]

Ralovich et al utilize a hybrid imaging system of fluoroscopy and intracardiac echocardiography (ICE). Radiopaque ball shaped markers are placed on a catheter and a monoplane projections is used with machine learning to detect the ball locations. The method then uses the location of the balls to determine the location and orientation of the ICE catheter and register the echo cone to the C-arm coordinate system. [25]

2.2.3 Path Calculations from a Known Geometry

Konings et al developed an algorithm based on elementary physics to simulate guidewire trajectory analytically. It incorporates the flexibility of the guidewire and the elasticity of the vascular wall. The set of equations is solved to minimize the energy of the guidewire bending and elastic wall deformation of the vasculature. Guidewire paths from the implementation of the algorithm with phantoms in two dimensions are shown in Figure 16. The simulation produced guidewire path accuracy to within 10% of the size of the lumen. [26]

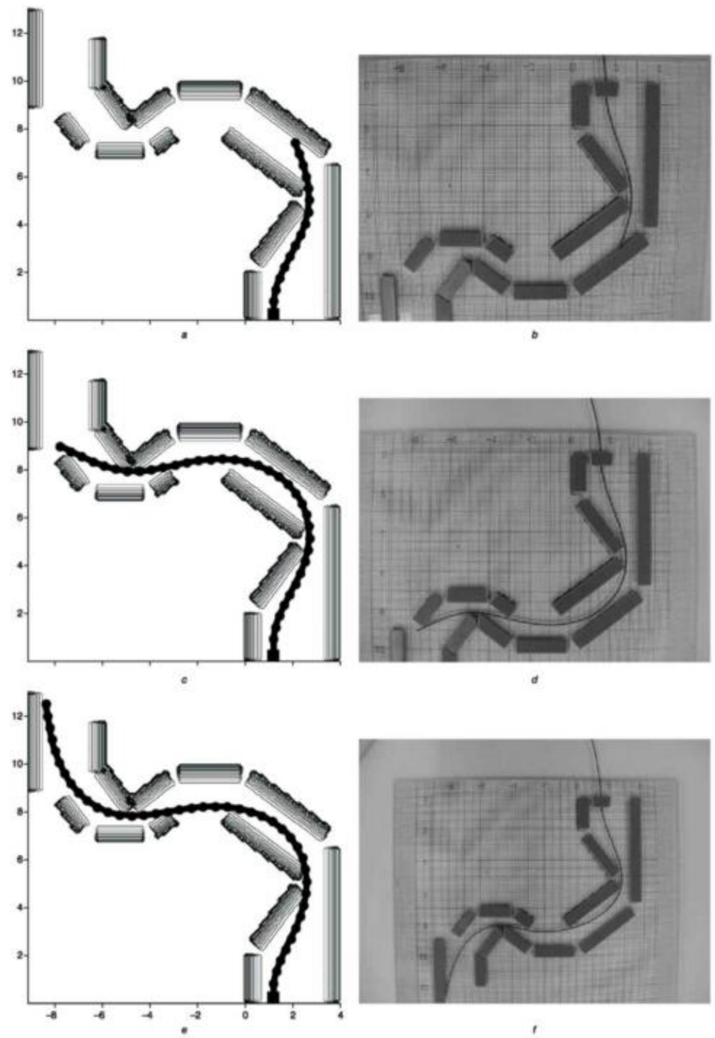

Figure 16. Results of validation experiments using planar vascular phantom. (a), (c), (e) Results of simulation corresponding to inserted length of guidewire of 7.75 cm, 17.90 cm, and 20.80 cm, respectively. (b), (d), (f) Photographs of guidewire in planar phantom, with the same inserted lengths. [26]

Alderliesten et al expanded on the work of Konings to discuss multiple techniques to develop a model representing guidewire geometry. The primary focus of the paper was to evaluate various models for tradeoffs between speed and accuracy. For clinical relevance and usefulness speed in the simulation is critical. If the computation takes too long to complete the simulation is not relevant for the physician.

The guidewire was modeled, shown in Figure 17, as a series of joint positions with a straight, rigid, incompressible segment, of constant length. The bending energy of the guidewire was calculated using Hook's Law and total energy for the guidewire was the sum of all segment energy. The energy of the vessel wall was calculated similarly. The sum of both total energies in the system is minimized.

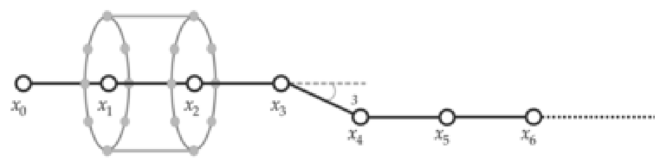

Figure 17. Guidewire defined by joint positions. Joint 0 represents the tip of the guidewire. Angle between the two segments connected by joint I is illustrated in joint 3. [27]

The algorithms compared in this analysis were an iterative analytical solution, a conjugate-gradient optimization, and a gradient leveraged iterated density-estimation evolutionary algorithm (GLIDE). The results of the algorithms were compared to a real guidewire and calculation times were assessed. The conclusion was that the significantly faster solution times of the gradient and GLIDE solvers were worth the small trade off in accuracy. Figure 18 and Figure 19 demonstrate these results.

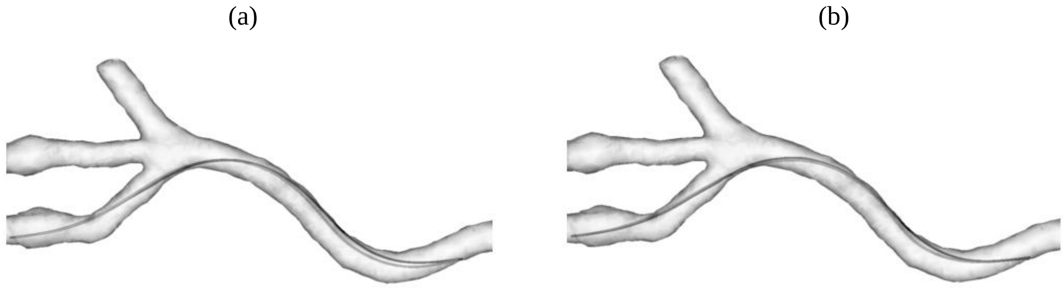

Figure 18. Guidewire simulation with two different algorithms. (a) Illustration of the reference guidewire configuration (black) and the simulated guidewire configuration (gray), resulting from the experiment based on the semianalytical approximation algorithm. An rms error of 1.22 mm is associated with this simulation result and simulation time of 20.36 s. (b) Illustration of the reference guide-wire configuration (black) and the simulated guidewire configuration (gray) resulting from the experiment based on GLIDE. An rms error of 1.12mm is associated with this simulation result and simulation time of 2.98s. [27]

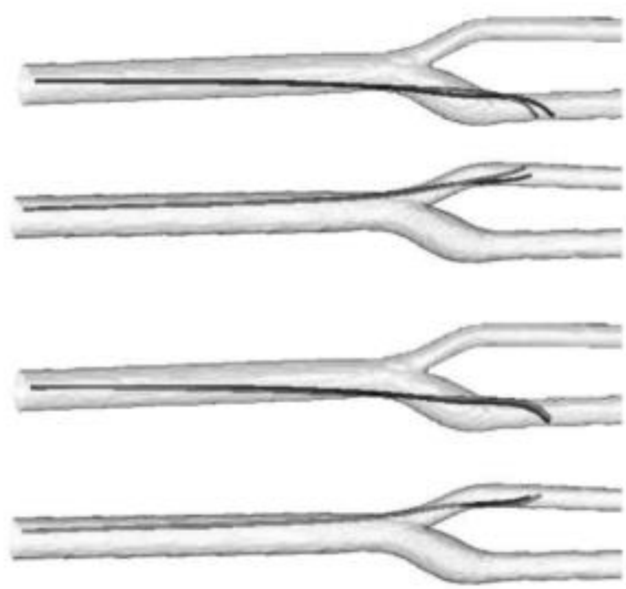

Figure 19. Illustrations of two simulation of the propagation of an intrinsically curved tip guidewire inside the carotid-bifurcation phantom. Two visualizations on the top illustrate the simulation results obtained with the semianalytical optimization algorithm. Two visualizations on the bottom illustrate the simulation results obtained with GLIDE. [27]

Korzeniowski et al developed a simulator for endovascular procedures utilizing a haptic feedback device, the Mentice Inc. Vascular Simulation Platform. The guidewire was modeled based on Cosserat Theory which assigns discrete sections of rod a coordinate system at the centerline of the material and calculates bend and twist deformations based on the differences between the frames. The model assumes inextensibility of the guidewire. Real-time simulation rates were achieved with an average error of 1.34±0.95 mm. [17] Figure 20 shows the results of the simulation.

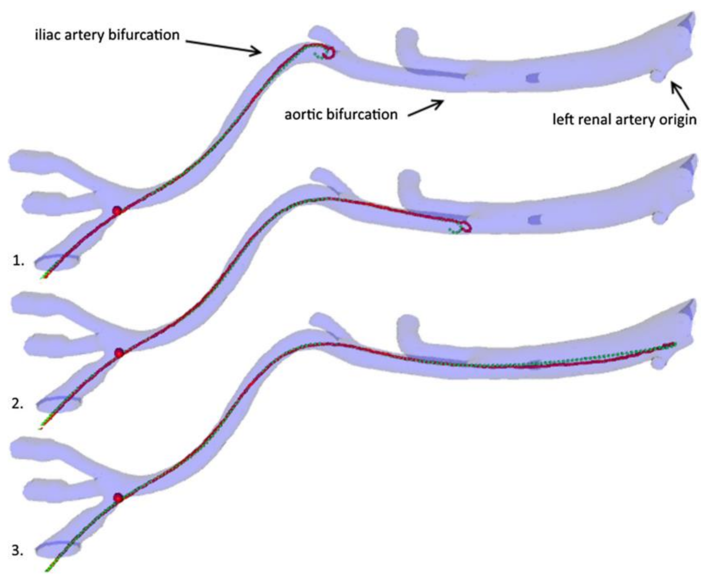

Figure 20. Reconstructed 3D geometry of the phantom showing the centerline of the guidewire in red and the simulated instrument centerline in green. [17]

Qui et al proposed the use of graph theory to simulate guidewire paths with an added iterative optimization step to reduce runtime. The minimum energy is calculated through the application of a shortest path algorithm to minimize the total energy of the guidewire. The process first uses an iterative refinement algorithm to reduce computation costs. The guidewire path is calculated from a set of spatial possible positions of the guidewire by finding the minimum energy path option. [28]

Schafer et al also implemented an approach based on known 3D vessel information. They expand on the work of previous models to reformulate the problem into a graph theory approach in an attempt to reduce computational run times. [29] The vessel centerlines are selected and sectioned. At each centerline point a mesh is drawn and vectors connect the mesh points. Energy for each vector connection from one mesh point to another is calculated and the total energy to go from the starting node to the end node is minimized.

Results show that increasing tortuosity reduces dependence on starting and ending locations. Spatial separation of 1.5cm or less between center points results in similar solutions. The conclusion based on varying stiffness parameters is that the spatial constraints of the vessel geometry have a larger effect than the guidewire stiffness.[29]

2.3 Current State of Technology Summary

The generation of technology to locate a catheter with the relative motion of a guidewire is not completely new. Methods have been developed and investigated to provide linear displacement information from catheter or guidewire motion. Additionally some of this has been applied to virtual reality simulations of endovascular procedures. The hardware methods known to have been developed are outlined in Table 3. The work from Cal Poly SWE Team Tech will be discussed in Chapter 3. The capability of any products or hardware based on the published patents investigated is unknown.

Table 3. Summary of displacement tracking technologies.

Author	Hardware Design	Capabilities (Resolution)
Cal Poly SWE Team Tech [30]	Photocell	4.5mm
	Rotary Encoder	0.03mm
	Mouse Trackball	0.06mm
Korzeniowski et al [17]	Mentice Inc Vascular Simulation Platform	Unknown
Luo et al [16]	Custom hardware	Unknown

Software methods have been developed to generate location information about guidewires placed in a patient. There is a strong desire to develop a method that can calculate and update this information in real time to apply to both simulations and real procedures. The majority of these methods utilize geometry pre-computed prior to the procedure. A summary of the methods' accuracy and calculation times are shown in Table 4.

Table 4. Summary of guidewire path calculation methods.

Author	Software Method	Accuracy	Calculation Time [seconds]
Konings et al [26]	Semi-analytical	10% of lumen diameter	
Alderliesten et al [27] [31]	Semi-analytical	1.23 mm (RMS Error)	20.36
	Conjugate-gradient optimization	1.45 mm (RMS error)	2.72
	GLIDE	1.12 mm (RMS error)	2.98
Korzeniowski et al [17]	Cosserat rod model	1..66 mm (RMS Error)	
Qiu et al [28]	Graph Theory	0.606 mm to 1.033mm (various phantoms)	5.9 to 4.1 (various phantoms)
Schafer et al [29]	Graph Theory	Approx 1 mm (RMS Error)	< 2 seconds

A novel development with this project was a calculation of the guidewire position using only the history of distal tip sensor position and marked landmark locations with no assumption of a known geometry prior to the procedure. The location history of the guidewire tip was used in combination with a graph theory approach to generate a predicted path for the guidewire. The recorded data provided a set of points to approximate the shape of the vasculature to which an approach similar to the one discussed by Schafer et al. This allowed for the calculation of a guidewire path without the prerecorded information about the vasculature from CT imaging or another method. The guidewire path can then be further extended to provide a calculation of catheter location. This method of determining the guidewire and catheter trajectory is discussed further in Chapter 6.

Chapter 3: Previous Work on this Project

This chapter covers a summary of the work that was completed prior the initiation of this thesis project. Over the course of the 2015 - 2016 academic year, the Cal Poly Society of Women Engineers Team Tech (SWE Team Tech) group was tasked to complete the initial work to develop proof of concept prototypes of three electromechanical system concepts and a proof of concept software demonstration of a catheter and guidewire localization system. Several prototype devices were developed and evaluated, and example visualization software was completed. In comparison to the SWE Team Teach project, this thesis sought to evaluate the results of the initial prototypes and continue development to a stage where the proof of concept could be demonstrated in a setting similar to a pre-clinical study.

3.1 Hardware

Three different mechanical hardware concepts were developed and proof of concept prototypes were tested. The designs consisted of a custom built photocell and roller device, a computer aided design (CAD) rendering is shown in Figure 21, a device utilizing rotary encoders, the prototype device is shown in Figure 22 and Figure 23, and a device utilizing the scroll ball and sensor from a computer mouse as shown in Figure 24.

The photocell device essentially created a custom encoder that allows the designer more direct control over the parameters of the device. Lasers are used to illuminate an alternating pattern of black and white divisions of a circle and a photocell reads the changes in reflected light intesnsity. The initial prototype did not meet the required specifications as it lacks a fine enough resolution, had too low of a response time, and could not distinguish between advancing and retracting motion. Each “tick” of the prototype photocell rotation corresponded to a 4.5mm movement of the tracked guidewire or catheter which is far greater than the desired sub-millimeter precision. Additionally the repsonse time of the photocell device did not allow for sufficient output speed.

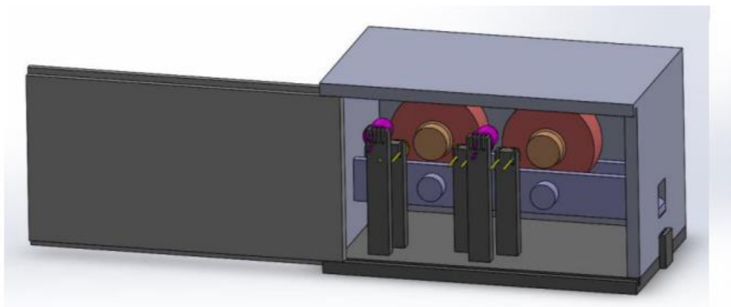

Figure 21. Design of the photocell roller measurement device. [30]

The rotary encoder device showed the most promise despite some of the issues it experienced. One point of difficulty was ensuring the encoder shaft rotation matches the movement of the guidewire as the guidewire passes over the encoder shaft. Inconsistent sliding motion over the shaft instead of continuous rolling resulted in large errors in the data output. The design implemented three encoders to introduce redundancy in the measurement but the core issue of inconsistent motion was not solved. The encoder had the advantage that through the use of quadrature, two output channels at a 90-degree phase shift, it is possible to measure both forward and backward motion. The prototype device had an output resolution of approximately 0.06 mm that would be sufficient to meet the design requirements.

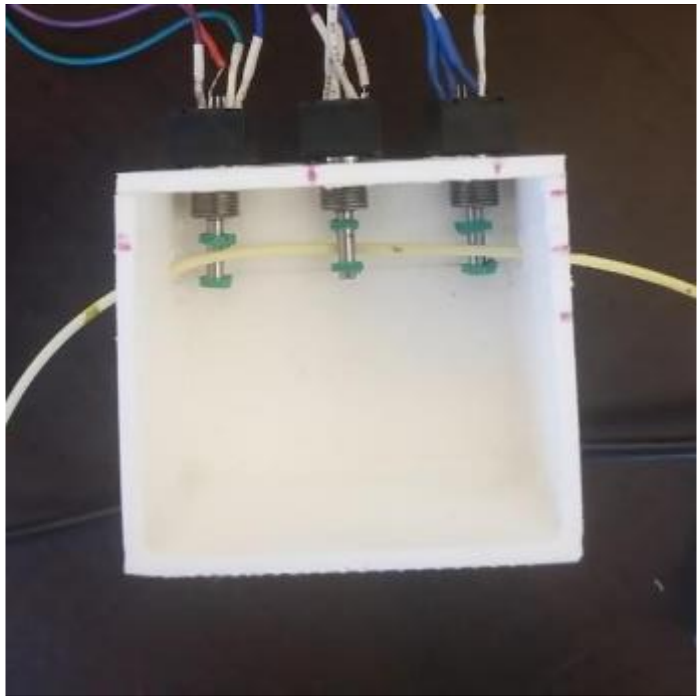

Figure 22. Design of the rotary encoder measurement device with the lid removed. [30]

Figure 23. The rotary encoder measurement device with the lid utilizing spring loaded bearings to maintain pressure on the catheter. [30]

The third prototype concept evaluated used a scroll ball tracking device that allows for both rotation movement measurement and axial movement measurement. The device design needed to accommodate both a catheter and a guidewire pressed against the track ball and integrate the signal outputs of the device into an Arduino.

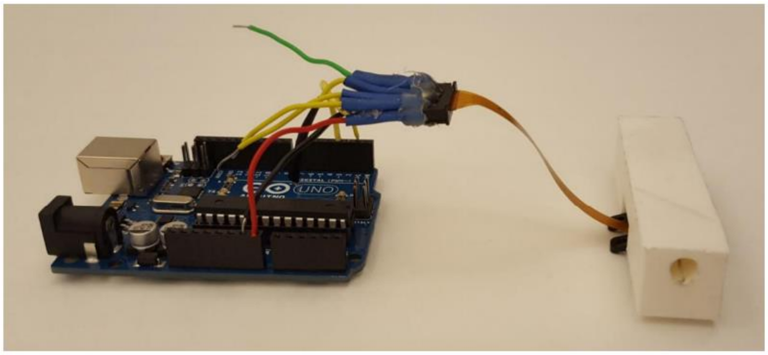

Figure 24. Prototype device utilizing the scroll ball from an Apple Mighty Mouse. [30]

The three prototype concepts were evaluated for accuracy and usability at the end of the 2015-2016 project. Based on the knowledge and experience of the SWE TeamTech members it was decided that pursuing an iteration and improved version of the rotary encoder device would be the most promising.

3.2 Software

The goal of the software portion of the Team Tech project was to develop a method for displaying the relative motion data captured from the catheter and guidewire in a manner that is relevant and helpful for the clinician. This involved interpreting the sensor data from the MediGuide sensor-enabled guidewire and calculating a predicted guidewire path. The predicted catheter location was drawn on top of the predicted guidewire path.

The SWE software team primarily focused on plotting the catheter placement on a line resulting from digital filtering of the MediGuide relative positon data. An aspect that needed more work was to develop a method for calculating the guidewire trajectory and path that is robust enough to determine when the guidewire is advanced down a bifurcation, retracted, and then advanced down another to result in a final path for the wire trajectory. The Team Tech algorithm did not differentiate the time-dependent path of the guidewire from the spatial representation of the vasculature. A representation of the team's algorithm results and graphical user interface (GUI) is shown in Figure 25.

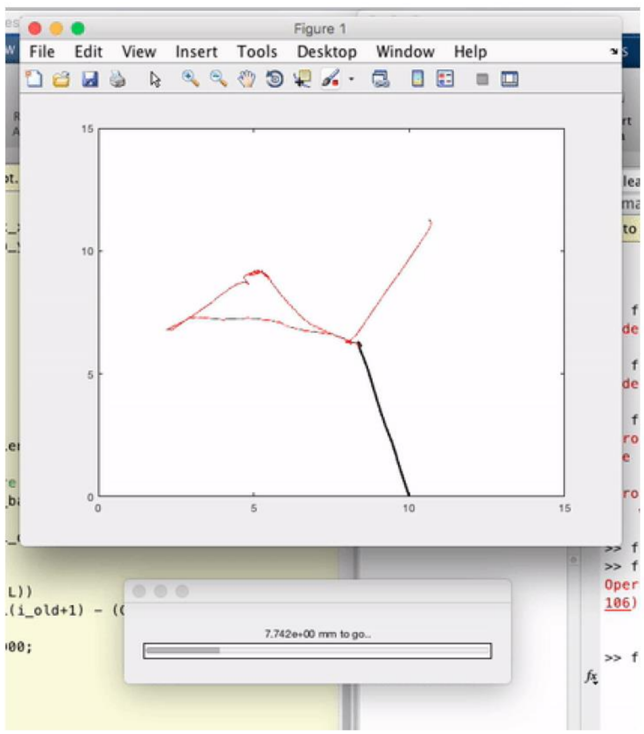

Figure 25. The GUI developed by the SWE Team Teach software subteam. [30]

3.3 System Use Process

The design of the systems developed by SWE was as described in Figure 26. The intended method of relative motion tracking was to backfeed the guidewire through the device and then forward feed the catheter over the guidewire. The measurement device would record the guidewire backfeed and the catheter forward feed. While in use motion of the guidewire would be calculated in software with the MediGuide system. This motion would be compared to the motion measured from the catheter and with the known backfeed length and prior knowledge of the total length of the guidewire the relative distance of the distal tips of the devices could be calculated.

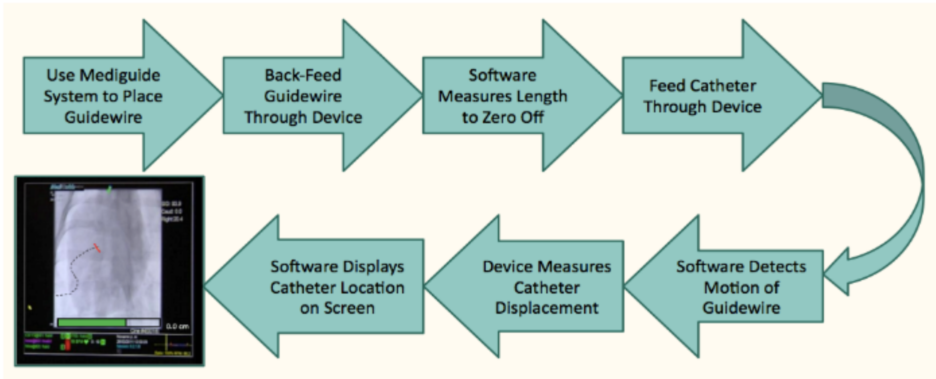

Figure 26. Outline of intended SWE team device use process. [30]

This intended system measurement methodology had multiple potential challenges. The motion of each of the two devices was measured with two different techniques and then compared to calculate the relative motion. This introduces additional error into the system as the uncertainty in each measurement propagates into the relative motion calculation. The guidewire is subject to movement from cardiac and respiratory motion in addition to the displacements caused by the operators actions making tracking accurate displacement from the software a challenge. Additionally, care would need to be taken during the initiation of the backfeed and forward feed of the devices to ensure that all the length of the devices was accounted for and no small segment was skipped.

3.4 Previous Work Summary

SWE Team Tech completed the initial work to develop feasible concepts and prototypes. Multiple design approaches were investigated simultaneously to evaluate several concepts. The construction of the devices and the evaluation through resulting testing indicated performance below expectations as outlined in Table 5. Each design had challenges with either resolution, error, or was challenging to interface with.

Table 5. Summary of SWE Team Tech device performance.

Device	Resolution	Error	Results
Photocell	4.5mm	Not Tested	No direction detection Slow response speed
Rotary Encoder	0.035mm	11% (best case single trial)	Inconsistent data due to slip on encoder shaft surface
Mouse Trackball	0.06mm	Not Tested	Sensor interface difficulties

The challenges discovered through the development of the initial prototype systems and the potential problems with the system use procedure several decisions were made to continue future development. The rotary encoder design was selected as the starting point for continued development due to the resolution and ease of interfacing with the sensor. It was decided that the hardware design should directly measure the relative motion of the guidewire and catheters instead of calculating the relative motion from multiple measurements. With regard to the software component of the project the focus was determined to be determining a spatial representation of the guidewire location instead of the time-dependent function developed by the SWE team. The goal of this thesis was to continue the work on the project, both hardware and software components, and build a device to adequately meet the specifications for accuracy.

Chapter 4: Hardware Design Process

4.1 Initial Concepts

The designs from the SWE Team Tech project were used as a starting point for continued development. The conclusion from the team was that the most promising option to test would be the rotary encoder based design as it provided the most consistent data. The photosensor design was, for all intents and purposes, a custom built encoder with much lower fidelity. The mouse trackball design had difficulty with accuracy and is more difficult of a sensor to interface with. It was decided that continued efforts would be focused on the improvement of the rotary encoder device with improved integration of the device with software.

The project scope required that the design function with both over-the-wire and rapid exchange type catheters as shown in Figure 27. Over-the-wire catheters pass fully over the guidewire and the guidewire exits out of the proximal end of the catheter. Rapid exchange catheters allow for faster swapping of catheters because the guidewire exits out of a port proximal to the catheter tip. This means that a shorter guidewire length can be used and the catheter does not need to be strung over the entire length of the guidewire.

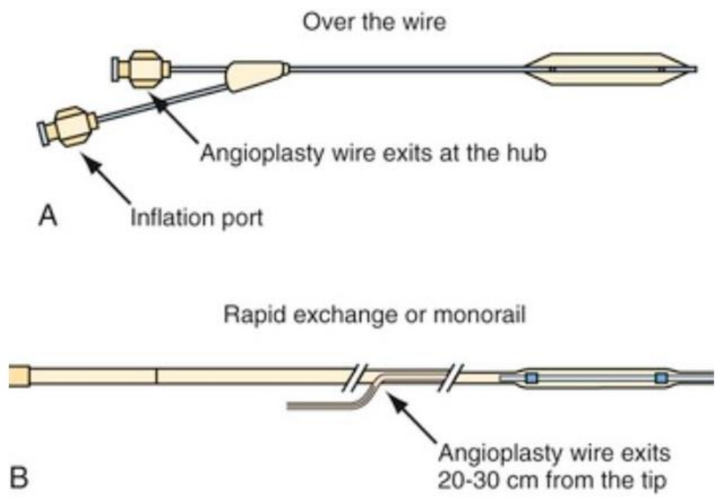

Figure 27. Illustration of the difference between over-the-wire and rapid exchange catheter designs. [4]

The conceptual design for integration with an over-the-wire catheter is depicted in Figure 28. The concept consists of a device that attaches to the Luer fitting on the proximal end of the catheter. The device measures the linear displacement change of the guidewire relative to the catheter as it is advanced. Using a set reference value determined with fluoroscopy the displacement of the catheter relating to the guidewire tip can be determined and displayed visually.

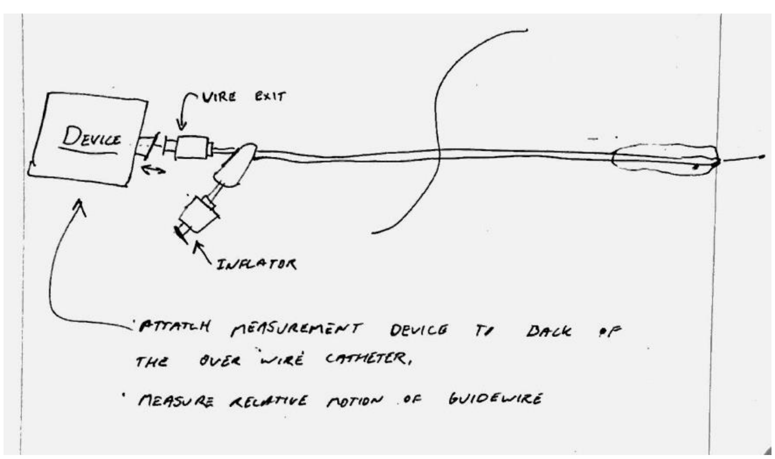

Figure 28. Sketch of the over-the-wire design concept that would connect to the Luer fitting on the back end of the catheter.

The conceptual design for integration with a rapid exchange catheter is depicted in Figure 29. The concept consists of a device that attaches between the proximal end of the catheter and the patient. The device measures the linear displacement change of the catheter relative to the guidewire as it is advanced. A small clip, pin, or other device is needed to ensure the guidewire position remains static relative to the measurement device. The advantage of this design is that a short length guidewire can still be used for the benefits of the rapid exchange catheter design. An implementation similar to the over-the-wire device that measured the guidewire motion would need an exchange length guidewire.

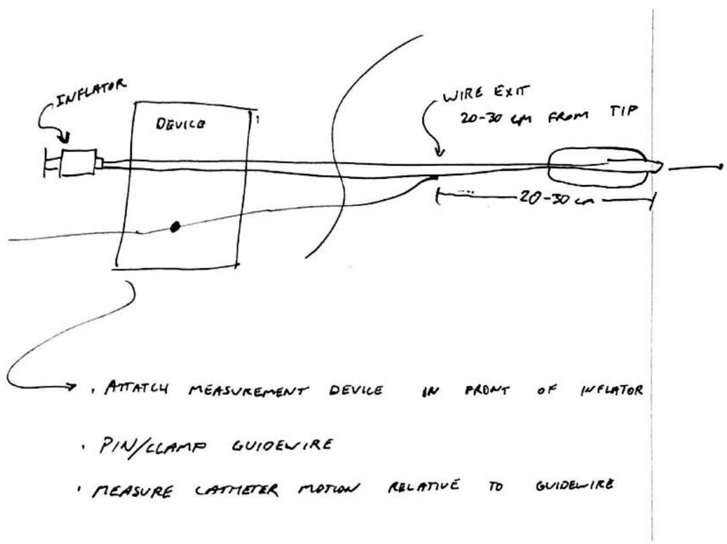

Figure 29. Sketch of the rapid exchange design concept utilizing a device with a guidewire clamp and measurement of catheter motion.

4.2 First Iteration Prototype

Prototype iterations of the rotary encoder device concept as an extension of the Team Tech device were developed. The first was a simplification of the TeamTech design and utilized a single encoder. The idler bearing was mounted on a spring loaded carriage riding over stainless steel dowel pins. A machined shaft was placed over the encoder shaft to allow for both better contact with the sensor via a set-screw and to allow for the possibility to swap various materials and coatings if desired to test for friction and grip variations. The prototype part is shown below in Figure 30.

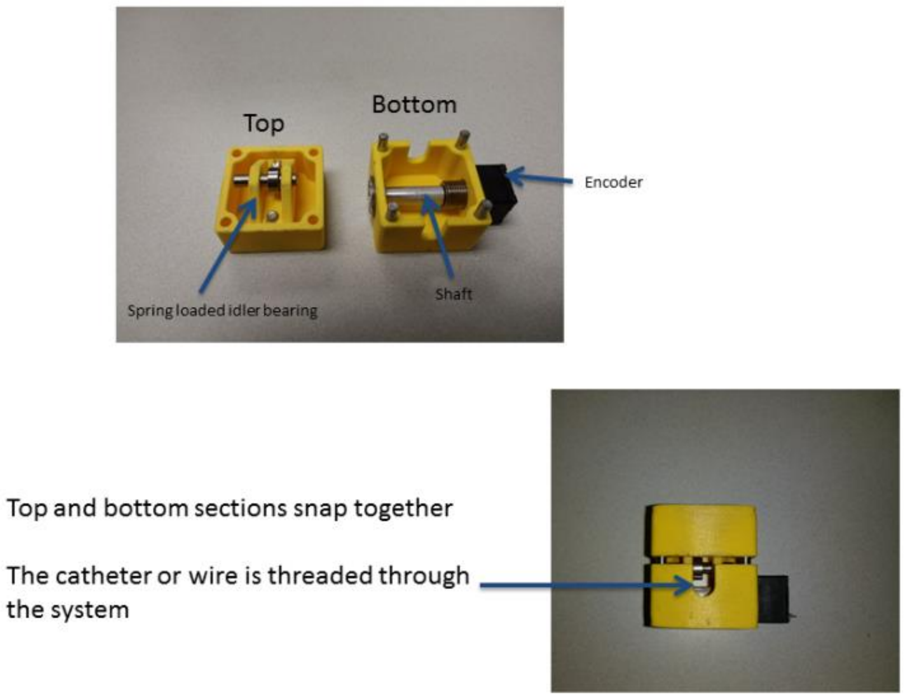

Figure 30. First prototype iteration of the rotary encoder guidewire measurement concept as would be utilized for an over-the-wire catheter.

This design exhibited several issues that led to the subsequent iteration. The friction fit of the lid over the dowel pins was not sufficient to resist the spring force and needed either a latching mechanism or a different design that allowed it to function without opening. Another problem was the spring force was too large to allow for guidewire insertion under the idler bearing. Instead, the catheter or guidewire was placed into the device and the lid closed on top which resulted in an extra step in the use of the device. This spring force and the support for the encoder shaft with a single external bearing and the bearings in the encoder resulted in the shaft binding under load. The spring loaded idler bearing places a radial load on the center of the encoder shaft, transmitted into the bearing in the encoder, but the deflection of the shaft was too large for the bearings and resulted in binding.

4.3 Second Iteration Prototype

These issues led to the second iteration of the design as shown in Figure 31 and Figure 32, which incorporated idler bearings on rockers instead of the linear motion of the first iteration. This design change was intended to allow the roller to more easily be pushed out of the way as a guidewire or catheter is inserted. Additionally, it utilized the option for two encoders to allow for checking data validity between the two measurement sources. Other changes included alignment blocks that ensure the guidewire was supported through the device as close as possible to the idler bearings. This was intended to prevent buckling or kinking the wire as it is pushed through the device. Friction results in an applied axial load to the wire and results in buckling of the guidewire when it is unsupported. The encoder shaft in this second iteration was supported by a bearing on both ends of the shaft to remove the transfer of the radial load on the shaft into the encoder which caused it to bind in the first iteration.

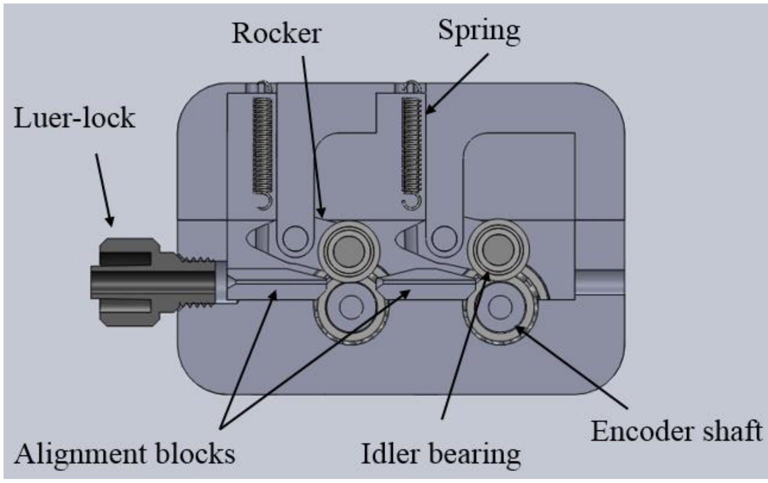

Figure 31. Section view of 3D model for the second rotary encoder design iteration

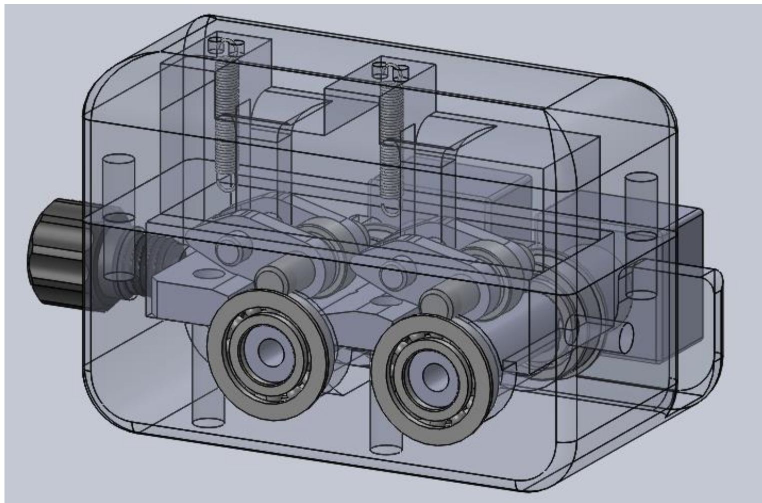

Figure 32. Assembly view of the 3D model of the second rotary encoder design with the outer casing set as transparent.

Like the first iteration, the second iteration was constructed of primarily 3D printed parts. The outer shell of the device is shown in Figure 33. One issue with this design was the small component size of the rocker links led to issues in the printing process. The problems are depicted in Figure 34.

Figure 33. Second rotary encoder prototype device iteration partially assembled.

Figure 34. Second iteration rocker link that proved difficult to 3D print and needs to be redesigned to function properly.

4.4 Third Iteration Prototype

The hardware design was revaluated due to the challenges with fabricating the small componenets. The device was redesigned with inspiration from the function of a wire-feed welding machine as shown in Figure 35. The device consists of a pinch roller that provides pressure on the wire or device that is being moved as it rolls between the pinch roller and an idler roller. The pinch roller pressure was moved with a thumbscrew and allowed for the user to adjust the device to the proper level of force to avoid excessive friction and binding while still allowing for the rolling motion of the tracked device on the rotary encoder shaft. Attached to one of the rollers was a rotary encoder. With a precisely known diameter of the encoder roller the displacement of the wire can be calculated.

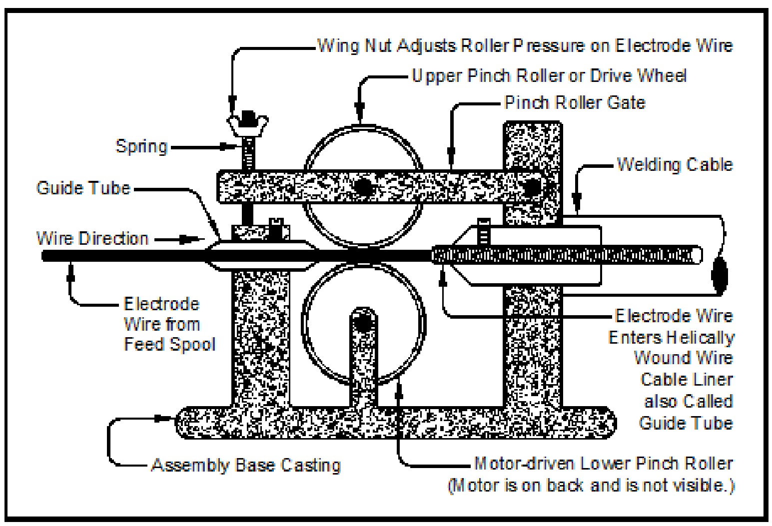

Figure 35. Diagram of a wire feed of a MIG welding machine. [32]

Two prototype devices were developed, one for over-the-wire type catheters and one for rapid exchange type devices. The over-the-wire prototype device attached with a Luer fitting to the proximal end of the device. The guidewire was passed through the Luer, over the encoder roller shaft, and then through a proximal guide pathway. The pinch roller was an idler bearing and was adjusted with a thumbscrew to provide an appropriate force on the wire. Too much force resulted in difficulty moving the wire through the device. Insufficient force resulted in slip of the guidewire over the encoder roller. A photograph of the prototype device is shown in Figure 36. An exploded drawing of the device is shown in Figure 37 and a cross sectional view is shown in Figure 38. Complete drawings for the prototype devices can be found in Appendix E.

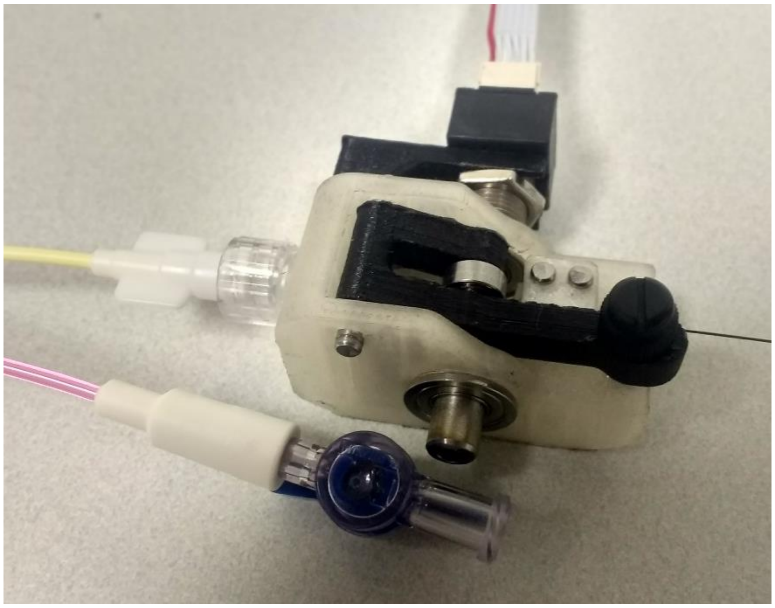

Figure 36. Prototype over-the-wire type device.

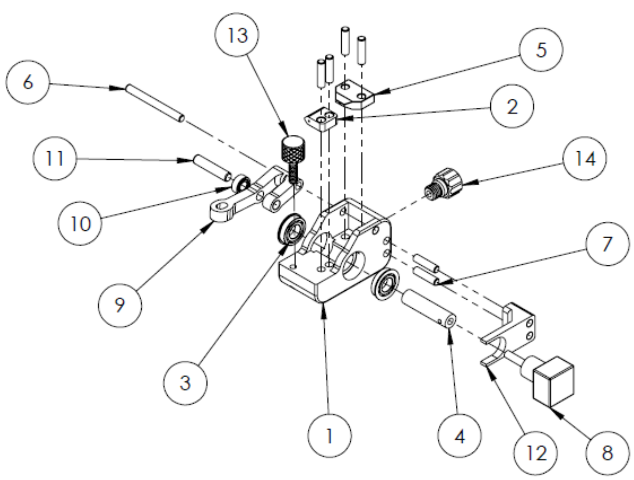

Figure 37. Exploded view of the over-the-wire device prototype.

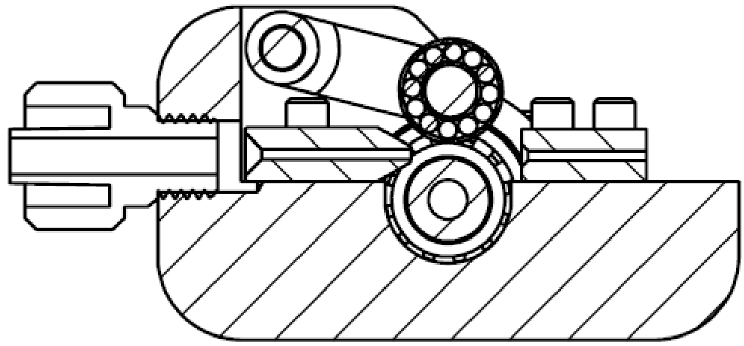

Figure 38. Section view of the over-the-wire prototype showing the path through the device for the guidewire.

The rapid exchange device was similar in construction to the over-the-wire device. Instead of the wire passing through the roller bearings, the catheter displacement was measured. The wire was pinned with a pinch bolt or thumb screw to the measurement device to ensure that the device measured the relative motion between the two devices. A photograph of the prototype device is shown in Figure 39. An exploded drawing of the rapid-exchange prototype device is shown in Figure 40 and a section view is shown in Figure 41.

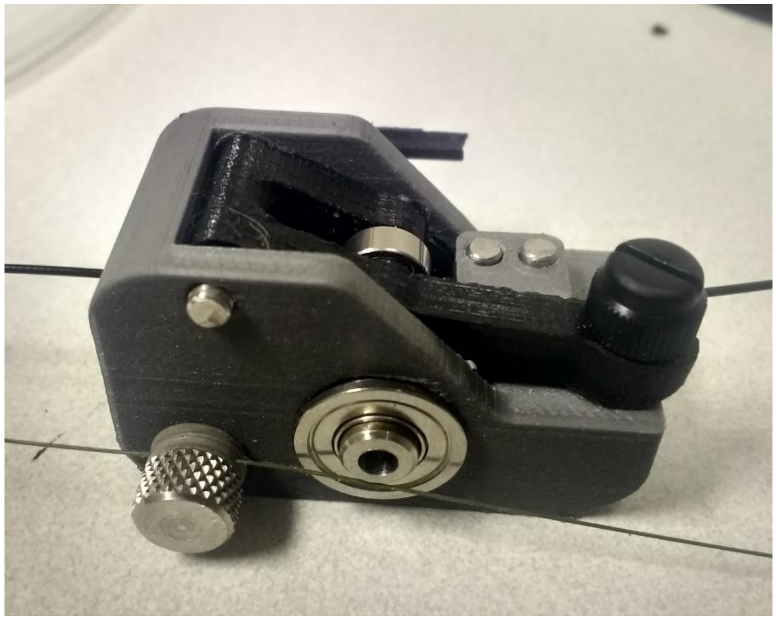

Figure 39. Prototype rapid exchange device.

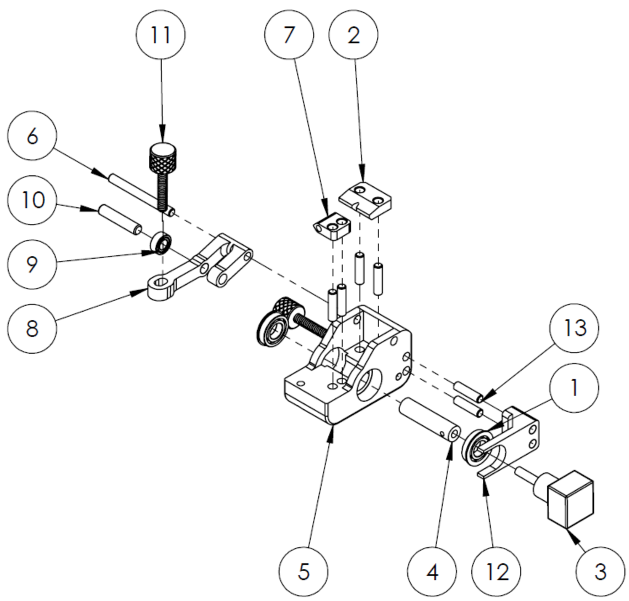

Figure 40. Exploded view of the rapid-exchange device prototype.

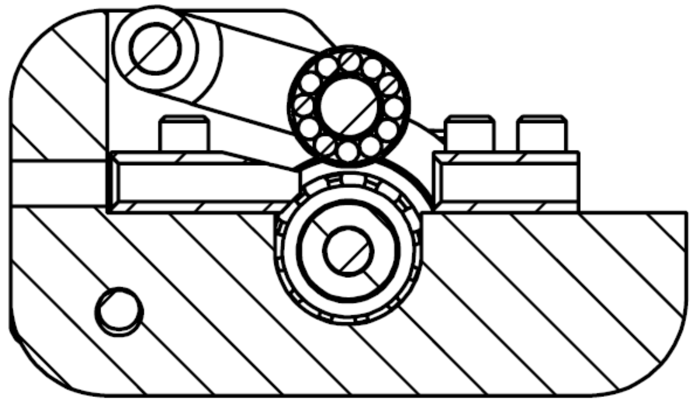

Figure 41. Section view of the rapid-exchange device prototype.

4.5 Hardware Design Summary

Multiple design iterations were conducted to develop a satisfactory functional prototype of the device based around a rotary encoder measurement method. The prototype device testing and results are discussed in Chapter 8. The key design concept centered around using an idler bearing that applied a normal force to the guidewire as it rolls over an encoder shaft. The force ensured continuous contact with the encoder shaft. The guidewire was supported by guides immediately before and after the bearing and shaft to support the wire and prevent buckling. The encoder shaft was supported by two radial bearings to prevent loading of the mechanical internals of the encoder.

In the rapid exchange variant the encoder measured the movement of the catheter and fixed the guidewire to the device. In the over-the-wire variant the encoder measured the movement of the guidewire and was fixed to the proximal Luer fitting of the catheter. Both devices provided a method to measure the relative motion between the catheter and the guidewire. The use of the devices in conjunction with the software side of the project is discussed in Chapter 7 and the measurement capability of the devices is discussed in Chapter 8

Chapter 5: Sensors, Electrical Design, and Integration with Software

This chapter covers the use of electronics, microcontrollers, and software to convert the mechanical movement of the guidewire to a numerical, linear displacement representation of the guidewire motion. The motion of the guidewire was tracked by the rotation of the shaft of a quadrature rotary encoder. The encoder had two channels, A and B, that were offset at 90 degrees phase to allow for determination of directional rotation. The encoder output high and low states from the two channels and that signal was interpreted by logic programmed into a microcontroller chip. The microcontroller sent the interpreted information to a computer running a program that interpreted the information and used it to display a graphical representation to the user. In this case, a MATLAB script displayed the user interface representing the relative locations of the catheter and guidewire with the information from the microcontroller. This chapter will cover the sensors used, the electrical wiring, the Arduino microcontroller prototyping board, and the MATLAB code that interfaces with the Arduino.

5.1 Sensors

Both of the prototype devices used the same sensor (Bournes ES14 Rotary Optical Encoder, P/N ES14A0D-E28-L064N) connected to an Arduino Uno microcontroller prototyping board. The rotary encoder provided a resolution of 64 pulses per revolution with 2-bit quadrature. This provided for the ability to measure clockwise and counter clockwise rotation of the encoder. Additionally with a total of four signal rise or falls per tick the sensor measured 256 pulses per revolution. The microcontroller interfaced with a computer running a MATLAB program through serial communication over the USB port as seen in the diagram in Figure 42.

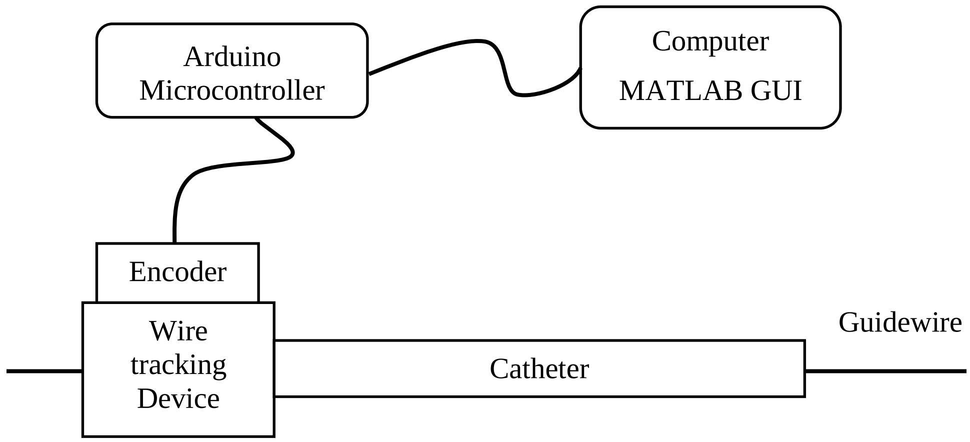

Figure 42. Schematic of connections between device and computer graphical output with an over the wire type device as an example.

5.2 Electrical

The encoder power and ground were connected to the 5v and ground of the Arduino. The data channels were connected to the two interrupt pins of the Arduino. Interrupt pins execute an action each time they are triggered and provide the fastest response rate the Arduino is capable of tracking as it will override other code execution to process the interrupt pin input. Pin 2 of the Arduino was connected to the A channel of the encoder. Pin 3 of the Arduino was connected to the B channel of the encoder. The encoder power was connected to the 5V supply from the Arduino and the Ground of the encoder was connected to one of the ground pins on the Arduino. The wiring of the device is shown in Figure 43.

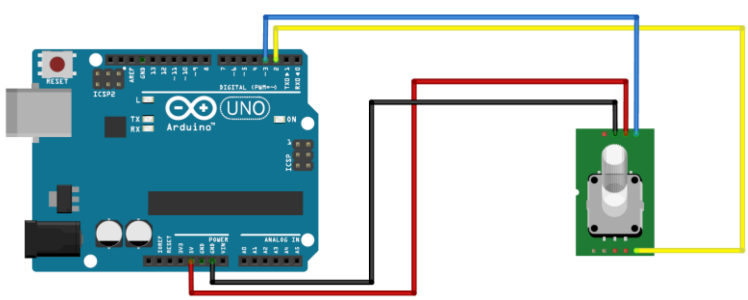

Figure 43. Diagram of Arduino and Encoder wiring.

5.3 Integration

The system required communication between multiple components. The Arduino read the information directly from the encoder and stored a count of directional encoder pulses. That count was passed from the Arduino to the MATLAB code, via serial communication through a USB cable, which used the information to display to the user the relative positions of the guidewire and catheter.

5.4 Arduino Code

The software running on the Arduino tracked the cumulative "ticks" of the encoder. A forward tick was added to the counter, a backwards tick was subtracted from the counter. The total number of ticks was output, on request, to the MATLAB script. The total motion of the measured device was calculated from the number of ticks, the ticks per revolution, and the diameter of the encoder shaft surface.

$$displacement = \frac{\#ticks\ counted}{256} * \pi D$$

The prototype devices used a shaft that with a nominal diameter of 0.25 inches. The shaft was measured to have a diameter of 0.2495 inches with a micrometer. This resulted in a displacement resolution capability of a single tick of the encoder corresponding to a movement of 0.00296 inches (0.0752mm). The higher precision the fabrication of the shaft and the smaller the shaft used for the encoder the more accurate the device can be. Additionally the device can be calibrated to handle the bias error that is introduced with a diameter that does not match the expected value.

Communication between the Arduino and the MATLAB script was handled over the serial port. On start up the MATLAB and Arduino performed a "handshake" to confirm that both are operational. The MATLAB code that the Arduino interfaces with dictated the rate of information transfer. MATLAB sent an ‘x’ character to the Arduino requesting the current encoder tick count. The Arduino then responded by printing the current value to the serial port. The MATLAB script could also reset the current encoder count, effectively zeroing the relative displacement, by sending the character ‘r’. The Arduino code is attached in Appendix A and the MATLAB script governing the communication with the Arduino and the user interface can be found in Appendix B.

5.5 MATLAB Code

MATLAB provided a convenient method to interact with external hardware, data processing, and basic graphical user interface (GUI) development for this project. Scripts and functions written in MATLAB implemented the software functionality for this project. The MATLAB scripts communicated with the Arduino microcontroller to get the current position measurement. Data recorded from the guidewire placement was exported from MediGuide and imported into the MATLAB program. The MATLAB program processed the imported data and used it to display, through a GUI, the current position of the guidewire and catheter

5.5.1 Arduino Communication

The Arduino was connected to the computer via a USB cable and communication was conducted through the serial protocol. Communication from MATLAB to the Arduino was carried out through sending characters. The function *arduinoSetup(comPort)* took input of a string indicating the computer communication port, ‘COM3’ is typical. It created a serial object at a specified Baud Rate and then initialized the connection. The code then paused for five seconds to allow the Arduino to start up. MATLAB would then send the character “a” to tell the Arduino it is ready to start.

The Arduino setup loop defined the pin connections and sets the pins to interrupt on changes. This allowed the encoder pulses to trigger various functions any time either the A or B channel initiates a pulse. The setup loop then initiated a while loop where it continually checks the serial input. If it received a serial input character “a” from MATLAB, indicating that MATLAB is ready to start, it exits the setup loop and begins the main loop of the code.

The main loop of the code continuously read from the serial input. If it received a character “x” it printed the current encoder count to the serial output. If it received a character “r” it reset the encoder count to zero. Meanwhile any pulse from the encoder triggered the interrupt routines which increment or decrement the encoder cumulative tick count dependent on the direction of motion. As mentioned, the Arduino code is attached in Appendix A.

5.5.2 Graphical User Interface

The graphical user interface (GUI) provided the connection between the operators and the sensing device. It displayed to the user the relevant information about where the guidewire and catheter was placed in the patient. This information was split into three panels in the display as shown in Figure 44. On the left panel the relative location of the catheter tip distance from the tip of the guidewire was shown and plotted over time. This distance was the distance along the guidewire the catheter would have to track as it is advanced with the wire pinned to reach the end of the guidewire. The function of this plot was to track the movements the clinician makes with the catheter. The middle panel plotted the predicted path of the guidewire, shown as the thin blue line. The catheter was assumed to follow directly on top of the path of the guidewire, shown here with the dark blue line and circle representing the tip of the catheter. The rightmost panel contained a numerical readout of the current distance from the tip of the guidewire and the buttons to control the display. The “Reset” button set the distance from the catheter to the guidewire tip to zero. The “Show Map” button displayed or hides the 3D map panel. The insert landmark buttons did nothing in this implementation but represent the process necessary when using the MediGuide system during the initial guidewire placement.

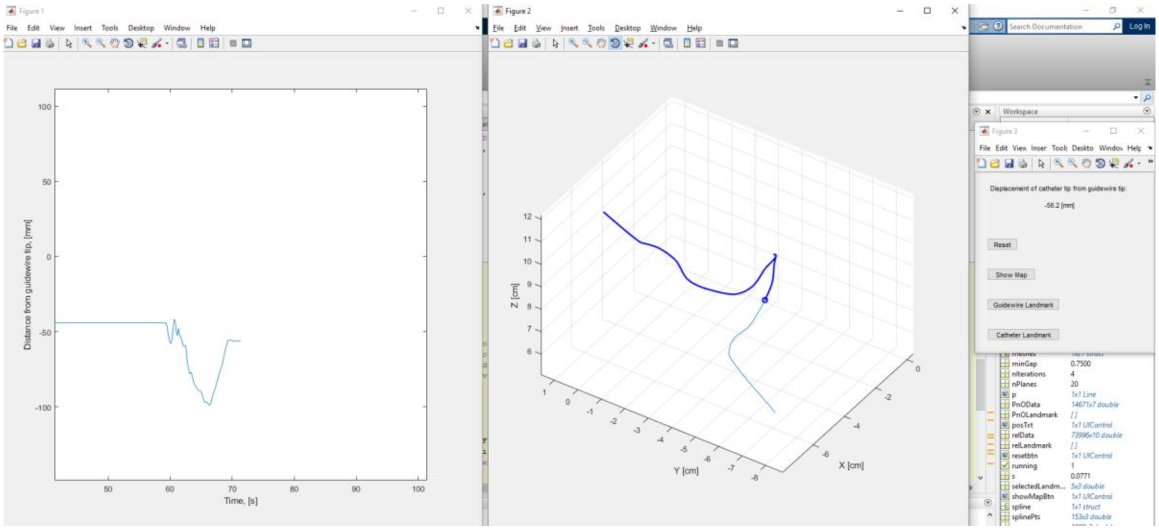

Figure 44. The graphical user interface in MATLAB displays the information relevant to the clinician.

At this stage of the project the user interface runs independently and parallel to the MediGuide system. This provides additional information to the user about the position of the catheter and guidewire. Future work to integrate the concepts here into an overlay of information on top of a fluoroscopy cine loop would be more advantageous. This will be further discussed in Chapter 9.

5.6 Sensors, Electrical, and Software Summary

The device prototype used a rotary encoder, Arduino microcontroller, and MATLAB software to implement the measurement methodology. The encoder was wired to the interrupt pins of the Arduino microcontroller. The Arduino used a quadrature encoder reading implementation that detected rising and falling peaks in both encoder channels. This provided both directional information and a sensor resolution of 256 ticks/revolution. Arduino software kept track of the cumulative sum of ticks in the forward and backwards direction. Forward movement was represented as an increment and backwards as a decrement of the total number.

Communication between the Arduino and MATLAB was handled by a serial communication protocol. On startup the two systems provided a confirmation of connection and function before entering the main loop. While running, the MATLAB code requested the current value from the Arduino and the Arduino responded with the current count. The MATLAB code could also send a signal to the Arduino to reset the displacement count to zero.

The MATLAB script used the data acquired from the sensor and microcontroller system to display a graphical interface to the user. One panel of the user interface displayed a scrolling tracker of the catheter-guidewire relative motion. This provided the user with information that the device is working and to evaluate the relative change in motion as a catheter and guidewire system was advanced or retracted. A second panel of the interface displayed a 3D map of the calculated guidewire trajectory and the current catheter placement overlaid onto that trajectory.

Chapter 6: Guidewire Data Processing

The next aspect of the project was to combine the hardware and electronics systems developed with software representing the location of the guidewire and catheter. This chapter discusses the processing of sensor enabled guidewire information to develop a predicted path of the guidewire. This path represents the location of the guidewire in 3D space based on the recorded spatial positions of the guidewire sensor during the procedure. The set of position coordinates from the MediGuide system was filtered based on frequency response, key “landmark” points in the data file were indicated by the user during guidewire placement, a predicted guidewire position was determined for the set of data points by an energy minimization fit algorithm. The position of the guidewire determined by the algorithm was used to display to the clinicians the location of the guidewire and the location of the catheter along the guidewire, in tandem to the existing MediGuide imaging modalities.

The scope of the project limited the amount of integration with the existing MediGuide system. Instead of directly interfacing with the MediGuide, for this project a software prototype was intended to run as a secondary system concurrent with a MediGuide procedure as a proof of concept. However there was still a need to transfer information recorded from the guidewire position sensor to the proof-of-concept system. The data output from the MediGuide was in two forms: Relative data and Position and Orientation data (PnO). Relative data contained 3-D coordinates of the MediGuide sensor position over time transformed to the coordinate system of a patient. A patient undergoing a procedure with MediGuide has a reference sensor (PRS) placed on their chest that provides an origin coordinate system for the data. The MediGuide system records the position of the devices relative to the imaging angulation and then transformed the data into the coordinate system of the PRS. Relative data did not contain the orientation information of the sensor. PnO data contained both the position and orientation of the sensor in 3D in the coordinate system of the C-Arm angulation.

The information from the MediGuide sensor enabled guidewire was used to generate a predicted path of the guidewire. The recorded spatial coordinates of the guidewire tip traced an outline of the vasculature that the tip traveled through. These data were used to predict the path of the guidewire. The data sets used to develop the method are discussed in section “6.1 Data Examples”. The data was processed to reduce noise in the signal as discussed in section “6.2 Data Filtering”. The method of determining a representation of the guidewire is discussed in section “6.3 Guidewire Path Fitting”.

6.1 Data Examples

Two datasets were provided for this project as a starting point to develop necessary software and algorithms for the system. The datasets were derived from recorded clinical procedures. The first was a recorded access of the right coronary artery (RCA). The second dataset was a recorded accesses two sides of a bifurcation in the left anterior descending artery (LAD). Figure 45 illustrates the locations of the arteries relative to the heart as a whole. Figure 46 and Figure 47 contain plots of the relative data files.

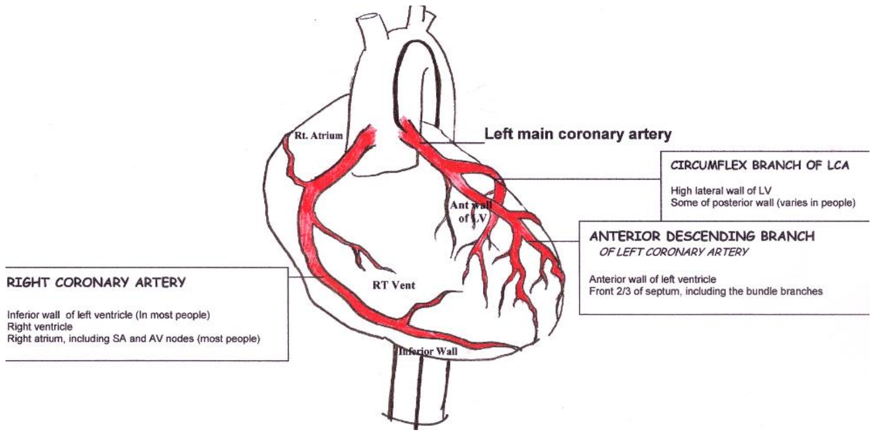

Figure 45. Illustration of the procedure that produced the example data guidewire path. [4]

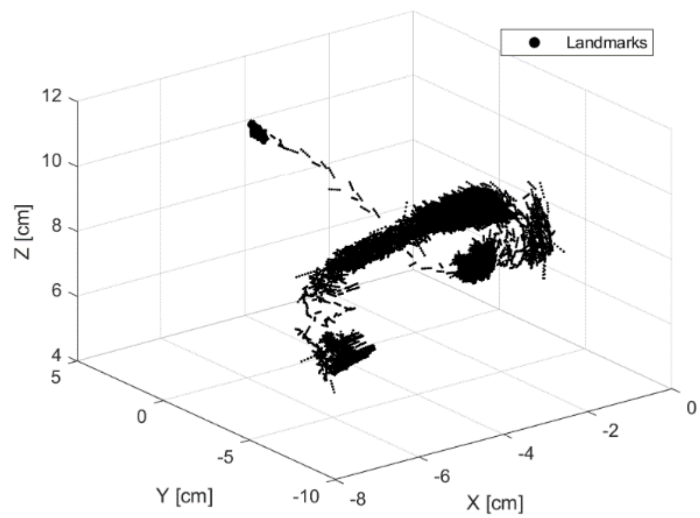

Figure 46. 3D scatter plot of relative position data for right coronary access.

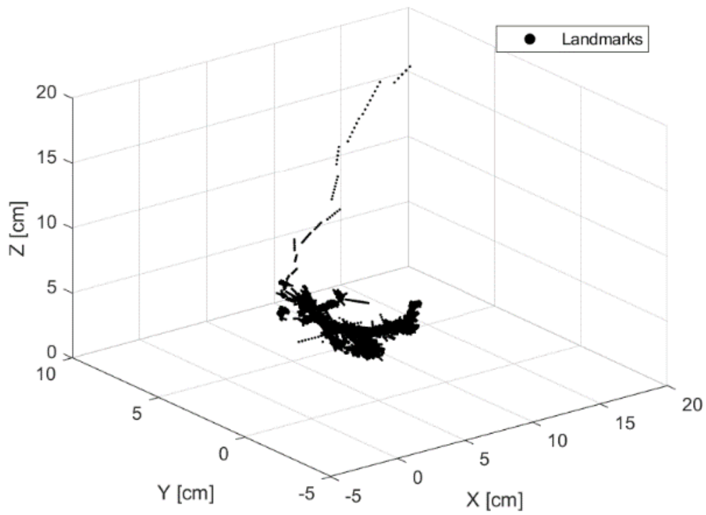

Figure 47. 3D scatter plot of relative position data for left anterior descending and circumflex access.

Additionally datasets were collected in an Abbott catheter intervention laboratory from benchtop models. These models utilized simplified geometry (curve, helix, and plastic coronary phantom) to provide data with reduced noise to assist development. Figure 48 through Figure 50 demonstrate the plots of these datasets.

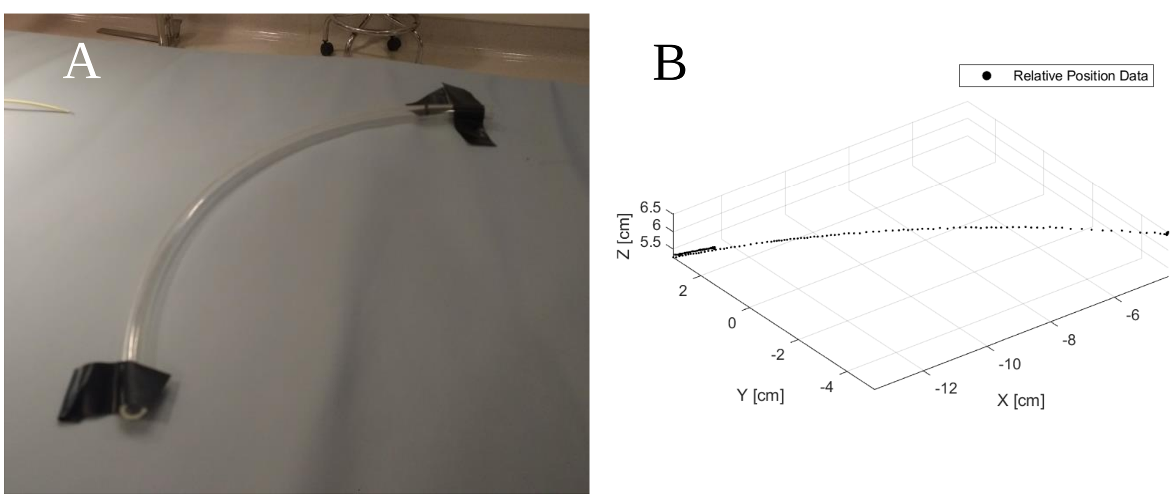

Figure 48. (A) Curve model and (B) dataset collected.

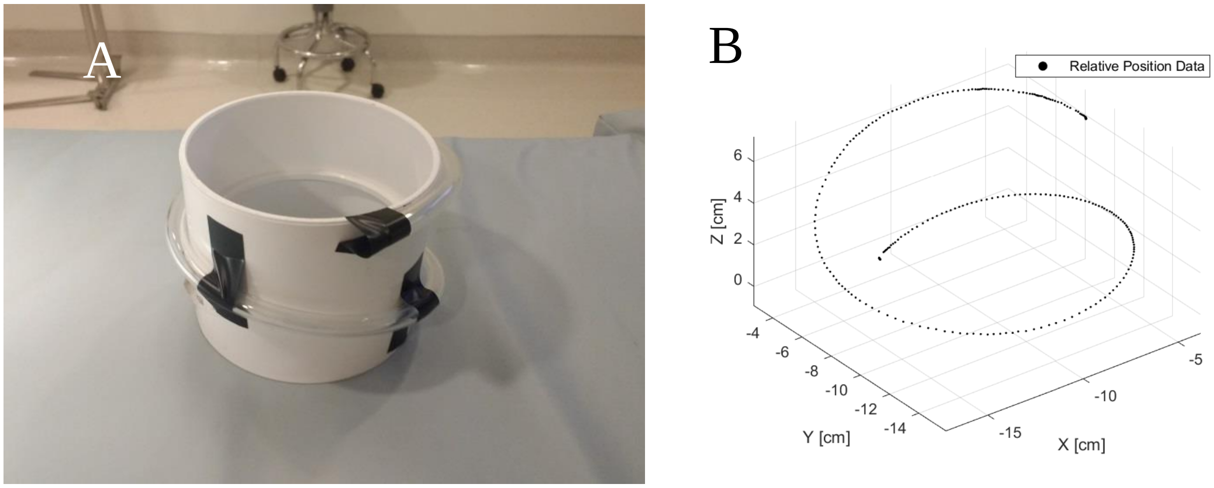

Figure 49. (A) Spiral model and (B) dataset collected

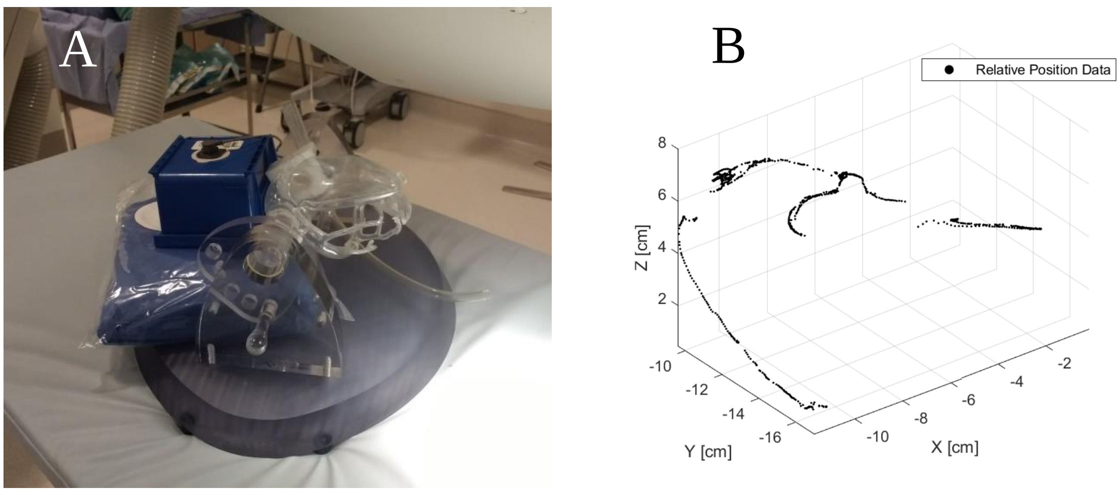

Figure 50. (A) Coronary model and (B) dataset collected

6.2 Data Filtering

The data derived from clinical use needed to be pre-processed before it could be used for determining a guidewire path. The data contained a significant amount of motion that did not represent the path traveled by the guidewire tip. This motion resulted from cardiac motion, respiratory motion, and electrical noise. Additionally, anytime there was a poor connection somewhere between the sensor and the tracking system, zeros were input into the position recording. These zero points were removed to avoid data errors. Figure 51 shows the X, Y, and Z position coordinate channels over time for the RCA dataset.

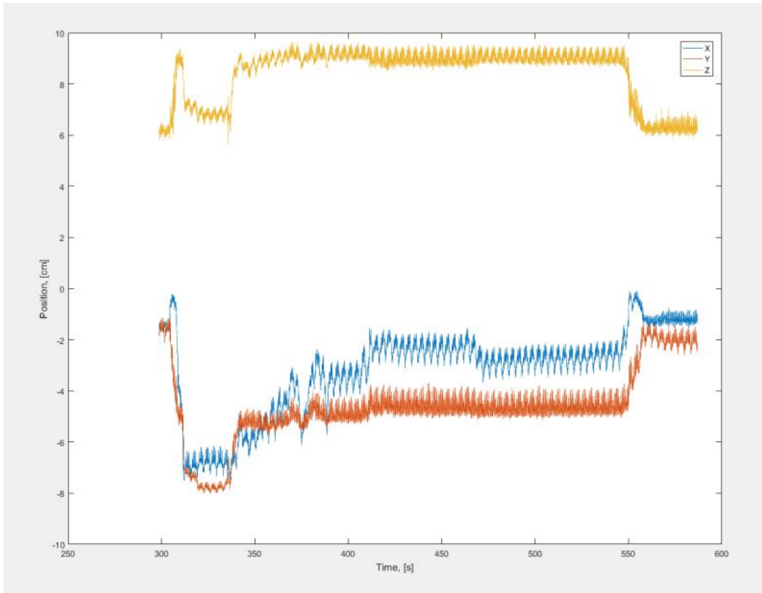

Figure 51. Three dimensional components of the relative guidewire tip location during right coronary access.

A lowpass Chebyshev Type II filter was chosen to smooth variations in the data. The variations are the result of noise, cardiac motion, and respiratory motion. The Chebyshev Type II filter was chosen as it minimizes the passband ripple where preservation of as much of the recorded signal as possible is desired. The filter was designed with the passband at 30 Hz, passband attenuation of 1 dB, the stopband at 40 Hz, and a stopband attenuation of 20 dB. The magnitude response plot of the filter is shown in Figure 52. The same filter was applied to each of the data channels independently. The results of the smoothing function and the relative data are shown in Figure 53.

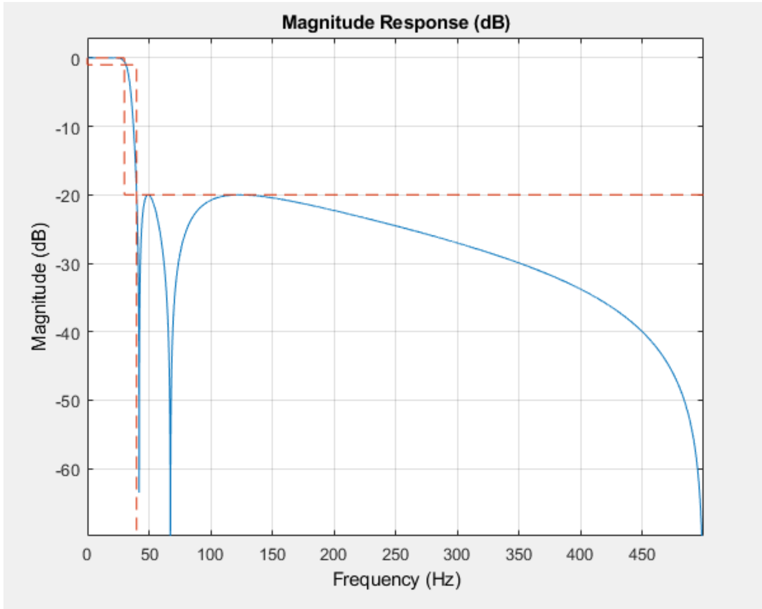

Figure 52. The magnitude response plot of the smoothing filter applied to the datasets.

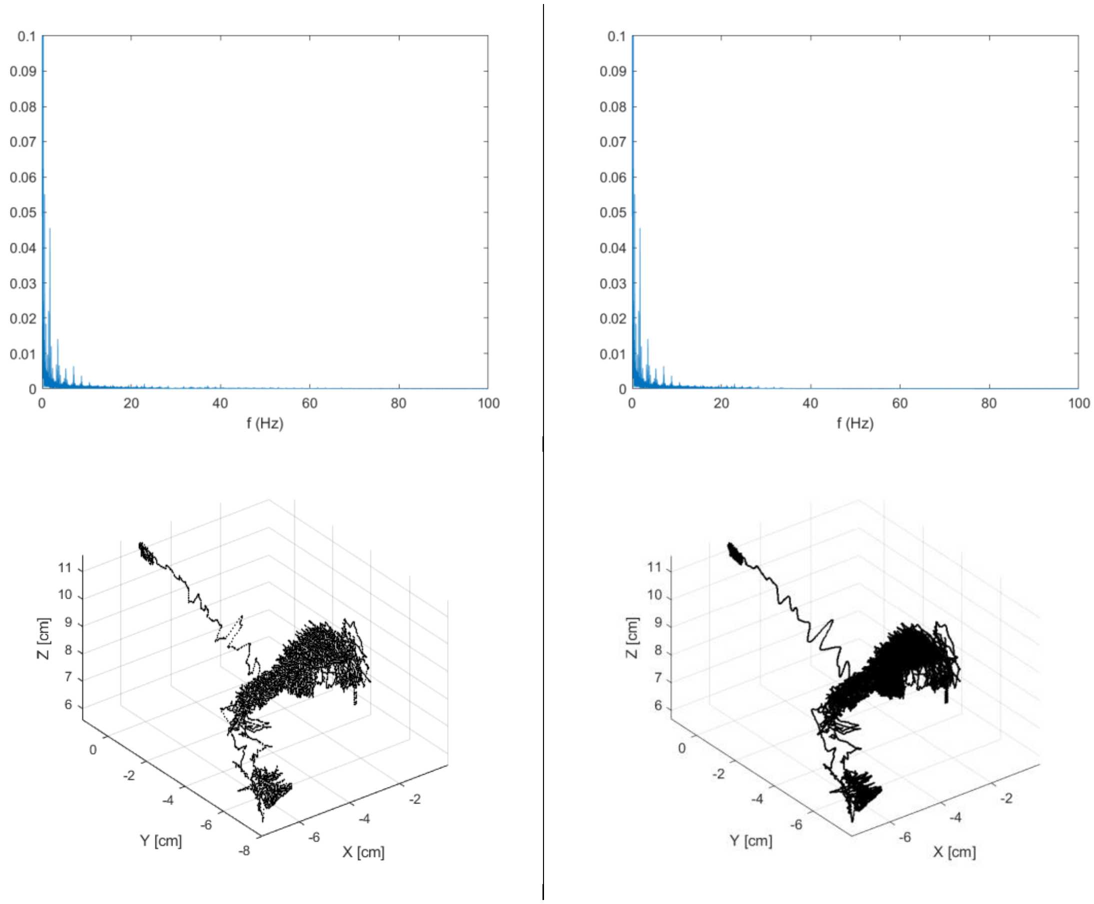

Unfiltered Data Filtered Data

Figure 53. Spectral density plot of the unfiltered X channel data. Filtered spectral intensity plot of the filtered X channel data. Unfiltered scatter plot of the RCA access provided data file. Filtered scatter plot of the RCA access provided data file

Another technique investigated in this project was the use of the orientation information in the PnO data files. An attempt was made to isolate the advancing and retracting motion of the guidewire from the cardiac and respiratory motion by determining when movement of the guidewire was orthogonal to the sensor orientation. This method was not used for the guidewire trajectory fitting algorithm but is addressed further in Chapter 9.

6.3 Guidewire Path Fitting

The determination of the trajectory of the guidewire was critical in conveying information to the clinician on the placement of the catheter tip relative to the guidewire tip. The guidewire tip contains the MediGuide sensor and the position of the guidewire tip is displayed by being overlaid onto the fluoroscopy cine loop. However, any section of the guidewire proximal to the sensor tip is invisible to the MediGuide magnetic navigation system. The prototype device system calculated a known displacement. In combination with a known trajectory of the wire, the relative displacement of the two devices was used to display the location of the catheter tip along the guidewire.

There are multiple aspects of the recorded position data that presented a challenge to determining a guidewire path. In the previously discussed literature from Chapter 2 some information about the boundaries of a possible guidewire path are known. In this implementation there was no prior assumption of any known path information except for a few locations where MediGuide landmarks have been placed. Some methods to address this limit would be to acquire a preoperative scan or intraoperative procedure to generate a map of the coronary artery tree. The first of the challenges of determining a path with the assumption of no known boundary information was the difficulty in cannulating an access point. A significant amount of time was spent at the entrance to a bifurcation as the clinician attempts to enter with the tip of the guidewire in the provided data sets. This resulted in large clusters of data points surrounding the access points or anywhere that the guidewire stayed still for an extended period of time. Conversely, the density of recorded position locations was much lower in sections of anatomy that were easier to traverse. Bifurcations add the complication that the final path of the guidewire did not depend on every section of recorded data as only one branch represented the current location of the wire.

The method discussed here is limited in scope to the capabilities of working in a capacity without integrating with any live data in the MediGuide system. Instead access was achieved, the guidewire was left in place, and the recorded data was exported from MediGuide and imported into the secondary computer system. MediGuide has the ability to place “Landmarks” into the data file that is exported. These landmarks mark the locations of significant anatomical markers such as the entry to arteries or other indicators. The implementation here required that landmarks the guidewire passes through be selected by the user. The results of this implementation showed that the placement and selection of landmarks has a significant effect on the resultant guidewire path. It is recommended that landmarks be placed at each bifurcation and the end of each branch. This placement allowed for the selection of landmarks that best generate a guidewire path. Future work of interest would be to automate bifurcation detection and landmark selection to allow the system to function with minimal user intervention. This will be discussed further in Chapter 9.

After the selection of initial landmarks to determine an initial path, the next challenge was determination of the optimal guidewire path. The implementation here used an energy minimization approach. The path that the guidewire takes was represented by the path that placed the wire in the lowest bending energy configuration. This means that sharp bends and high curvatures were limited and the path was optimized to provide the lowest energy for an estimated set of bounding conditions that are based on the input dataset of guidewire tip positions. This challenge was different from the literature previously discussed because it was done without the known boundary conditions from a preoperative analysis. Figure 54 outlines the procedure steps taken to achieve this result.

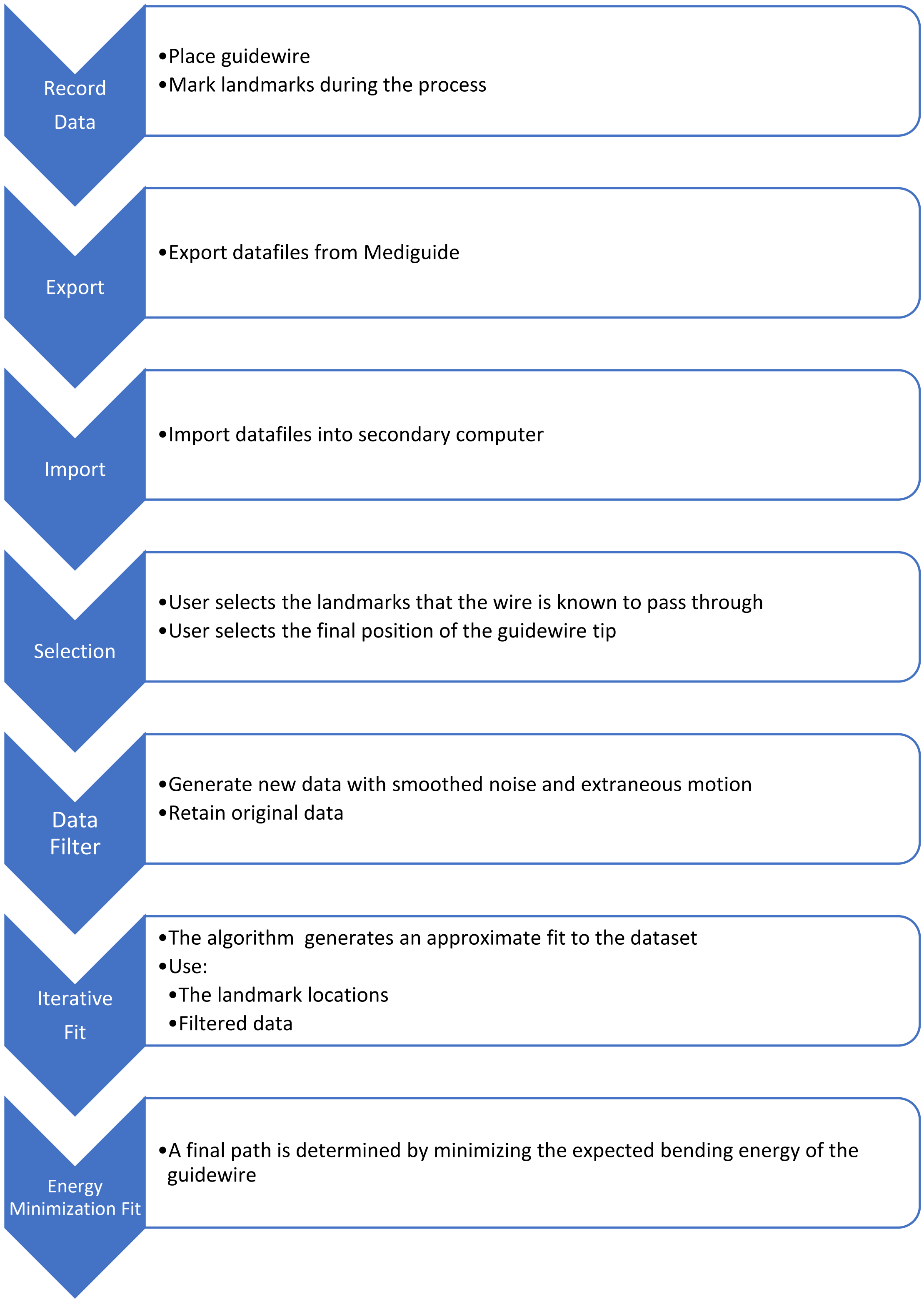

Figure 54. Diagram of the algorithm procedure to determine the optimal guidewire path.

6.3.1 Landmark Placement

Landmark markers were placed during the advancement and placement of the guidewire. The MediGuide system provides markers to mark specific anatomical locations but the landmarks can be used as needed. On export, the landmark was represented as a timestamp which can be correlated to a position in the relative or PnO dataset. Figure 55 and Figure 56 show the placement of a landmark from the MediGuide system.

Figure 55. Biplane MediGuide display of the placement of a landmark in the distal portion of an artery in a coronary phantom.

Figure 56. Biplane MediGuide display of the placement of a landmark with multiple other landmarks displayed.

6.3.2 Export and Import

The recorded position data was exported from the MediGuide system and imported into the secondary computer. The secondary computer matched the timestamps from the Landmarks to positions in the relative data. The display of relative data and landmark positions is shown in Figure 57. The data here appeared much smoother and with lower variation than the data shown previously because it was recorded from a fully static phantom, not a live subject. This resulted in significantly less variation in the data. The next set of examples all use data recorded from the plastic coronary artery model as shown in Figure 50. However, the same process can be applied to any of the datasets.

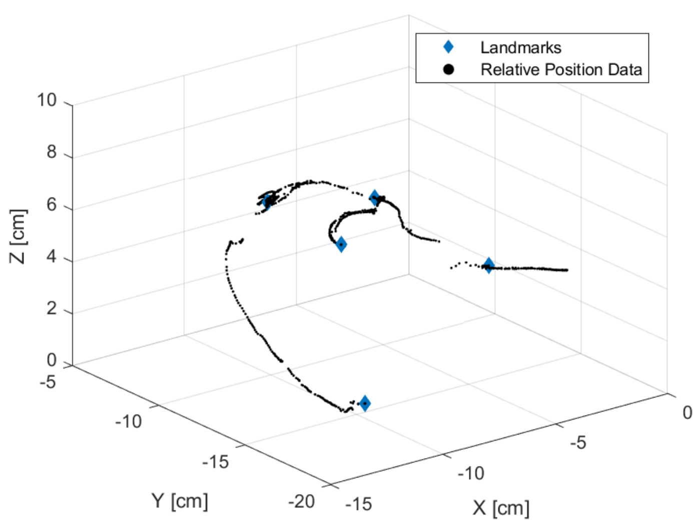

Figure 57. Plot of relative data with marked landmark locations at significant bifurcations and distal ends of the arteries.

The next step in the process was for the user to select the landmarks of interest in the order that the guidewire would pass through them. The user selected the most proximal point first, the next most proximal landmark (most likely at a bifurcation), and the final position of the guidewire tip. The landmark locations selected by the user were passed into the algorithm, discussed in sections 6.3.3 and 6.3.4, with the recorded data to generate a guidewire path.

6.3.3 Initial Spline Fit Algorithm

The software then fit an initial cubic piecewise polynomial spline between the selected landmark points. This initial spline was iterated to generate a fit close to the data points. This step was necessary because although time dependent data is provided in the recording, the aspect of interest is the spatial representation of the artery anatomy. During the placement of the guidewire there was backtracking over previously covered paths, and clustering of data resulting from attempts to cannulate different arteries. This is represented at the clusters of data points visible at the bifurcation landmarks. The results of this spline fit are shown in Figure 58. The code for the fit of the guidewire path can be found in Appendix C.

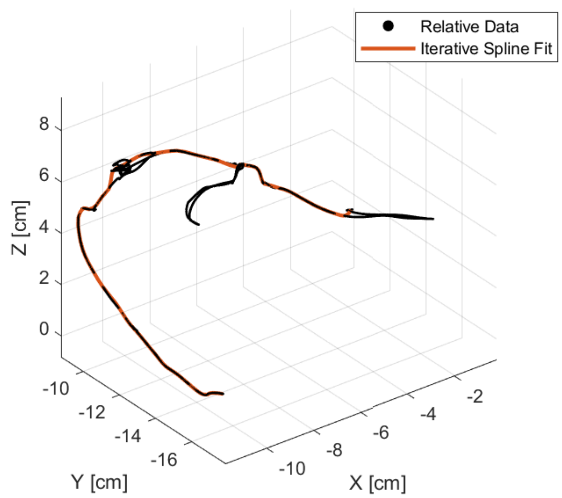

Figure 58. Relative data with spline fit to one of the artery branches.

6.3.4 Initial Spline Fit Algorithm Steps

The spline fit algorithm takes the initial spline fit and iterated on it to improve the fit and place the final fit closer to the dataset. In the initial spline fit each landmark was input as a point from which to generate the spline. The output spline function was then divided into sections half way between each landmark point used to build the previous iteration. A vector is drawn from the i-th build point to the i+1-th data point. Two planes normal the vector were placed with one passing through each point. All data points contained between these two planes were set as included data points for the next step. Then from the set of included data points, the data point closest to the point along the vector and halfway between the planes was selected to be part of the next set of points from which to build the spline. This process was repeated for each set of build points and each number of spline fit iterations until no points remain further apart then a defined minimum spacing or the number of algorithm iterations defined is reached. The results of the fitting algorithm are demonstrated in Figure 59.

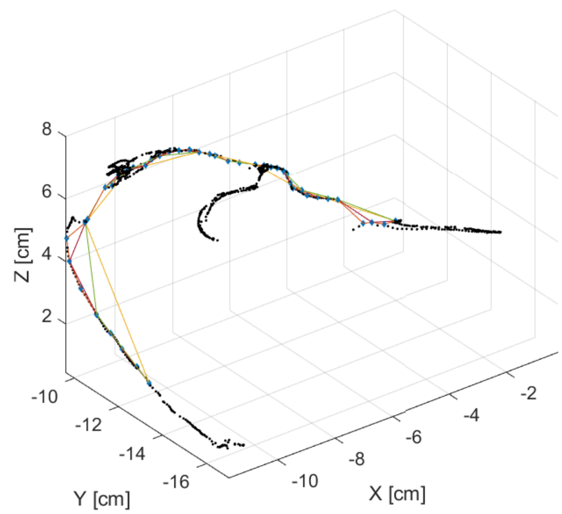

Figure 59. Example of each step in the initial spline fit iteration algorithm. The initial fit landmarks are shown in yellow and as the algorithm iterates it draws closer to the data set values. The final set of points used to build the piecewise cubic spline are shown as the blue diamonds.

<u>6.3.5 Graph Theory Implementation</u>

Graph theory provides an efficient method of determining the path of a guidewire through a known geometry. The method can be adjusted for guidewires of varying stiffness by adapting the calculation of the bending energy. [29] Graph theory represents data as nodes and edges between the nodes. Edges can be given values described as weights and can be defined to be directional or not. Algorithms have been developed to determine properties of graphs such as the shortest path from any node to any other, the set which is called the minimum spanning tree.

The implementation of a graph theory approach to determining guidewire locations through a known geometry optimizes the path by minimizing the total bending energy calculated for all segments of the guidewire. A confining geometry for the guidewire was defined by planes normal to the direction of the lumen. On each of these planes a set of spatial points were selected to create a planar mesh. Vectors were drawn from each point on each plane to the subsequent plane as illustrated in Figure 60.

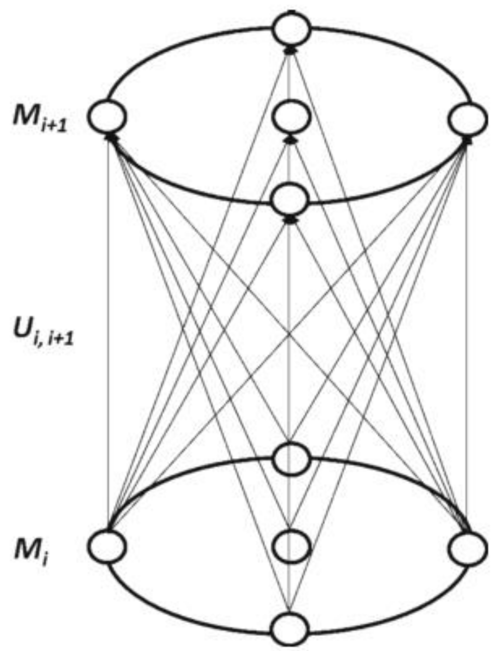

Figure 60. Creation of vector set $U_{i,i+1}$ consisting of the vectors $u_{i,j,i+1,k}$ connecting all points in two subsequent meshes, M_i and M_{i+1}.
[29]

Each of the vectors was treated as a "node" in the final graph. The edges connecting the vectors were set to be between each of the vectors (nodes) that share a common mesh point. Edge weights were calculated based on a representation of the bending energy of the guidewire which is a function of the guidewire properties (elastic modulus: E, second moment of area: I), the bend angle between the two vectors (θ), a bend energy scale parameter (α) and the distance spanned by the vectors.

$$\theta = \mathrm{acos}\left(\frac{u_{i,j,i+1,k} \cdot u_{i+1,k,i+2,1}}{|u_{i,j,i+1,k}| + |u_{i+1,k,i+2,1}|}\right) \qquad (1)\ [29]$$

$$Edge\ Weight = \frac{EI\theta^{\alpha}}{2 * |u_{i,j,i+1,k} + u_{i+1,k,i+2,1}|} \qquad (2)\ [29]$$

The elastic modulus was assumed to be 200 GPa for a steel wire, and α was set as 2 to compare to Hooke's law. [29] This edge weight was calculated for all edges in the graph. The graph was constructed with the built-in functions of the MATLAB graph functions to generate a graph object from a list of edges and edge weights. Then MATLAB's shortest path algorithm was applied from the first to last nodes. The output of shortest path is registered to points in 3D space saved during the graph construction to determine the spatial mesh points that the guidewire must pass through. The resulting guidewire fit is constructed as a cubic interpolating spline through the mesh points. As mentioned, the code for the graph theory fit can be found in Appendix C.

6.3.5.1 Mesh Plane Construction

The initial spline fit to the data points was used to determine where to attempt to build the mesh planes for the graph theory fit algorithm. The spline was divided into equal segments dependent on the desired number of planes. Increasing number of planes will improve the fit of the guidewire as it will be more tightly constrained to the data. However, increasing the number of planes will non-linearly increase the time for the algorithm to run. A set of twenty planes has been found to complete calculations relatively quickly while still providing reasonable results. [29]

The recorded data points between each segment of the divided up initial spline fit were found with the same method as used in the iterative spline fit. These points were projected onto a plane normal to the vector drawn between the two segment points on the spline. In the projected plane, a circle was drawn based on the point positions. The center of the circle was placed at the mean of the projected data points; the radius of the circle was calculated as the average of the maximum spread in each coordinate direction. The radius was bounded to a maximum of 2.5mm and a minimum of 0.5mm based on the reasonable range of coronary anatomy. [33]

On the circle drawn in the plane, points were selected to be used to build the vectors for the graph theory minimization. The number of points around the circle was variable, but will increase the calculation time of the algorithm non-linearly similar to the number of planes. The center point of the circle was also used to build the mesh plane.

The points were projected back into 3D space and translated to the section of the spline segment they were originally projected from. Figure 61 shows the construction of the mesh planes

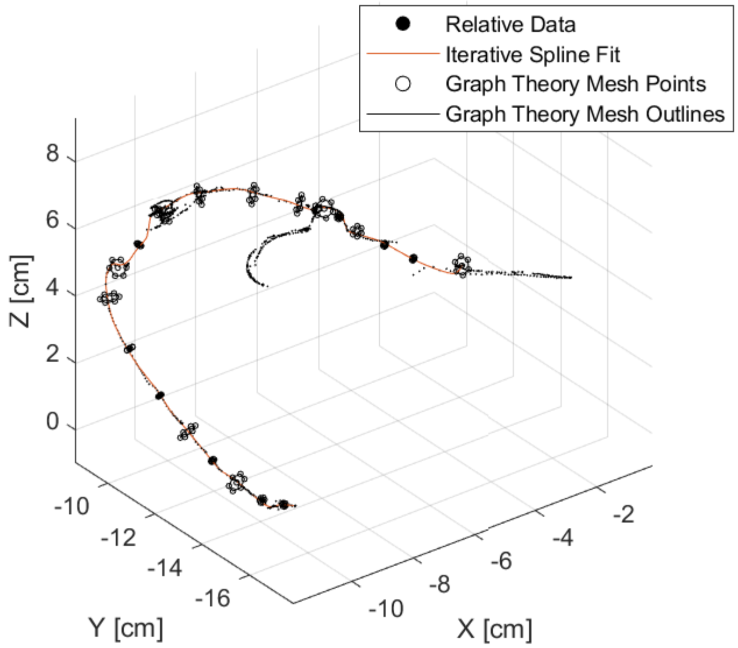

Figure 61. Representation of graph theory meshes derived from placement along the iterative spline fit.

6.3.5.2 Node List Construction

In a graph construction, a node list is a list of all the indices of the nodes of the graph. In this case it was all the vectors between the mesh points. To generate a list of these vectors the program used nested loops starting at the first set of two mesh planes and calculates the difference between the first point in one plane and every point in the subsequent plane. This was repeated for all points in the first mesh plane. At the same time a list of spatial mesh points was co-registered to the same indices as the list of vectors generated for later use. This made it possible to use the output of vector indices from a shortest path calculation to relate to the points in 3D space.

6.3.5.3 Edge List Construction

In a graph construction, an edge list is an array of values indicating which indices of nodes are connected to other node indices. In this case it represented the vectors that share a common mesh point. This was constructed in the program through nested loops starting at the first set of two mesh planes, the first vector connecting those two planes, and adding all the vectors from each connected mesh point in the next set of mesh planes. This was repeated for every vector in the first mesh plane and then the whole process was repeated for the next set of mesh planes.

With the edge list completed weights were calculated between each edge. The edge list was formatted as an Nx2 matrix. Column 1 was the index of the first vector. Column 2 was the index of the second vector. These indices can be entered into a MATLAB structure array of vectors generated earlier. The angle between the two vectors was calculated as discussed previously in Equation 1. This angle was used with the parameters determined for E, I, and α to calculate and edge weight for each set of graph nodes. The edge weight represented the bending energy of that segment.

A tighter angle between the vectors resulted in a tighter bend in the guidewire and would have a correspondingly higher energy. The stiffer the guidewire, either through the influence of the elastic modulus or through the influence of the second moment of area, resulted in a higher bending energy. This was normalized to the span of the segment between the mesh planes. Mesh planes covering a larger distance would result in a lower energy than a tight bend over a short distance.

6.3.5.4 Graph Theory Energy Minimization

The edge list could be input into the built in MATLAB support for graph theory operations. The function *digraph(E)* takes an edge list as an input and is used here to generate a graph object with directionality as the guidewire cannot form loops with or back on itself. The function *shortestpath(G, s, t)* takes a graph object, the starting node index, and the ending node index. It outputs the indexes of the nodes, connected by edges through which the sum of edge weights is minimized. This resulted in a minimized bending energy position of the guidewire. These indexes could be referenced back to the list of spatial mesh points generated when the list of vectors was constructed. These were used to generate a new spline fit to represent the guidewire trajectory. The result of these operations is shown in Figure 62.

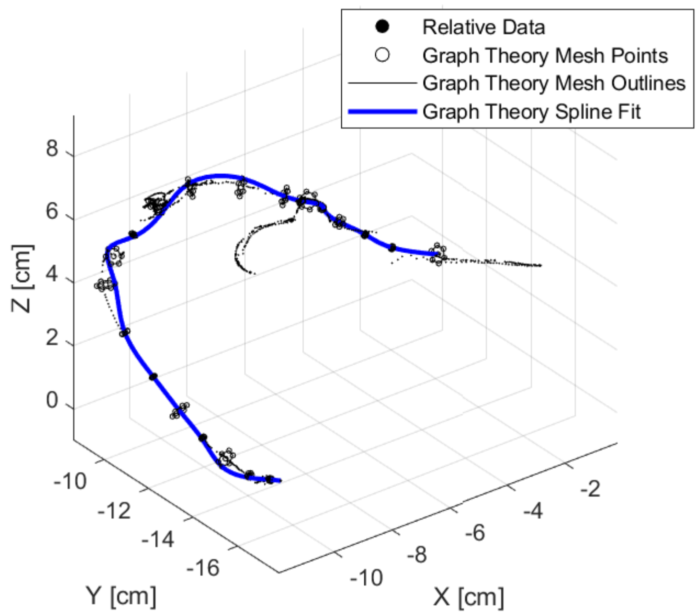

Figure 62. Representation of graph theory shortest path to minimize energy through the meshes.

6.4 Guidewire Data and Path Determination Summary

Determination of a path that represented the placement of the guidewire was a critical component of the project as it allows the user interface to represent the placement of the catheter relative to the guidewire tip in 3D space. The method developed here used the recorded data from the sensor in the distal tip of the guidewire in combination with a few marked locations to implement a fit of a guidewire with an energy minimization technique. Data from MediGuide was exported to MATLAB, landmark locations were indicated by the user, an initial fit was constructed to approximate the location and then an energy minimization fit was performed to represent the shape a guidewire would take within the restricted geometry of the vasculature. The next step was to combine the software developed with the previously discussed hardware into a proof-of-concept system as discussed in Chapter 7.

Chapter 7: System Integration and Use

The use of the prototype system integrates many different functional parts that must work in tandem with the process of an operator to achieve valid and relevant results. This chapter explains the process needed to use the device. The chapter will begin with an overview, and then will cover the set-up of the system, determination of the reference point, and use of the relative motion.

7.1 Overview

The prototype system involved the interactions of multiple components designed specifically for the proof of concept catheter localization system and the MediGuide system in its current state. The prototype device attached to the catheter and guidewire used in the MediGuide system. The MediGuide system used the sensor in the distal tip of the guidewire to track the position of the tool in 3D space. This information was displayed to the user as an overlay on a recorded fluoroscopy cine loop. The prototype system used data exported from the MediGuide system to display its own information relating the relative motion of the catheter and guidewire to the position of both tools in 3D. This was displayed as a 3D figure plotting the predicted guidewire trajectory and the catheter position along that trajectory. Eventually, development of this prototype into a clinical/commercial system would use the MediGuide data in realtime to not only display the sensor position at the tip of the guidewire but also a realtime-computed estimate of the guidewire trajectory and the relative position of the catheter tip and possibly also the catheter distal body. The schematic representation of the system is shown in Figure 63.

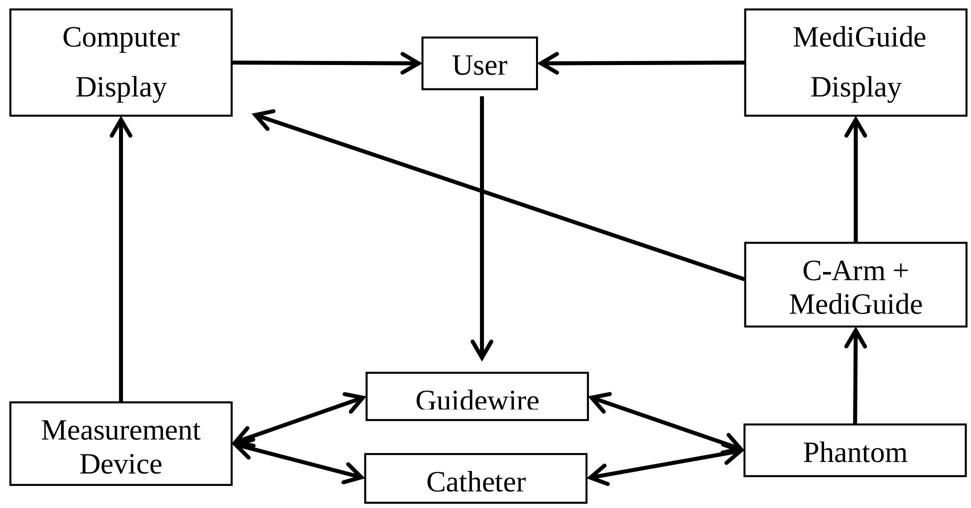

Figure 63. Diagram of the function of the prototype system as it functioned in this thesis project.

7.2 Reference Point Determination

In order to determine the relationship of the distal catheter tip and the distal guidewire tip a reference point needed to be set. This provided an initial location from which to calculate relative displacement for all following time points. In this implementation, fluoroscopy imaging was used to set an initial reference of zero displacement. The guidewire tip, indicated by a dot in the MediGuide overlay over the fluoroscopy image, was aligned with the tip of the catheter. Once in position the user selected the button in the MATLAB GUI to reset the displacement to zero. The user would then advance or retract the catheter and guidewire and the device would measure and display the relative position of the two tools.

7.3 Use of the System

The general process of using the system varied with the intended goals of the catheter localization. In some cases it might be advantageous to explore multiple branches of the vasculature to generate more data from which to build the guidewire fit simulation before exporting to the secondary computer. The process of using the prototype system is shown in Figure 64.

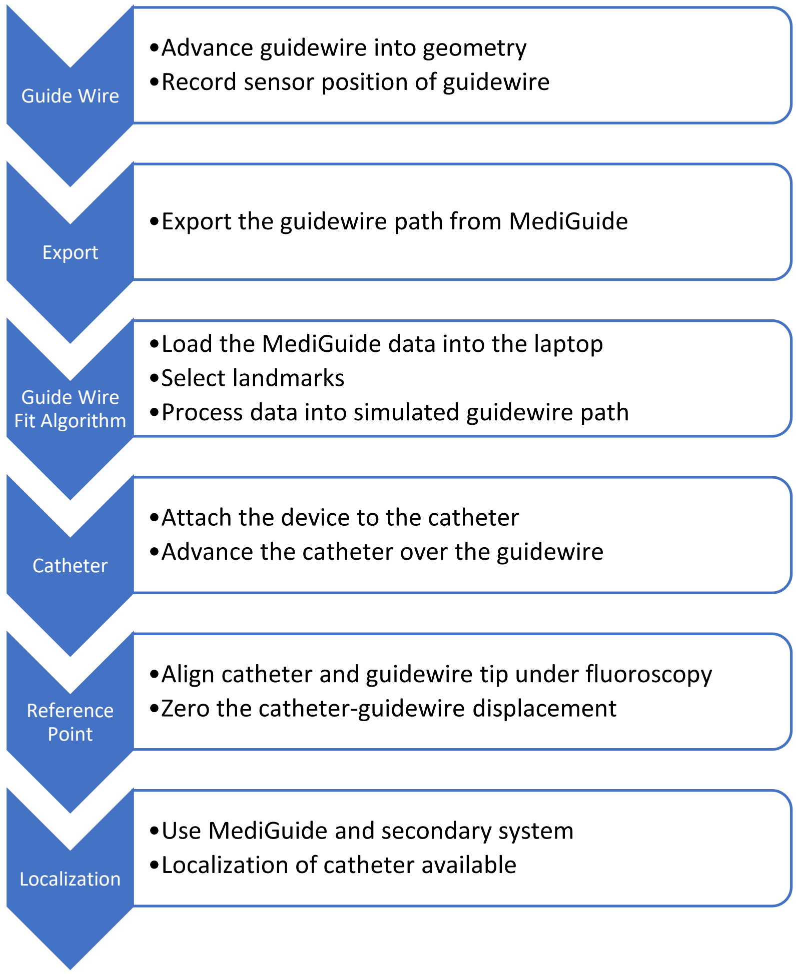

Figure 64. Process of using the prototype catheter localization system.

7.4 System Integration and Use Summary

The use of the prototype system involved the tracking of the placement of the guidewire with the MediGuide sensor and system. The recorded spatial positions of the guidewire as it was placed were exported to another computer. On the second computer the user selected the landmark locations of critical anatomical points and an algorithm generated a predicted path for the guidewire. A catheter and associated prototype measurement device was strung over the guidewire. A reference point for zero relative displacement was set by aligning the guidewire sensor with a radiopaque marker on the catheter under fluoroscopic imaging. The system can then be used by the operator to visualize the catheter displacement along the guidewire.

Overall the entire prototype system functionality has been explained in Chapter 4 through Chapter 7. The next step in the process was to conduct tests to evaluate the capabilities of the system for measurement accuracy and precision. These tests are explained in Chapter 8.

Chapter 8: Testing

This chapter discusses the testing conducted to evaluate the capabilities of the prototype system and determine the feasibility of implementation of the system a clinical environment. The accuracy and precision of the measurement device were tested to determine if they met the specifications outlined in Chapter 1. Additionally, the accuracy and precision of the device when used in a catheter lab were evaluated to quantify the additional complications of human operators and the process of using the device. As the work in this chapter will show, the measurement device was determined to be accurate to 0.7±0.03% (95% confidence) without a calibration of the device. With a calibration the measurement was expected to be 0.0±0.03% (95% confidence). When used in a catheter lab with fluoroscopic imaging in a method more similar to a clinical function the device measured displacement is expected to be -1.4±0.54mm (95% confidence) different than the actual displacement. The algorithm was evaluated by varying the parameters used for the execution of the process. A central composite design was used to generate a response surface of a response variable defining the fit quality and a response variable calculating the execution time for the algorithm. From this test an optimal set of parameters for the algorithm was determined. Details of the testing and analysis are explained through this chapter.

8.1 Device Testing

The over-the-wire device was tested to evaluate the measurement capability of the device. The device was clamped in the lower grip of an Instron 3342 test machine as shown in Figure 65.

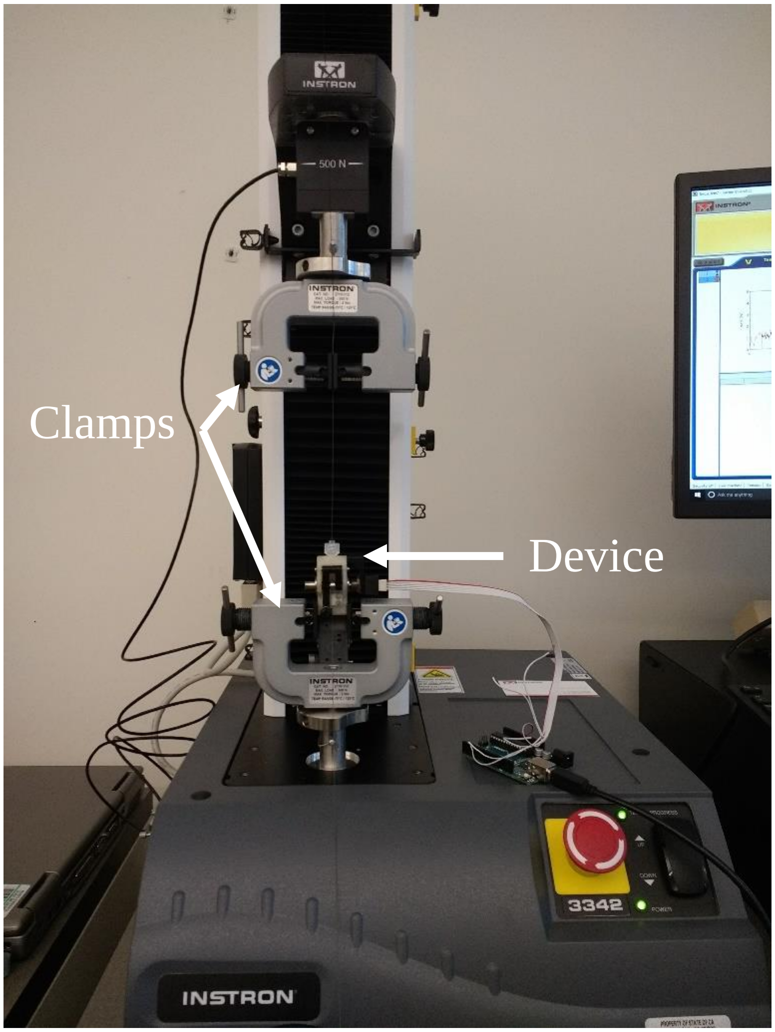

Figure 65. Testing set-up with the over-the-wire prototype device in the Instron 3342 test machine.

The measurement device was clamped in the lower grip of the Instron as shown in Figure 66. The guidewire was passed through the device and clamped with the thumbscrew mechanism carrying the idler bearing. The distal portion of the guidewire extending from the device was clamped into the upper grip of the Instron machine as shown in Figure 67.

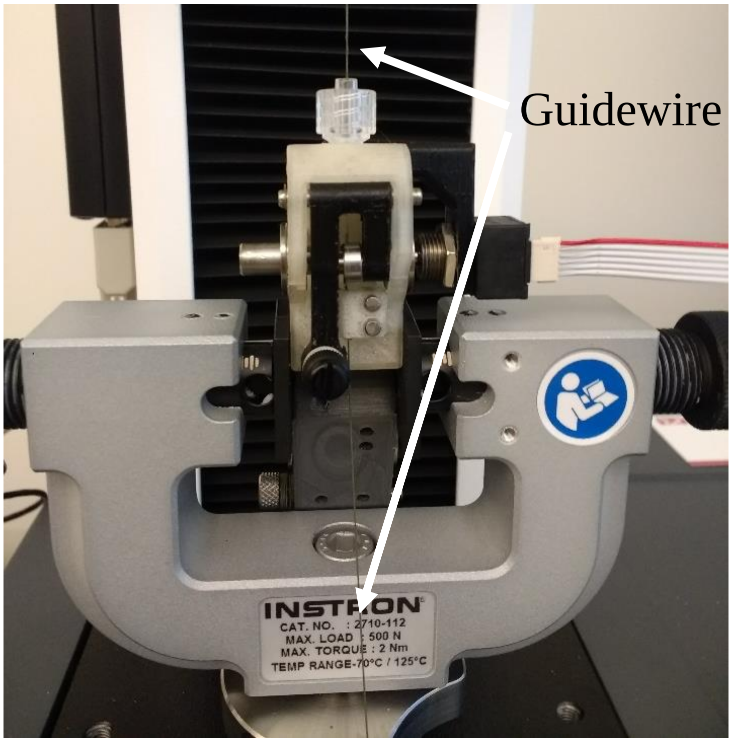

Figure 66. Over-the-wire prototype device mounted in the lower Instron grip.

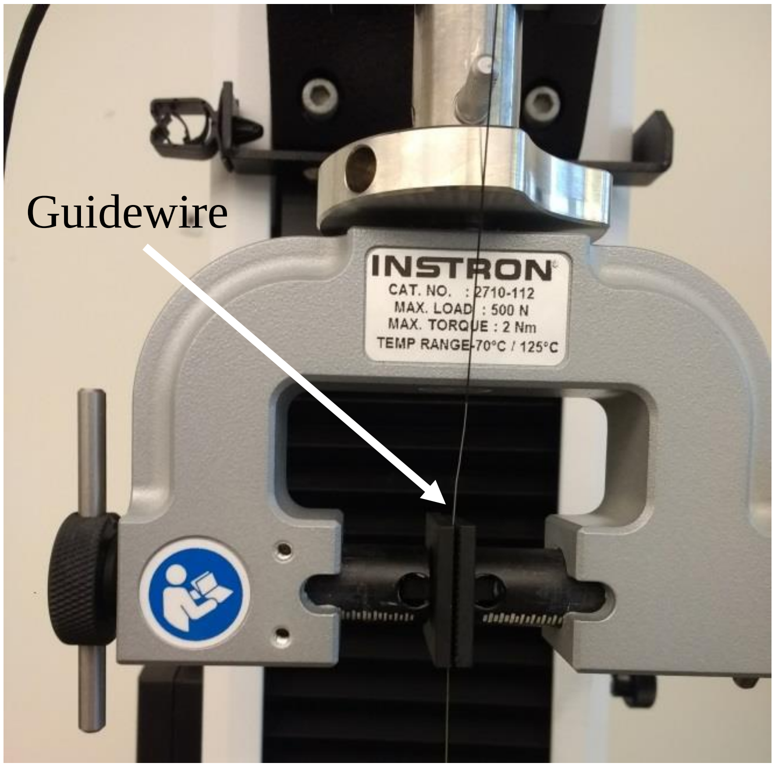

Figure 67. Distal portion of the guidewire clamped in the upper Instron grip.

The Instron was programmed to pull to a specified displacement at a set rate. Three levels were used for displacement (100mm, 175mm, and 250mm) based on the range of machine capabilities. Three levels were used for displacement rate (100mm/min, 500mm/min, and 1000mm/min) based on the range of machine capabilities.

The test results showed that there was a linear bias dependent on the displacement of the guidewire. Table 2 shows the average difference in displacement measured by the guidewire tracking device and the Instron calculated as the device measurement subtracted from the Instron measurement. Normalizing the displacement difference by the nominal displacement of the test resulted in a calculated error of 0.0069 mm per mm of displacement, or 0.7% error. It is possible to improve the device accuracy through calibration of the shaft diameter parameter in the software. In this case because the Instron measured consistently 0.7% higher the displacement/tick calculation should be increased by 0.7%.

The results of the testing indicated that the device, without an adjustment for calibration, read with an accuracy and precision 0.7±0.03% (95% confidence). If the displacement was adjusted to match the consistent bias error the expected measurement error is 0.0±0.03% (95% confidence). An example 100mm displacement would be expected to be in the range of 99.97mm to 100.03mm for 95% of repetitions. The data and calculations for the test can be found in Appendix G.

Table 6. Calculated difference between device and Instron displacement measurements.

Measurement	Target Displacement		
	100mm	175mm	250mm
Average Difference [mm]	0.69	1.14	1.67
Standard Deviation of Difference[mm]	0.08	0.18	0.11
Average Difference Normalized to Total Displacement Target [mm/mm]	0.0069	0.0065	0.0067

8.2 Catheter Intervention Lab Testing

Testing was conducted to evaluate the prototype catheter localization devices and procedures with data collected with the MediGuide system at in a catheter intervention lab at CPH, an Abbott facility. The goal of the tests was to acquire feedback on the process and to determine the localization precision and accuracy of the device. Additionally the time with access to the MediGuide software and hardware was used to collect datasets derived from moving the guidewire through a known geometry. Three benchtop phantoms were built using plastic tubing to create a model from which guidewire processing algorithms could be developed. The first shape used was a tube taped to the operating table in a straight line that resulted in a slight curve due to the storage of the tubing. The second shape was a spiral with a diameter of approximately 10cm made from the tubing wrapped around a PCV pipe. The third phantom used was a plastic benchtop coronary model. These models were previously shown in Figure 48 through Figure 50. The advantage of using the stationary benchtop models was that the guidewire signal was easier to work with without the complication of cardiac and respiratory motions.

<u>8.2.1 Dataset Acquisition</u>

The same process was used to build a dataset for each benchtop model. The model was secured to the operating table and the PRS sensor was placed near the model to provide an origin point for the coordinate system. A MediGuide enabled guidewire was connected the MediGuide system and then advanced through the model. At any key locations or bifurcations a landmark was placed in the MediGuide system. Additionally a landmark was placed at the final location of the guidewire. The guidewire was then retracted and the MediGuide recording was paused. The recorded datasets and the models used to generate them are shown in Figure 68 through Figure 70.

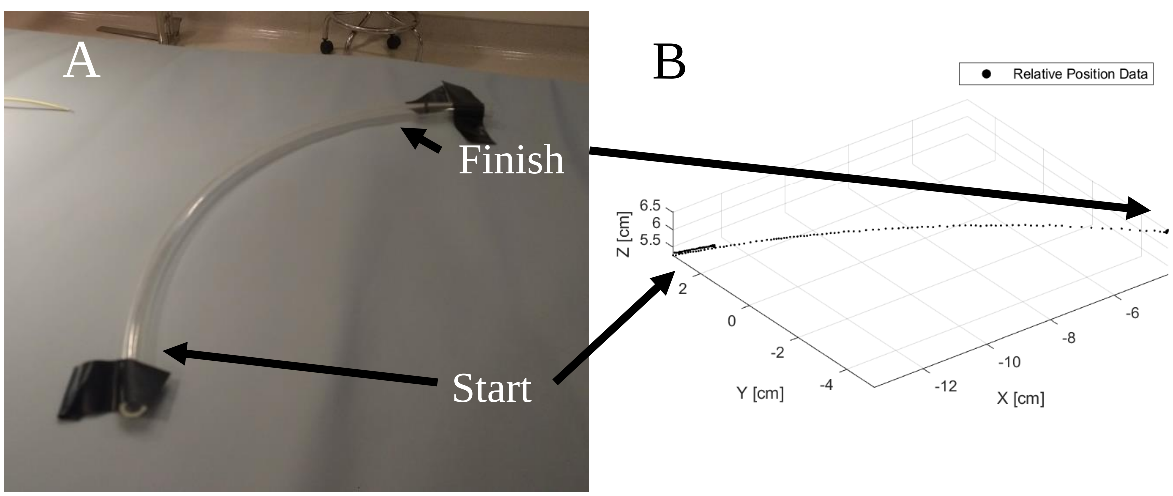

Figure 68. (A) Curve model and (B) dataset collected.

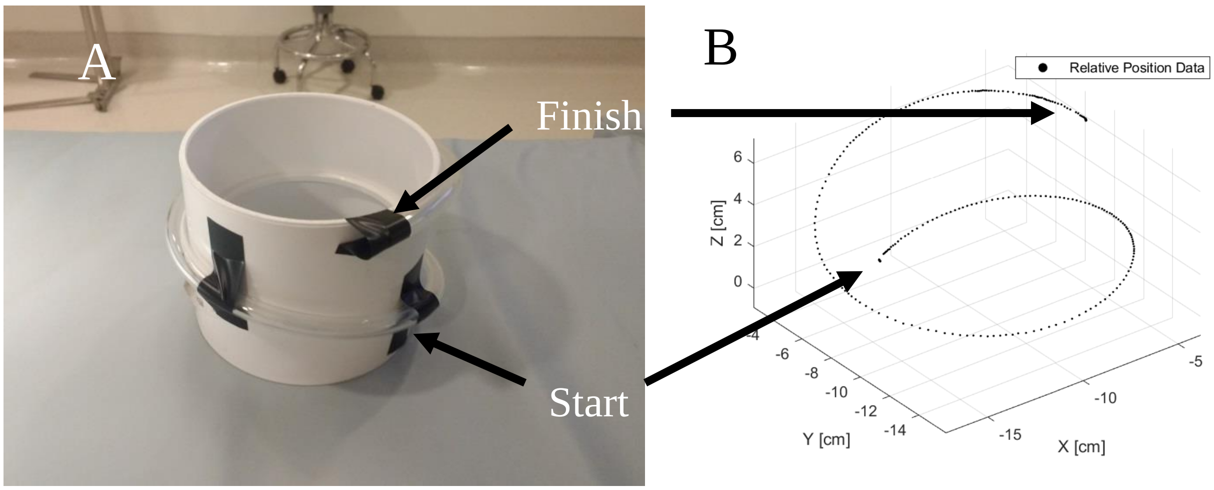

Figure 69. (A) Spiral model and (B) dataset collected

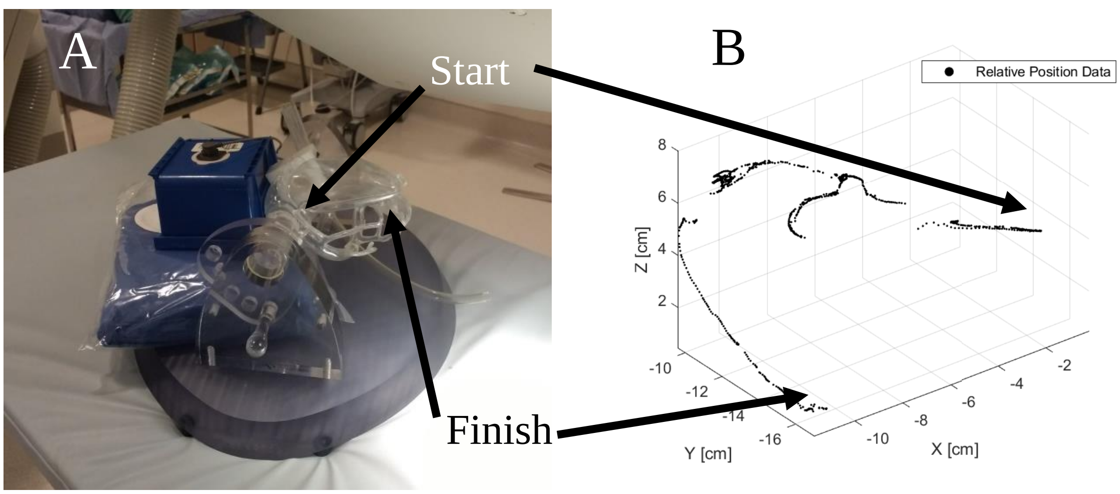

Figure 70. (A) Coronary model and (B) dataset collected

8.2.2 Device Use Process Evaluation

The flat curve tubing section was used to evaluate the device accuracy. The evaluation was attempted for both the over the wire catheter prototype and for the rapid exchange prototype. Evaluation of the over-the-wire device was completed but complications resulted in difficulties with the evaluation of the rapid exchange device as will be discussed.

The recorded dataset was loaded into the MATLAB program and the measurement device was connected to the computer via a USB cable. The guidewire was placed into the benchtop phantom along with the catheter strung over it. With the use of fluoroscopic imaging the MediGuide sensor overlay was aligned with the radiopaque tip of the guidewire. The guidewire was then advanced and retracted an arbitrary distance of several centimeters. The operator did not look at the catheter or guidewire in the phantom, instead they focused on the GUI read-out on the computer. The guidewire was retracted until the relative displacement read between 1 and 5mm. The distance from the catheter tip to the guidewire tip was measured and the distance measured by the device was recorded. The difference between these two measurements represents the error in the process and system combined.

The average difference between the actual catheter and guidewire displacement and that measured by the device was -1.4±0.54mm (95% confidence). The device consistently measured less than the relative displacement as a result of the process of aligning the initial reference point.

The same procedure was attempted with the rapid exchange prototype device. However the catheter available (Abbott Dragonfly Optis Imaging Catheter) had an exit port for the guidewire approximately 2cm proximal to the distal tip of the catheter. A distal radiopaque maker is 4mm from the distal tip of the catheter. A drawing of the catheter is shown in Figure 71. The close proximity of the exit port and the distal radiopaque maker made alignment of the catheter and guidewire a challenge without losing the guidewire from the lumen of the catheter. These challenges made alignment of the catheter and guidewire reference point difficult to achieve. Additionally because the guidewire is only retained in a short distal portion of the catheter lumen, there is more freedom for movement between the guidewire and catheter that would not be observed as a change at the distal tip because of slack in the wire or catheter. The more constrained the members are to the vasculature the less effect this had but when the members were external to a tube or structure there was significant movement that was not translated to the distal tips of the devices.

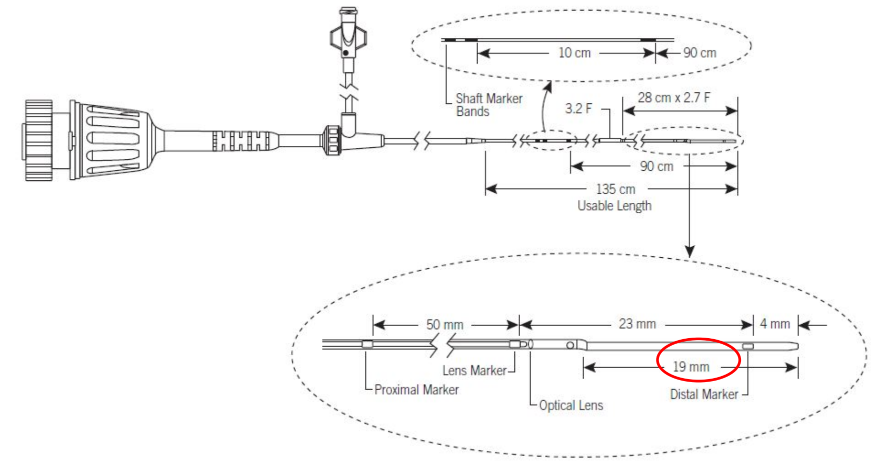

Figure 71. Dragonfly Optis Imaging Catheter dimensions. The distal lumen length dimension is highlighted in the red circle..

8.3 Guidewire Fit Algorithm Testing

The algorithm developed to fit a guidewire path was evaluated to analyze the effects of various parameters on the quality of the fit and the runtime of the algorithm. An inscribed central composite design with a quadratic response surface was used to evaluate both fit response and runtime. The design was centered on the parameters that appeared to produce reasonable results that were found through trial and error experimentation with the algorithm. The range of parameters and descriptions of parameter meaning is shown in Table 7. The goal of this analysis was to determine the optimal parameters for the algorithm. The code for the experimental design can be found in Appendix D.

Table 7. Guidewire Fit Algorithm Parameters

Parameter	Description	Low	Center	High
Number of Iterations [-]	The numbers of iterations the initial spline fit algorithm conducts	1	4	8
Minimum gap [cm]	The gap size between fitted points in the initial spline fit beyond which no more points are attempted to be fit	0.48	0.75	1.5
Between Plane Radius [cm]	When calculating the points contained between two planes, the distance outside of the range to be included in that set.	1	5	10
Close Point Radius [cm]	When finding the closest points to a selected point, the radiuses beyond which points are not considered.	1	4	8
Number of Planes [-]	The number of planes from which to implement the graph theory approach.	5	20	40
Number of Points [-]	The number of points in each mesh in the graph theory approach.	3	6	12

The analysis was conducted for the datasets available and replicated twice per dataset with variation introduced by the user selected landmark locations. To run the analysis, a dataset was selected and landmark points of interest were chosen. The code then ran and evaluated the set of parameters in every variation and recorded the results for each experiment. The data was analyzed in Minitab with a stepwise full quadratic model. The datasets used were treated as a block in the model. The stepwise model evaluates the significance of included factors through sequential addition and removal to determine the minimum model that best represents the response variable. After the completion of the stepwise model a response surface optimization was conducted to compare the effects of algorithm parameters on fit quality and runtime.

8.3.1 Fit Quality Analysis

Fit quality was measured by calculating a sum square error for the fit path compared to the relative dataset it was built from. The resulting spline fit was evenly sectioned into twenty segments. A vector tangent to each section point on the curve was calculated and planes were constructed normal to the vector and passing through the previous and subsequent section points of the fit. The points between the two constructed planes were selected. The distance from the fit point to the mean of the points between the planes was calculated. This was repeated for all sections of the guidewire. The sum of these distances represented the quality of the fit.

The fit quality was analyzed in Minitab with a stepwise quadratic response surface methodology. A Box-Cox optimal λ transformation was applied to normalize the fit response data. This determined an optimal $\lambda = -0.25$. A stepwise analysis was performed to determine the minimum relevant parameters with α to include or exclude a factor of 0.15. The ANOVA table for the transformed analysis is shown in Table 8. The significant factors on the resulting fit were the quadratic number of initial spline fit iterations performed, the quadratic effect of the distance limit when calculating the closest points, and the linear effect of the number of planes used in the graph theory fit. The assumptions for the model were evaluated in Figure 72. The main effects plot is shown in Figure 73.

Table 8. Analysis of Variance for Transformed Fit Quality Response

Source	DF	Adj SS	Adj MS	F-Value	P-Value
Model	10	15.6762	1.56762	1528.70	0.000
Blocks	5	15.5672	3.11345	3036.15	0.000
Linear	3	0.0694	0.02313	22.56	0.000
Iterations	1	0.0021	0.00215	2.09	0.148
ClosePoint	1	0.0311	0.03105	30.28	0.000
nPlanes	1	0.0360	0.03595	35.06	0.000
Square	2	0.0135	0.00677	6.60	0.001
Iterations*Iterations	1	0.0029	0.00292	2.85	0.092
ClosePoint*ClosePoint	1	0.0123	0.01226	11.95	0.001
Error	884	0.9065	0.00103		
Lack-of-Fit	449	0.5788	0.00129	1.71	0.000
Pure Error	435	0.3277	0.00075		
Total	894	16.5827			

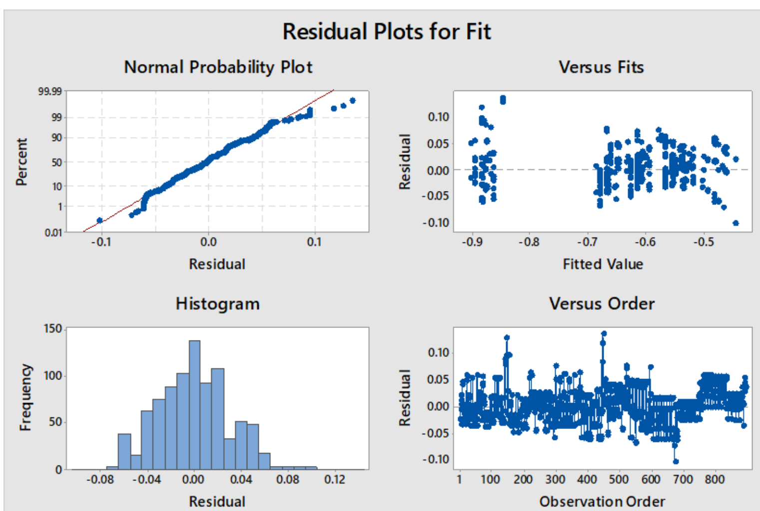

Figure 72. The residuals of the fit quality analysis. Normality is shown by the Normal Probability Plot, Equal Variance is shown by the Residual vs Fit plot, and Independence is shown by the Residual vs Time plot.

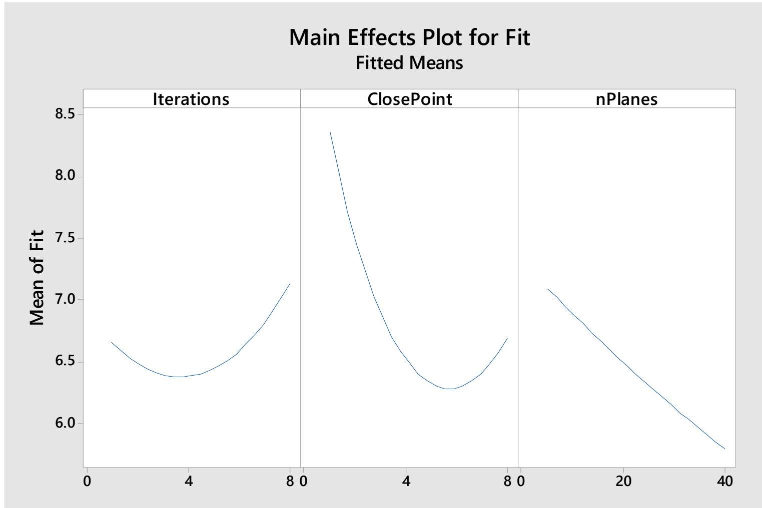

Figure 73. Main effects plot of significant factors affecting fit quality. A lower value represents a closer fit of the simulated trajectory to the dataset. Units for the closest point parameter are centimeters and for Iterations and nPlanes it is the number of items.

<u>8.3.2 Execution Time Analysis</u>

To be applicable to a clinical use the algorithm must be relatively fast. Simulation in real time would provide live updates of a predicted shape and position of the guidewire to the clinicians. In order to evaluate the feasibility of providing real-time updating simulated position to the operators the calculation time for the algorithm using a range of parameters was evaluated.

The runtime was evaluated with the use of MATLAB tic-toc functions. The time was measured from the function call to the initial spline fit and ending at the output of the spline function point array. The calculation of the fit quality was not included in the runtime. The runtime was analyzed with a stepwise quadratic response surface methodology. The ANOVA table for the transformed data in the runtime analysis is shown in Table 9. The residuals were analyzed in Figure 74. The variance was explained primarily with the interaction effects shown in the interaction plots of Figure 75.

Table 9. Analysis of Variance for Transformed Runtime Response

Source	DF	Adj SS	Adj MS	F-Value	P-Value
Model	22	18.6884	0.84947	851.07	0.000
Blocks	5	16.8633	3.37266	3378.99	0.000
Linear	6	0.5578	0.09296	93.14	0.000
Iterations	1	0.0180	0.01804	18.07	0.000
minGap	1	0.0546	0.05458	54.68	0.000
BetweenPlane	1	0.0033	0.00334	3.35	0.068
ClosePoint	1	0.0245	0.02449	24.53	0.000
nPlanes	1	0.3587	0.35873	359.41	0.000
nPoints	1	0.0119	0.01192	11.94	0.001
Square	3	0.0215	0.00718	7.19	0.000
Iterations*Iterations	1	0.0180	0.01796	18.00	0.000
ClosePoint*ClosePoint	1	0.0058	0.00579	5.80	0.016
nPlanes*nPlanes	1	0.0047	0.00465	4.66	0.031
2-Way Interaction	8	0.0777	0.00972	9.73	0.000
Iterations*minGap	1	0.0347	0.03471	34.78	0.000
Iterations*ClosePoint	1	0.0086	0.00859	8.60	0.003
Iterations*nPlanes	1	0.0092	0.00916	9.18	0.003
minGap*BetweenPlane	1	0.0036	0.00356	3.56	0.059
minGap*ClosePoint	1	0.0036	0.00358	3.58	0.059
minGap*nPlanes	1	0.0031	0.00307	3.08	0.080
BetweenPlane*ClosePoint	1	0.0021	0.00210	2.10	0.147
ClosePoint*nPlanes	1	0.0127	0.01272	12.75	0.000
Error	872	0.8704	0.00100		
Lack-of-Fit	437	0.6748	0.00154	3.43	0.000
Pure Error	435	0.1956	0.00045		
Total	894	19.5588			

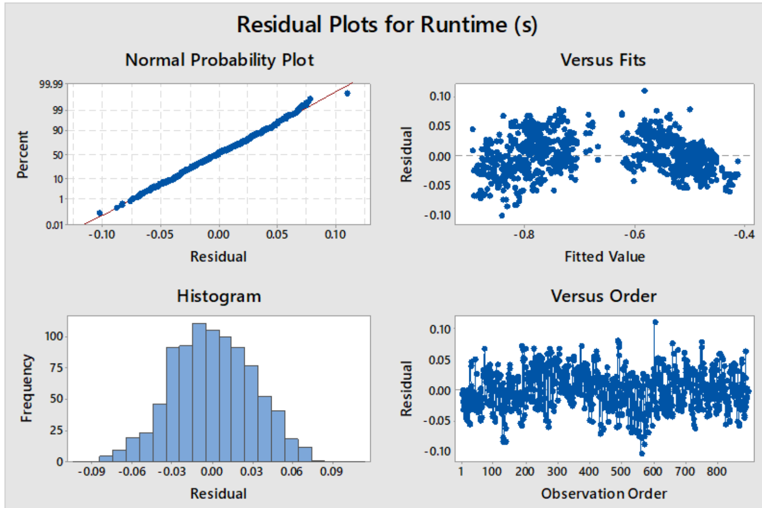

Figure 74. The residuals of the algorithm runtime analysis. Normality is shown by the Normal Probability Plot, Equal Variance is shown by the Residual vs Fit plot, and Independence is shown by the Residual vs Time plot

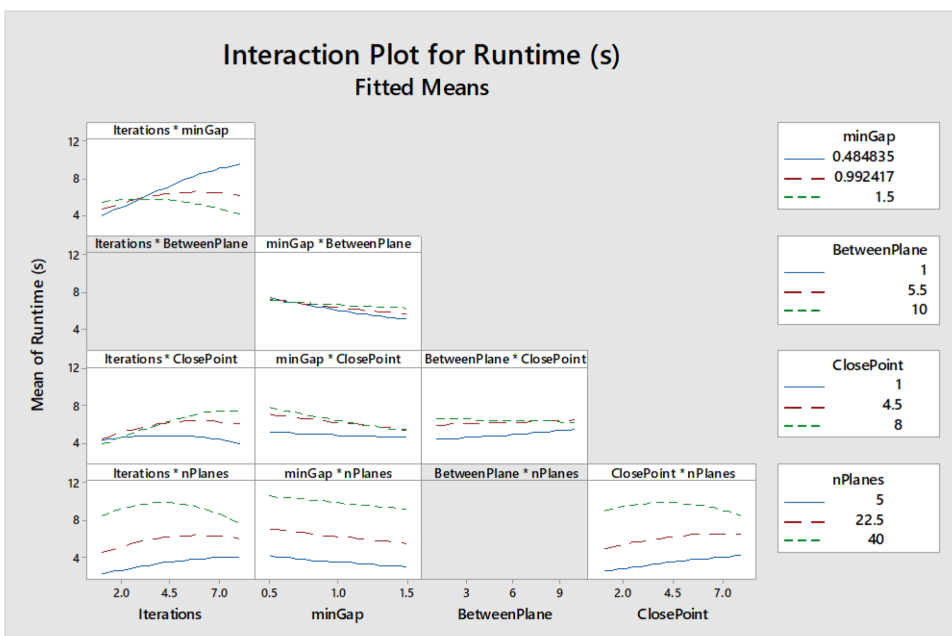

Figure 75. Interaction effects plot for algorithm runtime. A lower value indicating less time for the algorithm to calculate the guidewire position is desirable.

8.3.3 Response Surface Optimization

A response surface optimization was conducted in Minitab with the significant factors to determine the optimal settings for the guidewire fit algorithm. The optimization attempted to minimize the fit quality error value and the runtime simultaneously with an emphasis of the fit quality. The parameters resulting from the optimization are shown in Figure 76. An example dataset with a fit calculated with these parameters (runtime of 5.63 seconds) is shown in Figure 77. For comparison, the results of the algorithm with the worst parameters in the range (runtime 1.34 seconds) is shown in Figure 78. Both of these analyses used the coronary model phantom as an example.

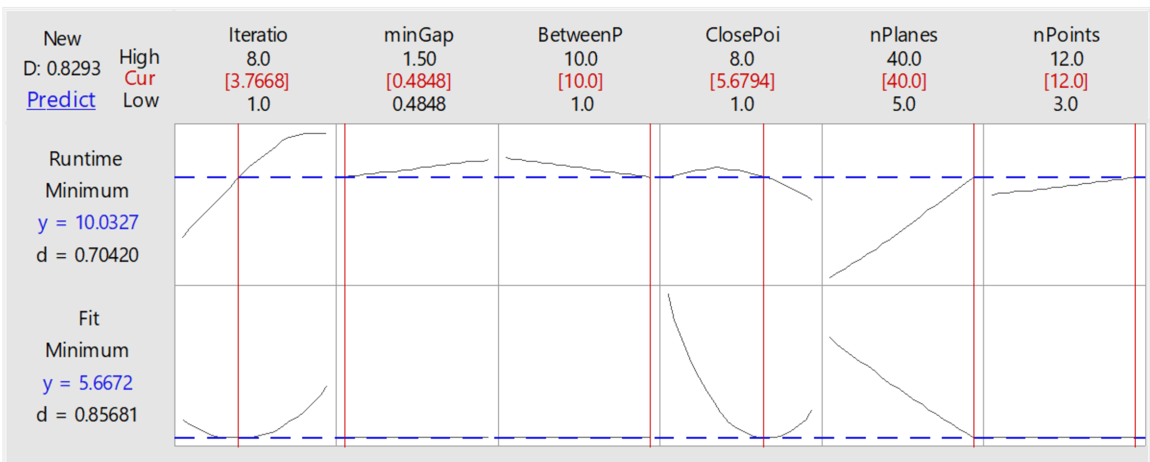

Figure 76. Fit quality response surface optimization to minimize runtime and fit error.

Parameter	Best Fit Quality	Shortest Runtime
Number of Iterations [-]	4	1
Minimum gap [cm]	0.48	1.5
Between Plane Radius [cm]	5	10
Close Point Radius [cm]	5.7	8
Number of Planes [-]	40	5
Number of Points [-]	12	3

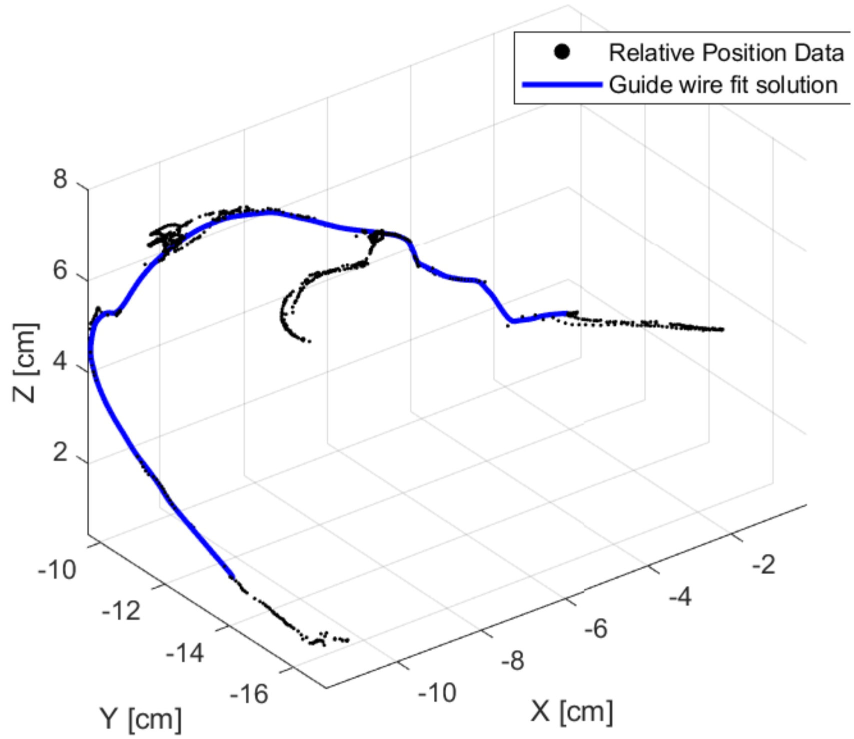

Figure 77. Guidewire fit solution resulting from the best algorithm optimization.

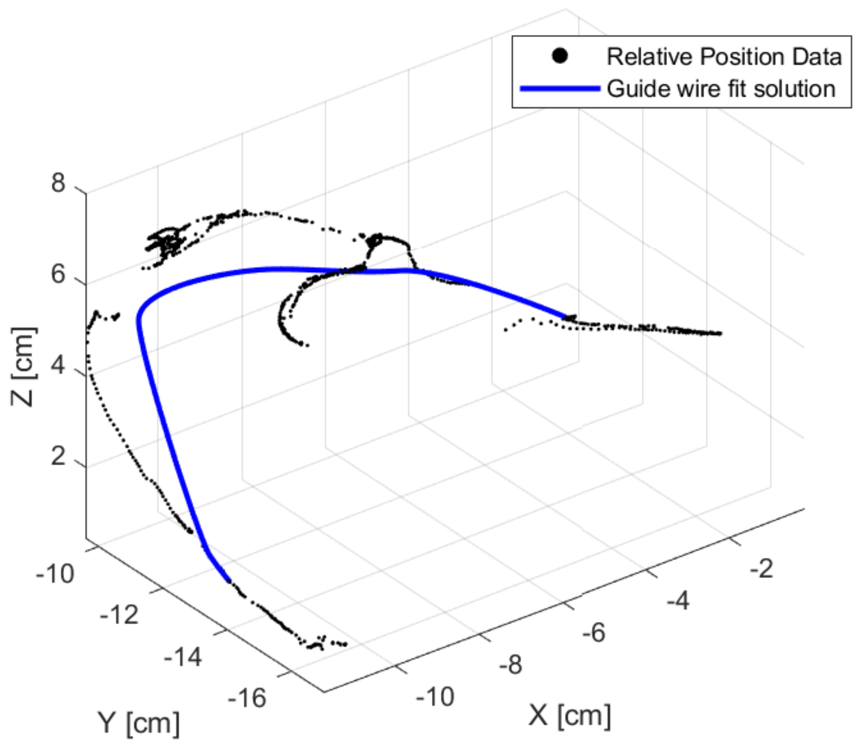

Figure 78. Guidewire fit solution with the worst parameters in range of the response surface optimization.

8.4 Testing Summary

The components of the prototype system were tested to evaluate the capabilities of the prototype and the potential for implementation. The prototype electro-mechanical device was evaluated, the use procedure of the device in an interventional catheter lab setting was evaluated, and the software algorithms to calculate a guidewire trajectory were evaluated.

The over-the-wire device by itself was determined to be accurate to 0.7±0.03% (95% confidence). In use it was accurate to 1.4±0.54mm (95% confidence). The parameters to develop the best simulation of the guidewire trajectory were determined and resulted in a calculation time dependent on the number of data points in the file and the resolution for the algorithm. For an implementation optimized for quick execution the runtime is on the order of 5 seconds. A more accurate fit takes around 20 seconds. Overall these results indicate the initial feasibility of the system to benefit clinicians by providing additional information about catheter localization and reduce radiation dosage from fluoroscopy. The implications of these results will be discussed in Chapter 9. However there are still remaining challenges that were not addressed in this project and more development work to be completed. The future work and directions of further investigation and development will also be discussed in Chapter 9.

Chapter 9: Discussion and Conclusion

9.1 Summary

The intent of this thesis was to evaluate the feasibility of expanding the Abbott MediGuide technology through the use of an external device to track relative motion of catheters and guidewires and to develop a prototype device and prototype software to prove the concept. With the use of a sensor enabled guidewire, the goal was to localize a catheter without a sensor in it. This would open up the capabilities of the MediGuide navigation system to be used with interventional tools not designed with sensors integrated into them.

The research conducted covered multiple disciplines from mechanical design to software algorithms. First, an overview of the existing literature and patents on similar devices was evaluated and the literature surrounding the concept of guidewire path simulation and calculation of guidewire positions from both image-based and sensor-based methods was investigated. The literature investigation of previously proposed device hardware design guided the development of prototype hardware for this device particularly the use of a rotary encoder to measure the linear motion. The prototype hardware was constructed for over-the-wire and rapid exchange type catheters. Investigation of research into device tracking systems and the development of algorithms for simulating guidewire trajectories influenced the development of the software prototype for the project. The existing techniques were evaluated and adapted to the special conditions assumed in this project to create a method of calculating a predicted guidewire trajectory without prior knowledge of the vascular geometry. Using data provided by Abbott from patient interventions and data collected in a catheterization lab with custom built phantoms an algorithm and method of calculating a predicted guidewire path was developed.

The hardware and software components of the project were evaluated through an array of testing. The prototype device was evaluated in isolation and in a use scenario in the Abbott catheterization laboratory. The mechanical and electrical components of the device exceed the accuracy requirement. Use of the device in an environment like a catheter lab introduces additional challenges to the measurement that shows promise but does need more work to reach the desired level of accuracy which will be discussed further in this chapter. The software algorithms to generate a simulated guidewire path were evaluated and tuned to generate the best response to the data sets available.

9.2 Discussion

The project began with an outline for the specifications and goals of the prototype device. These are outlined again here in Table 10 along with the results of the work on this project. This section will address each specification, how the specification was addressed and any challenges remaining. The implications of the work will be discussed to conclude.

Table 10. Specifications for the prototype system with the results of evaluation and testing

Spec No.	Specification	Description	Target	Achievements
1	Resolution	Output resolution of the device	± 0.5 mm	0.08 mm
2	Precision	Consistent reliability of the device data output must be better than this value	± 0.5 mm	Device ± 0.03%: In use: ± 0.54 mm
3	Output Speed	The device must output live data within this range of frequencies	30 – 60 Hz	20 Hz
4	Ease of use	The device must minimally interfere with the current procedure used for cardiac intervention. Specified as additional procedure time	< 5 min	See section 9.2.4
5	Cost	Typical budget for a Cal Poly MEDITEC Project	$5000	Single Prototype: $100
6	Safety	No injury or damage to equipment, physicians, or patients.	Pass	See section 9.2.6

9.2.1 Resolution

The target for the project was to provide a resolution of ±0.5mm for measurement. In the current embodiment with the quadrature rotary encoder with 64 pulses per revolution and a nominal encoder shaft diameter of 0.25 a resolution of ±0.02mm was achieved. This represents the finest resolution possible of the device with a single pulse of the encoder representing 0.02mm of linear motion of the guidewire or catheter as it rolled over the encoder shaft.

9.2.2 Precision

Precision represents the repeatability or variability in the measurements. The goal for the project was to have a precision within ±0.5mm. The prototype device, when tested in a displacement controlled tensile movement of the guidewire, exhibited a variability of 0.03% (95% confidence) of the nominal displacement. The device was also evaluated in an interventional catheter laboratory to simulate conditions more similar to using the device in a clinical scenario. The precision observed in this test, for total displacements under 10cm, was ±0.54mm (95% confidence).

9.2.3 Output Speed

The output speed of the system was specified at 30-60Hz to be able to display the motion smoothly in real time as the catheter was moved relative to the guidewire. The system displayed information at the refresh rate of MATLAB drawing functions which was capped at 20Hz for stability. Although this does not provide a perfectly smooth image of the motion it is still sufficient to display the information to the user without significant latency.

Where the project falls short on runtime is the calculation of the guidewire path. This calculation depends on the size of the data set generated when the guidewire placement was recorded with the MediGuide sensor. The calculation of the guidewire path took on the order of 10 seconds to complete. Future work in this area is discussed in section 9.3.2.

9.2.4 Ease of Use

The prototype devices, over-the-wire and rapid exchange, integrate into the workflow with a few changes compared to a standard procedure. The over the wire device attached to the proximal end of the catheter. Once attached in place to the proximal Luer fitting, there were only a few additional steps to use the device compared to an intervention without it. The first additional step was the guidewire positioning data needed to be transferred from the MediGuide system to the secondary computer. The second additional step was to use the fluoroscopy system to set the reference zero displacement position between the catheter and guidewire. Following those steps the catheter and guidewire system was used as normal and the prototype device tracked the relative motion of the two components.

The rapid exchange device requires similar changes to procedure as the over the wire device. The data needs to be transferred from the MediGuide to the secondary computer the same it does with the over-the-wire device. The catheter was placed into the measurement device and then strung over the guidewire. The proximal end of the guidewire was pinned to the measurement device with a thumbscrew to allow the device to measure catheter motion relative to the guidewire. Future work on this system would to develop a method to attach the measurement device to the introducer sheath of the catheter this is discussed further in section 9.3.

9.2.5 Cost

The total cost of the prototype devices is low. The devices are simple consisting of 3D printed prototype components, hardware such as bearings and dowel pins, and electronics. Table

11 shows the approximate costs of the components used to construct the prototype devices. The project was completed within the budget given.

Table 11. Approximate cost of the prototype devices.

Component	Approximate Cost
3D Printed Parts	$0
Bournes ES14 64PPR Encoder	$65
Arduino Uno	$30
McMaster hardware	$10
Total	$105

9.2.6 Safety

The prototype devices described in this paper were designed to be fully external to the patient. They functioned by measuring the motion outside the patient and applying that relative motion to describe the relative positions of the catheter and guidewire inside the patient. Safety concerns with the devices include removal of devices as rapidly as possible if necessary and sterility. Removal of devices from the patient is not significantly different than in a typical procedure as the device is fully external. The device would need to be sterilized with a process that does not damage electronic systems as the measurement functioned through contact of the guidewire or catheter.

9.3 Future Work

9.3.1 Device

The prototype device was functional, but not at the level of a marketable product. Future work should aim to improve the ergonomics and integration of the product so that it is easier to hold, and the components are protected. Development of a more advanced prototype should move the electronics from the Arduino prototyping board to a more compact custom printed circuit board with only the components needed for the device. The Arduino has many more pins and functionality than are needed for the device and its design as a prototyping system with easy access and reusable headers results in a bulky form factor. An improved design would contain all the device components into a neat package that adds minimal intrusion into the clinician's workspace or workflow.

Another direction of improvement on the prototype device would be to move away from the rotary encoder and move towards the development of a non-contact, or a light contact measurement system. The prototype device, with the idler bearing and mechanical rotary encoder measurement, does introduce friction into the system. From the standpoint of the operator of the interventional tools, additional friction is a hindrance and should be minimized. A system that utilized an optical or other form of non-mechanical measurement of guidewire or catheter motion, if it could be made to be precise and reliable, would most likely improve on the results shown here. The Vascular Simulation Platform from Mentice Inc, uses optical sensors to track the position and rotation of catheters and guidewires. [17] The benefits of this method include lower friction without the need to maintain rolling motion of the device over the encoder shaft and the ability to measure both linear and rotational motion of the device. It may also be more compact and easier to package into a product than the mechanical device as it would have no moving parts.

A weakness in this project is adapting the device to rapid exchange catheters. In the rapid exchange catheter available the close proximity of the distal radiopaque marker and the proximal exit port for the guidewire made use of the system challenging as margin of error to avoid loss of the guidewire from the catheter lumen was small. Future work should attempt to address the challenges presented by rapid exchange catheters similar to the one investigated here. With regard to hardware implementation an area of interest may be develop an introducer sheath or introducer attachment through which both the catheter and guidewire both pass through. Two sensors could independently measure the displacement of each device. A potential method to address the issue of losing the guidewire from the catheter lumen while setting the initial reference point would be to develop a method to set the reference point without the need to directly align a radiopaque marker and the guidewire sensor. This could be done by using a fluoroscopic image to measure the distance from a radiopaque marker to the guidewire sensor, advancing or retracting the guidewire a known small displacement, and then measuring the distance from the marker to the sensor again. From this information it would be possible to calculate the linear offset from the catheter radiopaque marker to the guidewire sensor.

9.3.2 Guidewire Algorithm

Data filtering was performed prior to estimating a guidewire trajectory with the recorded guidewire distal tip position data. The filtering was performed with a low-pass filter with minimal results at removing the large motions caused by cardiac and respiratory motion. Future work in data filtering techniques include further utilization of the PnO data from the guidewire sensor and coordination with electrocardiogram (ECG) data. It would be possible to use the orientation information to determine the direction of motion relative to the guidewire tip orientation. This could be used to filter out movement perpendicular to the orientation of the guidewire such as what could be caused by cardiac motion while the guidewire is in the coronary vasculature. Additionally with an ECG recording at the same time as the MediGuide navigation, movements of the guidewire could be correlated to sections of the cardiac cycle. This could be used to limit data recording to only a single portion of the cycle or configuration of the heart.

The guidewire fit simulation algorithm was tested, tuned, and evaluated based on the datasets available. Future investigations should develop a method to compare the guidewire path with a real guidewire in the same spatial constraints. This would assist with improving the development of the algorithm. Additionally it would be beneficial to test the algorithm in both benchtop models and in vivo models. A study to evaluate the effectiveness of the technique in the much more complicated scenario of in vivo testing would bring with it many more issues to address. For example, processing the data in real time would be challenged with compensating for cardiac and respiratory motion of the subject, and error and noise in the signal. When the connection to the MediGuide system is poor the system records rows of zeros for the position. Cardiac and respiratory motions introduce movement into the dataset that does makes determining a representation of the real geometry of the vasculature difficult. Two of the datasets analyzed previously contained cardiac and respiratory motion but the correlation of the fit guidewire path was evaluated with respect to the recorded data and not evaluated with respect to the real vascular anatomy.

To be truly useful the algorithm must be able to run in real time or near real time. To make this happen, the algorithm would need to be directly connected to the MediGuide system so that new data can be incorporated as it is collected and so that the continuously updating position of the distal guidewire tip can be incorporated into the calculation and display. A refresh rate of approximately 20 frames per second would appear smooth to the operator. Achieving this would require a total calculation time of 0.05 seconds, much faster than the algorithm currently operates. This could be improved through implantation of a more efficient algorithm and improving the current process with more computationally efficient methods. Even moving the algorithm from MATLAB to a language like C may achieve some performance improvements. Additionally it would most likely be possible to implement a similar technique to the one developed here, but modified to function on continuous new data generated in the MediGuide system. The position data from the distal tip of the guidewire could be used to estimate a bounding geometry of the vasculature. Simultaneously the system could use the estimated bounding geometry with a method similar to the one discussed here to calculate a guidewire trajectory. This would allow the algorithm to function without the need to calculate every part of the solution from the ground up for each frame to display to the user. Instead the algorithm could make smaller updates and modifying the model as more data is collected.

9.3.3 Testing

This work provides a starting point that evaluated the feasibility of a catheter localization device and system. It would be beneficial to conduct more research into the feasibility of the system with access to more resources and catheter laboratory time. An aspect of the work that warrants further investigation is to determine methods or techniques that would produce better localization accuracy and precision results in a catheter lab type environment. One large source of error in the measurement device results from the need to register an initial reference point of zero displacement. Future work should be undertaken to determine a method to more accurately determine the initial reference point. This future method could use the fluoroscopy as done in this paper or some alternative method.

An important aspect of the device concept that needs to be tested is the fluoroscopy time reduction. It remains unknown if the implementation of the proposed devices would result in a lower fluoroscopy dose in a clinical or pre-clinical procedure. It would be expected that the proposed device may fall somewhere between a traditional procedure and the benefits shown with MediGuide enabled procedures. Future work should design a test and evaluate the differences radiation exposure for a traditional procedure without the MediGuide technology, a procedure with MediGuide sensors in both the catheter and guidewire, and a procedure with the sensor enabled guidewire and the proof-of-concept device. Some of the concepts initially developed here such as simulated guidewire trajectories could also be applied to procedures with MediGuide enabled tools to further enhance the capabilities of the system.

9.3 Implications of the Work

The application of the MediGuide system has already shown benefits with reduction in procedure time, reduction in radiation dose, [6], [34], and improved ergonomics through moving the C-Arm out of the way when the imaging does not need to be live. [34] The prototype system developed in this project, if translated into a clinically applicable commercial device, would both bring the benefits of the MediGuide technology to a wider variety of interventional tools without embedded sensors. Beyond just applying the current technology to more devices the ability to simulate the position of a guidewire or catheter in the vasculature adds value to the system. Currently only the distal tips of devices where the sensors are placed are displayed by the MediGuide system. The ability to display information about the guidewire and catheter shape and position proximal to the distal tip adds additional capabilities to the system that may prove useful to the operators in clinical procedures.

The existing work to track guidewires and catheters is mostly limited to virtual reality surgical training systems. These systems provide a method of to virtually simulate endovascular procedures and train physicians on procedures without the risk of training on patients. These systems include the Procedicus VIST (Mentice), Simsuite (Medical Simulation Corporation), Angiomentor (Simbionix), and CathLabVR (CAE Healthcare). [35] These systems provide the capability to simulate a variety of procedures using hardware to track catheter motion and software to simulate the procedure and provide a calculation of feedback forces. The device developed in this project miniaturizes the tracking ability to something that can be used with interventional tools and remain external to the patient. This technology could be applied to the simulation systems as well as the clinical use intended with the original project concept.

9.4 Conclusion

This thesis has created a prototype system to demonstrate the feasibility of a catheter localization system. The prototype system used a sensor enabled guidewire tracked in the Abbott MediGuide system in combination with an external measurement device that attached to the catheter. The external device measured the relative motion between the guidewire and the catheter. Using the information from the sensor tracking, the system displayed the position of the catheter to the guidewire in a 3D spatial representation and provided a predicted measurement of the difference between the placements of the distal tips. This provided a starting point for further development and refinement of the concept. Future work would aim to improve the mechanics of the device, improve the guidewire trajectory simulation, integrate more seamlessly with the MediGuide system, and further prove the effectiveness of the concept with radiation dose testing.

Appendices

References

[1] M. Y. Flugelman *et al.*, “Medical positioning system: a technical report.,” *EuroIntervention*, vol. 4, no. 1, pp. 158–60, May 2008.

[2] H. Heidbuchel *et al.*, “Practical ways to reduce radiation dose for patients and staff during device implantations and electrophysiological procedures,” *Europace*, vol. 16, no. 7, pp. 946–964, 2014.

[3] S. Condino *et al.*, “Simultaneous tracking of catheters and guidewires: Comparison to standard fluoroscopic guidance for arterial cannulation,” *Eur. J. Vasc. Endovasc. Surg.*, vol. 47, no. 1, pp. 53–60, 2014.

[4] L.-P. Richer, “Provided courtesy of Louis-Philippe Richer.” .

[5] S. J. M. Inc, “MediGuide™ Technology: Navigating Away from Live X-Ray Clinical Compendium.” St Jude Medical.

[6] B. THIBAULT *et al.*, “Reducing Radiation Exposure During CRT Implant Procedures: Single-Center Experience With Low-Dose Fluoroscopy Settings and a Sensor-Based Navigation System (MediGuide),” *J. Cardiovasc. Electrophysiol.*, vol. 27, no. 11, pp. 1337–1343, Nov. 2016.

[7] C. Piorkowski and G. Hindricks, “Nonfluoroscopic sensor-guided navigation of intracardiac electrophysiology catheters within prerecorded cine loops,” *Circ. Arrhythmia Electrophysiol.*, vol. 4, no. 4, pp. 36–39, 2011.

[8] P. Sommer, S. Richter, G. Hindricks, and S. Rolf, “Non-fluoroscopic catheter visualization using MediGuide technology: experience from the first 600 procedures,” *J. Interv. Card. Electrophysiol.*, vol. 40, no. 3, pp. 209–214, 2014.

[9] R. Sidhu, J. Weir-Mccall, F. Cochennec, C. Riga, A. Dimarco, and C. D. Bicknell, “Evaluation of an electromagnetic 3D navigation system to facilitate endovascular tasks: A feasibility study,” *Eur. J. Vasc. Endovasc. Surg.*, vol. 43, no. 1, pp. 22–29, 2012.

[10] A. Schwein *et al.*, “Flexible robotics with electromagnetic tracking improves safety and efficiency during in vitro endovascular navigation,” *J. Vasc. Surg.*, vol. 65, no. 2, pp. 530–537, Feb. 2017.

[11] S. B. Lewis and M. J. Eberle, “Optical Pullback Sensor For Measuring Linear Displacement of a Catheter or Other Elongate Member,” US 2003/0187369, 2003.

[12] G. Kornblau and S. Ben-Ari, “Locating a Catheter Tip Using a Tracked Guide,” US2008/0262473 A1, 2008.

[13] P. T. Anderson, “Catheter Guidewire Tracking System and Method,” US 2009/0062739, 2009.

[14] A. F. Bolger and C. Tacklind, “System and Method for Monitoring Intraluminal Device Position,” 5,437,290, 1995.

[15] F. C. Van Egmond and C. T. Lancee, “Electronic Catheter Displacement Sensor,” 5,709,661, 1998.

[16] M. Luo, H. Xie, L. Xie, P. Cai, and L. Gu, “Computerized Medical Imaging and Graphics A robust and real-time vascular intervention simulation based on Kirchhoff elastic rod,”

Comput. Med. Imaging Graph., vol. 38, no. 8, pp. 735–743, 2014.

[17] P. Korzeniowski, R. J. White, and F. Bello, “VCSim3: a VR simulator for cardiovascular interventions.,” *Int. J. Comput. Assist. Radiol. Surg.*, 2017.

[18] S. A. M. Baert, M. A. Viergever, and W. J. Niessen, “Guide-wire tracking during endovascular interventions,” *IEEE Trans. Med. Imaging*, vol. 22, no. 8, pp. 965–972, 2003.

[19] Y. Ma *et al.*, “Real-time x-ray fluoroscopy-based catheter detection and tracking for cardiac electrophysiology interventions,” *Med. Phys.*, vol. 40, no. 7, 2013.

[20] F. Milletari, V. Belagiannis, N. Navab, and P. Fallavollita, “Fully Automatic Catheter Localization in C-Arm Images Using ℓ1-Sparse Coding,” in *Lecture Notes in Computer Science (including subseries Lecture Notes in Artificial Intelligence and Lecture Notes in Bioinformatics)*, vol. 8674 LNCS, no. PART 2, 2014, pp. 570–577.

[21] T. Petković, R. Homan, and S. Lončarić, “Real-time 3D position reconstruction of guidewire for monoplane X-ray,” *Comput. Med. Imaging Graph.*, vol. 38, no. 3, pp. 211–223, 2014.

[22] S. Condino *et al.*, “Electromagnetic navigation platform for endovascular surgery: how to develop sensorized catheters and guidewires,” *Int. J. Med. Robot. Comput. Assist. Surg.*, vol. 8, no. 3, pp. 300–310, Sep. 2012.

[23] L. Gepstein, G. Hayam, and S. A. Ben-Haim, “A Novel Method for Nonfluoroscopic Catheter-Based Electroanatomical Mapping of the Heart : In Vitro and In Vivo Accuracy Results,” *Circulation*, vol. 95, no. 6, pp. 1611–1622, Mar. 1997.

[24] K. Lam, J.-L. Bigcas, A. Luong, W. Yao, and M. J. Citardi, “Flexible microsensor technology for real-time navigation tracking in balloon sinus ostial dilation,” *Allergy Rhinol.*, vol. 8, no. 1, pp. 20–24, 2017.

[25] K. Ralovich, M. John, E. Camus, N. Navab, and T. Heimann, “6DoF Catheter Detection, Application to Intracardiac Echocardiography,” in *Lecture Notes in Computer Science (including subseries Lecture Notes in Artificial Intelligence and Lecture Notes in Bioinformatics)*, vol. 8674 LNCS, no. PART 2, 2014, pp. 635–642.

[26] M. K. Konings, E. B. van de Kraats, T. Alderliesten, and W. J. Niessen, “Analytical guide wire motion algorithm for simulation of endovascular interventions,” *Med. Biol. Eng. Comput.*, vol. 41, no. 6, pp. 689–700, 2003.

[27] T. Alderliesten, P. A. N. Bosman, and W. J. Niessen, “Towards a Real-Time Minimally-Invasive Vascular Intervention Simulation System,” *IEEE Trans. Med. Imaging*, vol. 26, no. 1, pp. 128–132, Jan. 2007.

[28] J. Qiu, Z. Qu, H. Qiu, and X. Zhang, “An improved real - time endovascular guidewire position simulation using shortest path algorithm,” *Med. Biol. Eng. Comput.*, vol. 54, no. 9, pp. 1375–1382, 2015.

[29] S. Schafer, V. Singh, P. B. Noël, A. M. Walczak, J. Xu, and K. R. Hoffmann, “Real-time endovascular guidewire position simulation using shortest path algorithms,” *Int. J. Comput. Assist. Radiol. Surg.*, vol. 4, no. 6, pp. 597–608, Nov. 2009.

[30] C. P. S. U. SWE-Team-Tech, “2015-2016 Team Tech Project: Catheter Localization,” 2016.

[31] T. Alderliesten, M. K. Konings, and W. J. Niessen, “Modeling Friction, Intrinsic Curvature, and Rotation of Guide Wires for Simulation of Minimally Invasive Vascular Interventions,” *IEEE Trans. Biomed. Eng.*, vol. 54, no. 1, pp. 29–38, Jan. 2007.

[32] F. Marlow and P. J. Tallman, *Welding Know-How*. Metal Arts Press, 2012.

[33] J. T. Dodge, B. G. Brown, E. L. Bolson, and H. T. Dodge, “Lumen diameter of normal human coronary arteries. Influence of age, sex, anatomic variation, and left ventricular hypertrophy or dilation,” *Circulation*, vol. 86, no. 1, pp. 232–246, Jul. 1992.

[34] M. VALDERRABANO, S. GREENBERG, H. RAZAVI, R. MORE, K. RYU, and E. K. HEIST, “3D Cardiovascular Navigation System: Accuracy and Reduction in Radiation Exposure in Left Ventricular Lead Implant,” *J. Cardiovasc. Electrophysiol.*, vol. 25, no. 1, pp. 87–93, Jan. 2014.

[35] S. M. Green *et al.*, “The current state of medical simulation in interventional cardiology: A clinical document from the Society for Cardiovascular Angiography and Intervention’s (SCAI) Simulation Committee,” *Catheter. Cardiovasc. Interv.*, vol. 83, no. 1, pp. 37–46, Jan. 2014.

Appendix A: Arduino Code

This appendix contains the code for the Arduino microcontroller system. The code implements a method to read a 2 bit quadrature encoder. The code also implements a communication protocol over a serial port between the Arduino and a MATLAB script.

```
#define encoderPinA 2
#define encoderPinB 3

volatile int encoderPos = 0;
String inputStr = "";
volatile char startCheck = 'b';
char input;

void setup() {
  // put your setup code here, to run once:

  pinMode(encoderPinA, INPUT);
  pinMode(encoderPinB, INPUT);
  attachInterrupt(0, doEncoderA, CHANGE);
  attachInterrupt(1, doEncoderB, CHANGE);
  Serial.begin(9600);

  inputStr.reserve(200);

  while (startCheck != 'a') {
    input = Serial.read();
    if (input == 'a') {
      startCheck = 'a';
      Serial.println("Starting");
      delay(100);
    } else {
      delay(100);
    }
  }
}

void loop() {
  // put your main code here, to run repeatedly:
  if(Serial.available()){
    char inChar = (char)Serial.read();
    if (inChar == 'r') {
      encoderPos = 0;
    } else if (inChar == 'x') {
      Serial.println(encoderPos);
    }
  }
  //Serial.println(encoderPos);
  //delay(1/60*1000); //output at 60Hz
}
```

```
void doEncoderA(){
  if(digitalRead(encoderPinA) == HIGH) {
    if(digitalRead(encoderPinB) == LOW) {
      encoderPos = encoderPos + 1;
    }
    else {
      encoderPos = encoderPos - 1;
    }
  }
  else {
    if(digitalRead(encoderPinB) == HIGH) {
      encoderPos = encoderPos + 1;
    }
    else {
      encoderPos = encoderPos - 1;
    }
  }
}

void doEncoderB(){
  if(digitalRead(encoderPinB) == HIGH) {
    if(digitalRead(encoderPinA) == HIGH) {
      encoderPos = encoderPos + 1;
    }
    else {
      encoderPos = encoderPos - 1;
    }
  }
  else {
    if(digitalRead(encoderPinA) == LOW) {
      encoderPos = encoderPos + 1;
    }
    else {
      encoderPos = encoderPos - 1;
    }
  }
}
```

Appendix B: MATLAB Arduino Interaction Code and User GUI

This appendix contains the MATLAB script and function files that implement the communication with the Arduino microcontroller and display the graphical user interface (GUI).

```
% Main.m
% This script builds the guidewire path, runs the user interface, and
% interacts with the Arduino microcontroller that is recording signals from
% the rotary encoder device.
```

Clean up workspace before starting

```
%clear
close all
clc
delete(instrfindall)
format compact
```

New File import

```
% Data Import
% Load datapoints in
% Pick Example Type
[relData, PnOData, relLandmark, PnOLandmark] = selectDataset(1);

% Filter Data
% Low pass filter below 1500hz.
% Remove noise in the data.
[filtData, dataInterp] = myLowPass(relData);

% Select Landmarks
% User indicates which points int the relative 3D position data are
% relevant to their interests. The algorithm will use this to develope a
% representation of the predicted guidewire path.
selectedLandmarks = selectLandmarks(relLandmark, filtData);
```

Fit Guidewire Path

```
%Default Settings
nIterations = 4;
minGap = 0.75; %cm
betweenPlaneRadius = 5; %cm
```

```
closePointRadius = 4; %cm
nPlanes = 20;

[spline, splinePts, buildPts] = iterativeSplineFit(selectedLandmarks, relData,
nIterations, minGap, betweenPlaneRadius, closePointRadius);
[graphFitPoints, meshes] = graphTheoryFit(dataInterp, splinePts, nPlanes);
```

Set Up

```
running = true;
%Communication port for the Arduino
comPort = 'COM3';

%Interpolate a finer resolution using cubic spline interpolation
vq = interp1(linspace(0,1,size(graphFitPoints,1)), graphFitPoints, linspace(0,1,1000),
'pchip');
xdata = vq(:,1);
ydata = vq(:,2);
zdata = vq(:,3);

%Initialize Arduino serial communication
ard = arduinoSetup(comPort);

% Encoder shaft diameter
d = 0.2475; %inches
% Encoder shaft circumference
c = d*pi; %inches
% Displacement per encoder tick
s = c/256; %inches
s = s*25.4; %mm
```

Plot Set-up

```
%Time axis
x = [0];
%Position axis
y = [0];

%Generate plot parameters
encoderDataFig = figure;
encoderDataFig.Position = [0 200 800 800];
ax = axes(encoderDataFig);
ax.Position = [0.1100 0.1100 0.7750 0.8150];
p = plot(ax, x, y);
xlim(ax, [0, 60])
xlabel('Time, [s]')
ylim(ax, [-500, 500])
ylabel('Distance from guidewire tip, [mm]')
```

```
%Generate catheter position figure
cathPosFig = figure;
cathPosFig.Position = [810 200 800 800];
ax2 = axes(cathPosFig);
ax2.Position = [.1100 .1100 .775 .8150];
hold on
guidewirePlot = plot3(ax2, xdata, ydata, zdata);
catheterPlot = plot3(ax2, xdata(1), ydata(1), zdata(1));
hold off
axis equal
grid on
view(3) %default 3D view
xlim(ax2, [min(xdata)-1, max(xdata)+1]);
xlabel('X [cm]')
ylim(ax2, [min(ydata)-1, max(ydata)+1]);
ylabel('Y [cm]')
zlim(ax2, [min(zdata)-1, max(zdata)+1]);
zlabel('Z [cm]')
cathPosFig.Visible = 'off';

%Generate control window figure
controlFig = figure;
controlFig.Position = [1620 500 300 300]; %[left bottom width height]
bg = uibuttongroup('Visible', 'off', 'Position', [ 0 0 1 1]);

posTxt = uicontrol(bg, 'style', 'text', 'Position', [20 200 240 80]);

resetbtn = uicontrol(bg, 'Style', 'pushbutton', 'String', 'Reset', ...
    'Position', [20 170 50 20], 'Callback', @resetEncoder);
resetbtn.UserData = ard;

showMapBtn = uicontrol(bg, 'Style', 'pushbutton', 'String', 'Show Map', ...
    'Position', [20 120 80 20], 'Callback', @showMap);
showMapBtn.UserData = cathPosFig;

gwLandmarkBtn = uicontrol(bg, 'Style', 'pushbutton', 'String', 'Guidewire Landmark', ...
     'Position', [20 70 120 20], 'Callback', @guidewireLandmark);
gwLandmarkBtn.UserData = ard;

cathLandmarkBtn = uicontrol(bg, 'Style', 'pushbutton', 'String', 'Catheter Landmark', ...
     'Position', [20 20 120 20], 'Callback', @catheterLandmark);
cathLandmarkBtn.UserData = ard;

bg.Visible = 'on';

disp('GUI set-up complete')
```

GUI Plotting Functions

```
tic
i = 1;
```

```
%Continuous Loop
while running

fprintf(ard, 'x'); %tell arduino to send position
pause(0.01) %wait for arduino to respond
currTime = toc; %get time passed since tic
val = fscanf(ard, '%d'); %read value from arduino
y(i) = val*s;
x(i) = currTime;
currentPos = val*s;
i = i+1;
%Plot of relative motion vs time, scrolling plot
arduinoPlotRealTime(encoderDataFig, ax, p, x, y);
%Plot of catheter and guidewire positions, 3D plot.
cathMap(cathPosFig, ax2, guidewirePlot, catheterPlot, currentPos);
%Text indicating measured relative displacement
set(posTxt, 'String', {'Displacement of catheter tip from guidewire tip: ', ' ',
horzcat(num2str(currentPos, '%.1f'), ' [mm]')});

end
```

Button Functions

```
function resetEncoder(source, event)
ard = source.UserData; %retrieve Arduino serial object stored in resetbtn.Userdata
fprintf(ard, 'r'); %send char 'r' to arduino which takes that as a reset to 0
end

function showMap(source, event)
h = source.UserData;
if strcmp(h.Visible,'off')
    h.Visible = 'on';
else
    h.Visible = 'off';
end
end

function guidewireLandmark(source, event)
setGuidewireLandmark(source.UserData)
display('Guidewire Landmark Set')
end

function setGuidewireLandmark(ard)
display('Sending reset command to Arduino')
fprintf(ard, 'r');
end

function catheterLandmark(source, event)
setCatheterLandmark(source.UserData)
display('Catheter Landmark Set')
```

```
end

function setCatheterLandmark(ard)
fprintf(ard, 'x'); %tell arduino to send position
pause(0.01) %wait for arduino to respond
val = fscanf(ard, '%d')
display(strcat('Current Distance to Guidewire Tip', val))
end
```

Published with MATLAB® R2017b

```
function [] = arduinoPlotRealTime(h, ax, p, x, y)
%arduinoPlotRealTime Plots the distance (mm) measured by the arduino and
%encoder.
%
%   Input
%   h: figure handle
%   ax: axes handle
%   p: plot handle
%   x: x dataset, time
%   y: y dataset, displacement

set(p, 'XData', x, 'YData', y);
set(h, 'Visible', 'on');
%Scale axis as needed
ylim(ax, [min(y)-50 max(y)+50])

%Show 60 seconds of data at a time
%Scroll forward from 30 seconds onward
if max(x) > 30
    xlim(ax, [max(x)-30, max(x)+30])
else
    xlim(ax, [0, 60])
end

end
```

Published with MATLAB® R2017b

```
function [ s ] = cathMap(h, ax, p1, p2, currentPos )
%cathMap Draws the guidewire path and the path of the catheter over it
%
%   Input
%   h: figure handle of plot figure
%   ax: axes handle of plot axes
%   p1: plot handle of 3D line plot of guidewire
%   p2: plot handle of 3D line plot of catheter
%   currentPos: double, value indicating the current difference in relative
%       displacement
%
%   Output
%   s: double, length of catheter in plot

s = 0; %Guidewire path length
for i = 1:length(p1.XData)-1
    %ds is the difference in two sequential points in the guidewire plot
    ds = sqrt((p1.XData(i+1)-p1.XData(i))^2 + ...
        (p1.YData(i+1) - p1.YData(i))^2 + ...
        (p1.ZData(i+1) - p1.ZData(i))^2);
    ds = ds*10; %convert cm to mm

    %Add up all distances to get total length
    s = s + ds;
end

if currentPos > 0
    %When guidewire is retracted proximal to the catheter tip
    disp('Catheter tip distal to guidewire tip')
else
    % Cathter is along same path as guidewire minus the relative
    % displacement difference
    cathLength = s + currentPos;
    cathDrawLength = 0;
    i = 1;
    while cathDrawLength < cathLength
        dl = sqrt((p1.XData(i+1)-p1.XData(i))^2 + ...
            (p1.YData(i+1) - p1.YData(i))^2 + ...
            (p1.ZData(i+1) - p1.ZData(i))^2);
        dl = dl*10; %convert cm to mm
        cathDrawLength = cathDrawLength + dl;
        i = i+1;
    end

    hold on
    %Plot catheter up to the i-th position along the guidewire
    set(p2, 'XData', p1.XData(1:i), 'YData', p1.YData(1:i), 'ZData', p1.ZData(1:i))
    %Set the catheter plot as blue and thick
    set(p2, 'Color', 'b', 'Linewidth', 2)
    %Place a marker at the tip of the catheter plot
    set(p2, 'Marker', 'o', 'MarkerIndices', i)
    hold off
```

```
end
end
```

Published with MATLAB® R2017b

Appendix C: MATLAB Guidewire Fit Code

This appendix contains the MATLAB functions used to produce a predicted guidewire path to the recorded MediGuide position data from the guidewire navigation.

```
function [spline, splinePoints, buildPoints] = iterativeSplineFit(selectedLandmarks,
relData, iterations, minGap, betweenPlaneRadius, closePointRadius)
%iterativeSplineFit Given a set of initial landmark points this function
%iterates a given number of time to refine the fit.
%   Detailed explanation goes here

n = iterations;
buildPoints = selectedLandmarks;
for i = 1:n
    landmarks = landmarkInterp(buildPoints, relData, minGap, betweenPlaneRadius,
closePointRadius);
    buildPoints = landmarks;
end

%Natural cubic spline fit to the build points of interest, ppform.
spline = cscvn(buildPoints(:,:)');
%Find a set of points for the spline from the ppform.
splinePoints = fnplt(spline)';

disp('Initial spline fit complete')

end
```

Published with MATLAB® R2017b

```
function [landmarksOut] = landmarkInterp(landmarksIn, data, minGap, betweenPlaneRadius,
closePointRadius)
%landmarkInterp Given a set of points and a data file this function
%determines a point of interest halfway between each set of points.
%
%   Input:
%   landmarksIn: n x 3 matrix, given set of landmarks
%   data: n x 4 matrix, dataset that is being fit to
%   minGap: double, number representing the distance between two landmarks
%       below which an interpolation will not be performed
%   betweenPlaneRadius: double, radius used when calculating the poitns of
%       interest between two landmarks. Greater than this and points will not
%       be included.
%   closePointRadius: double, radius used when calcuating the close points
%       to a point of interest. Greater than this and points will not be
%       included.
```

```
%
%   Output:
%   landmarksOut: set of landmarks found
%

%Find the largest distance between any two landmarks
    [~, biggestGap] = findLongestDistance(landmarksIn);

%Array of landmark locations
%Start with the first input landmark
landmarks = [landmarksIn(1,:)];

for i = 1:size(landmarksIn,1)-1
    %select two sequential landmarks
    p1 = landmarksIn(i, :);
    p2 = landmarksIn(i+1, :);


    %If the distance between the two selected landmarks is greater than or
    %equal to one-quarter of the largest gap, execute this block
    len = norm(p1-p2);
    if( len >= 0.25*biggestGap && len > minGap)

        %Find the middle point between the landmarks
        pMid = (p1+p2)./2;

        %Generate the set of points found between two planes and within a distance. Each
plane
        %passes through a landmark and is normal to the vector between the
        %planes
        pointsAvailable = pointsBetweenLandmarks([p1;p2], data, betweenPlaneRadius);

        %Find the points within a distance, d, of the line drawn between
        %the two vectors and within the set of pointsAvailable.
        %d = 4; %cm
        closePoints = findClosestPoint(pMid, pointsAvailable, closePointRadius);

        %If the set of points is not empty
        if ~isempty(closePoints)
            %Select the closest point
            pSelect = closePoints(1, :);

            if norm(pMid - pSelect) > closePointRadius
                %disp('Overreach')
                pSelect = p1;
            end

            landmarks = vertcat(landmarks, pSelect, p2);
            %disp('Non-empty close points set')
        else
            landmarks = vertcat(landmarks, p2);
            %disp('Empty close points set')
        end
```

```
    else
        landmarks = vertcat(landmarks, p2);
    end
end

landmarksOut = vertcat(landmarks, landmarksIn(end, :));

end
```

Published with MATLAB® R2017b

```
function [data, dataInterp] = myLowPass(relData)
%myLowPass Implements a low pass filter on the recorded dataset.
%   Input: dataset, n x 4 [time x y z]
%
%   The function interpolates a cubic spline between the recorded
%   datapoints to improve the response of the filter.
%
%   Passband Frequency: 1500 Hz
%   Stopband Frequency: 2000 Hz
%   Passband Attenuation: 1
%   Stopband Attenuation: 20
%
%   Output:
%   data: n x 4 matrix of filtered data
%   dataInterp: n x 4 matrix of data after interpolation before filtering



relData(:,1) = relData(:,1)./1000;
n = size(relData,1);

interpFreq = 1000000; %Hz
interpStep = 1/interpFreq;

t = relData(:,1);
tt = t(1):interpStep:t(end);
dataInterp = interp1(t, relData(:,2:4), tt, 'spline');

Fpass = 1500;
Fstop = 2000;
Apass = 1;
Astop = 20;

d = designfilt('lowpassiir', ...
  'PassbandFrequency',Fpass,'StopbandFrequency',Fstop, ...
  'PassbandRipple',Apass,'StopbandAttenuation',Astop, ...
  'DesignMethod','cheby2','SampleRate',interpFreq);

data = [tt' filtfilt(d, dataInterp)];
```

```
dataInterp = [tt', dataInterp];
disp('Data Filter Complete');

end
```

Published with MATLAB® R2017b

```
function [includedPoints] = pointsBetweenLandmarks(landmarks, data, dist)
%pointsBetweenLandmarks Finds set of 3D points contained between two other
%points
%
%   Input
%   landmarks: 2x3, points to be searched between [x y z]
%   data: nx4, the datset to be evaluated [t x y z]
%   dist: double, the range to evaluate for the max distance from the line
%   drawn between the two landmarks.
%
%   Output
%   includedPoints: nx3 matrix, points between the two landmarks [x y z]

% Selective point fits between landmarks

% The equation of a plane that contains the point [x0 y0 z0]
% with normal vector [a b c] is given by,
% a(x-x0) + b(y-y0) + c(z-z0) = 0;

%Vector Between landmarks
p1 = landmarks(1,:);
p2 = landmarks(2,:);
r = p2 - p1;

%Normal Plane at each Landmark
% Plane 1: a*x + b*y + c*z = a*x0 + b*y0 + c*z0;
% Plane 2: a*x + b*y + c*z = a*x1 + b*y1 + c*z1;
%Select subset of data between the planes
% If  plane1 < [x y z] < plane2 or plane1> [x y z] > plane2

plane1 = r(1)*p1(1)+r(2)*p1(2)+r(3)*p1(3);
plane2 = r(1)*p2(1)+r(2)*p2(2)+r(3)*p2(3);

includedPoints = [];

%Parfor to parallelize for faster execution time
parfor i=1:size(data,1)
    point = data(i, 2:4);

    pointVal = r(1)*point(1)+r(2)*point(2)+r(3)*point(3);

    pointDistance(i) = norm(cross(abs(point - p1), abs(point - p2))/norm(p2-p1));

    if ((plane1 < pointVal && pointVal < plane2) ...
```

```
            || (plane1 > pointVal && pointVal > plane2)) ... %Is it between the two
planes?
            && (pointDistance(i) < dist) %Is it within a distance dist?
        includedPoints = vertcat(includedPoints, point);
    end
end
end
```

Published with MATLAB® R2017b

```
function [outputArg] = findClosestPoint(x, data, distanceLimit)
%findClosestPoint Finds the set of points closest to a point within a
%bound.
%   Input
%   x: 1x3 vector, Input point of interest, [x y z]
%   data: n x 3 matrix, dataset of interest [x y z]
%   distanceLimit: double, bound on calculating set of points
%
%   Output
%   outputArg: set of points with the close bound
%

if isempty(data)
    outputArg = [];
    return;
end

%If data file is very large limit points for speed
% n = size(data,1);
% if n > 100000
%     data = data(1:ceil(n/100000):end,:);
% end

%Find relative position vector from point of interest to every data point
difference = x - data;
%Pre aloccate distance vector
distance = zeros(size(difference,1),1);

for i = 1:size(difference,1)
    %Calculate distance to every point in the dataset
    distance(i) = norm(difference(i,:));
end

%Sort distances and get index array
[B,I] = sort(distance);
%Use index array to sort datapoints from closest to furthest
data = data(I, :);
%Select only the data that is within the range of interest
inBoundsData = data(distance<distanceLimit, :);

outputArg = [];
```

```
if isempty(inBoundsData)
    outputArg = findClosestPoint(x, data, distanceLimit+1);
else
    ind = zeros(length(distance),1);
    for i = 1:length(distance)
        if distance(i) < distanceLimit
            ind(i) = i;
        end
    end
    outputArg = data(find(ind),:);
end



end
```

Published with MATLAB® R2017b

```
function [circle3DTranslate] = circFit3D(points, normalVector, vectorOrigin, nPoints)
```

```
%circFit3D Uses a set of 3D points, a vector, and an origin, and generates a circle fit
%to the points projected into the normal plane of the vector
%
%   Input
%   points: nx3 matrix, set of 3D points to be projected
%   normalVector: 1x3 matrix, normal vector the plan the points will be
%       projected onto
%   vectorOrigin: 1x3 matrix, spatial coordinates of the vector
%   nPoints: int, the number of points in the circle fit
%
%   Using the given vector a unit normal vector is created and a basis for
%   a plane normal to the vector is created. The 3D points are projected
%   onto the plane basis to create a projection of the poitns. The center
%   of the circle fit is placed at the mean of the points in the local x
%   and y coordinates. The radius used is the average of the max-min in
%   each coordinate direction.
%
%   Depending on the number of points requested in the circle fit points
%   are calcuated centered at the circle fit center and at the fit radius
%   spaced evenly around the circle.
%
%   The radius is bounded by the range of 0.05cm to 0.25cm based on
%   phyiosological data of coronary anatomy.
%
%   The 2D circle fit is projected back into the 3D space it was generated
%   from and translated to the origin of the input vector.
%
%   Output
%   cicle3DTranslate: n x 3 matrix of points in the circle fit, [x y z]
%
```

```
% Find projection plane unit normal vector
unitNormal = normalVector/norm(normalVector);

% Plane basis
uv = null(unitNormal);

% Projected Points onto plane
p2DinPlane = points*uv;

%[xc,yc,R,a] = circfit(p2DinPlane(:,1), p2DinPlane(:,2));
xc = mean(p2DinPlane(:,1));
yc = mean(p2DinPlane(:,2));
xspan = max(p2DinPlane(:,1)) - min(p2DinPlane(:,1));
yspan = max(p2DinPlane(:,2)) - min(p2DinPlane(:,2));
R = (xspan+yspan)/2;

interval = pi/(nPoints/2);
th = (0:interval:2*pi-interval)';

% Upper and lower limits on radius
lowLimit = 0.05;
upperLimit = 0.25;
if size(points,1) < 3
    R = (lowLimit+upperLimit)/2;
else if R < lowLimit
        R = lowLimit;
    else if R > upperLimit
            R = upperLimit;
        end
    end
end

circle = [R*cos(th)+xc R*sin(th)+yc];
```

Back into 3D coordinate system

```
circle3D = (circle*uv.');
centerCircle3D = mean(circle3D);
T = vectorOrigin - centerCircle3D;
circle3DTranslate = [centerCircle3D; circle3D] + T;

end
```

Published with MATLAB® R2017b

Appendix D: MATLAB Guidewire Fit Design of Experiments Code

This appendix contains the script file used to execute the guidewire fit algorithm on multiple datasets. The script applies the same functions to variations of algorithm fit parameters and then evaluates the results with a fit quality function and a recording of the time to execute the function.

Guidewire Path Fit Analysis DOE

- Central Composite Design Inscribed due to limits on reasonable values
- One center point because there is no variation with identical input
- 2 Replicates with user selected points
- Response Variables:
    - fitQuality
    - Runtime
- Factors: 6
    - Iterative Spline Fit
        1. nIterations
        2. minGap
        3. betweenPlaneRadius
        4. closePointRadius
    - Graph Theory Fit
        5. nPlanes
        6. nPoints

Set Up

```
clear
close all
clc
format compact

% Get or Start parallel pool workers
pp = gcp;
disp('Parallel Pool started')
```

Design Set Up

```
%Default Values used as center points
nIterations = 4;
minGap = 0.75; %cm
betweenPlaneRadius = 5; %cm
closePointRadius = 4; %cm
nPlanes = 20;
nPoints = 6;

testParamDefault = [nIterations, minGap, betweenPlaneRadius, closePointRadius, nPlanes,
nPoints];
```

```
%Generate central composite design standard order matrix
dCC = ccdesign(6, 'fraction', 0, 'center', 1, 'type', 'inscribed');

testParams = zeros(size(dCC,1), length(testParamDefault));

%Modify ccd standard order matrix with test parameters
for i = 1:length(testParamDefault)
    testParams(:,i) = dCC(:,i)*testParamDefault(i)+testParamDefault(i);
end

%Modify ccd design due to limits on algorithm functions
testParams(:,[1, 5, 6]) = round(testParams(:,[1,5,6])); %Iteration number, plane number,
point number: must be integers
testParams(testParams <= 0) = 1; %No parameter should be less than or equal to zero
testParams(testParams(:,5)<5, 5) = 5; % Minimum of 5 planes for graph theory fit
testParams(testParams(:,6)<3, 6) = 3; %Minimum of 3 points on mesh plane
```

Data Import

```
% Define the datasets and landmark selections to be used before running.
% Can run multiple sets of data or landmarks in one run. Output is into a
% struct with data required for each run and response for each run stored
% within the struct.


%Datasets = [1 3 5a 5b 1 3 5a 5b]
%dataSets = [1 3 5 5 1 3 5 5]
%[2a 2b 2a 2b]
dataSets = [2 2 2 2];

for i = 1:length(dataSets)
    %Pick Example Type
    [relData, PnOData, relLandmark, PnOLandmark] = selectDataset(dataSets(i));

    %Filter Data
    [filtData, dataInterp] = myLowPass(relData);

    % Select Landmarks
    selectedLandmarks = selectLandmarks(relLandmark, relData);

    %Struct of test data selections
    Test(i).relData = relData;
    Test(i).selectedLandmarks = selectedLandmarks;
    Test(i).dataInterp = dataInterp;
    Test(i).filtData = filtData;

end
```

Fit Guidewire Path

```
%For every dataset selected previously
for j = 1:length(dataSets)
    results(j).responseVars = zeros(size(testParams,1), 2); %[fitQuality runTime]

    failedRunsIndex = [];

    %For all test parameters in the standard order matrix
    for i = 1:size(testParams, 1)
        disp(strcat('DOE test run: ', num2str(i)))

        %Define parameters for the algorithm
        nIterations = testParams(i,1);
        minGap = testParams(i,2);
        betweenPlaneRadius = testParams(i,3);
        closePointRadius = testParams(i,4);
        nPlanes = testParams(i,5);
        nPoints = testParams(i,6);

        %Try-Catch due to non-robust algorithm. Sometimes fails, in that
        %case zeros are entered into the response and handled later in the
        %data analysis. Replication is important to help mitigate this.
        try
            %Record the start time
            tic

            %Fit the guidewire path
            [spline, splinePts, buildPts] = iterativeSplineFit(Test(j).selectedLandmarks,
Test(j).relData, nIterations, minGap, betweenPlaneRadius, closePointRadius);
            [graphFitPoints, meshes] = graphTheoryFit(Test(j).relData, splinePts,
nPlanes, nPoints);
            vq = interp1(linspace(0,1,size(graphFitPoints,1)), graphFitPoints,
linspace(0,1,1000), 'pchip'); %interpolate the spline

            %Record the end time
            runtime = toc;

            testData = Test(j).filtData(1:10:end,:);

            %Evaluate the quality of the fit
            fitQuality = fitQualityEval(testData, vq);
        catch
            runtime = 0;
            fitQuality = 0;
            failedRunsIndex = [failedRunsIndex i];
        end

        %Store results in the results struct.
        results(j).responseVars(i,:) = [fitQuality, runtime];

    end
end
```

Published with MATLAB® R2017b

Appendix E: Prototype Device Drawings

ITEM NO.	PART NUMBER	DESCRIPTION	QTY.
1	Bottom	PRIMARY COMPONENT OF DEVICE	1
2	AlignmentBlockExit	GUIDEWIRE EXIT ALIGNMENT GUIDE	1
3	57155K304	1/2 X 1/4 FLANGE BEARING R188	2
4	EncoderShaft	ENCODER SHAFT	1
5	AlignmentBlockEntry	GUIDEWIRE ENTRY ALIGNMENT GUIDE	1
6	90145A477	5/32 18-8 DOWEL PIN	1
7	90145A471	1/8 X 1/2 18-8 DOWEL PIN	6
8	ES14	BOURNES ES14 ROTARY ENCODER	1
9	ClampArm	ILDER BEARING CLAMPING ARM	1
10	57155K371	SEALED BEARING, R155-2Z	1
11	90145A490	5/32 X 3/4 18-8 DOWEL PIN	1
12	EncoderMount	ENCODER MOUNT	1
13	93585A015	KNURLED KNOB 6-32 X 1/2	1
14	51525K241	LUER LOCK FITTING 1/4"-28 UNF	1

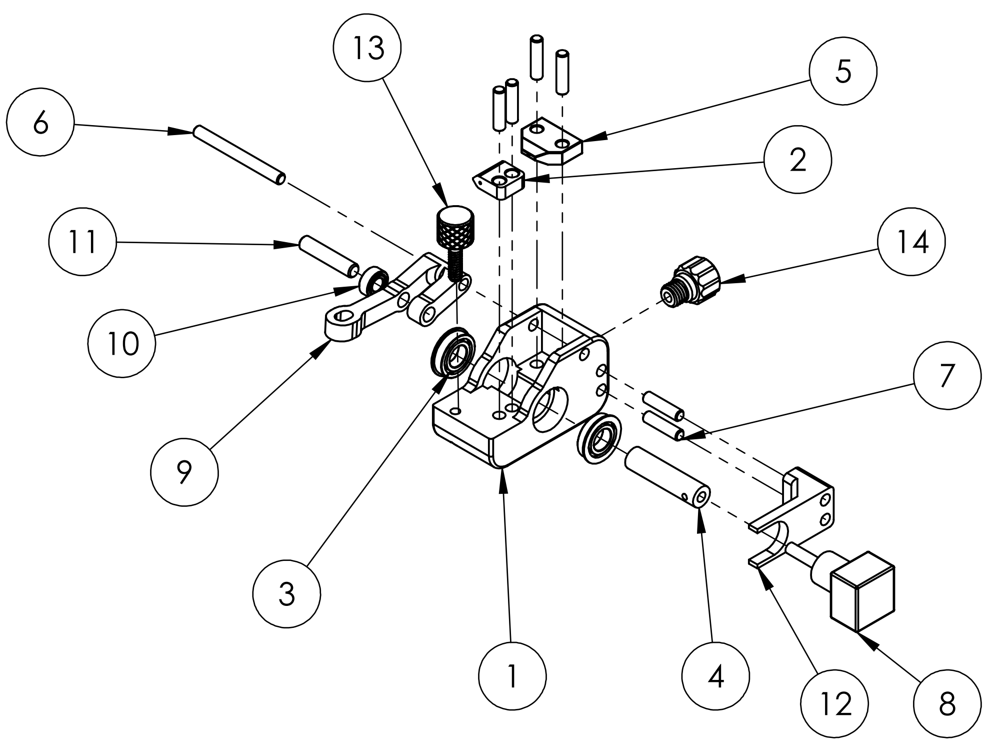

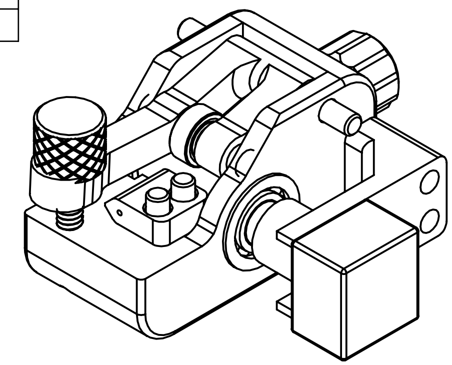

SCALE: 1:1

Cal Poly Biomedical Engineering Catheter Localization Thesis Project		Title: OVER-THE-WIRE PROTOTYPE	Drwn. By: A. EVARD
		Date: 5/14/18 / Scale: 1:2	

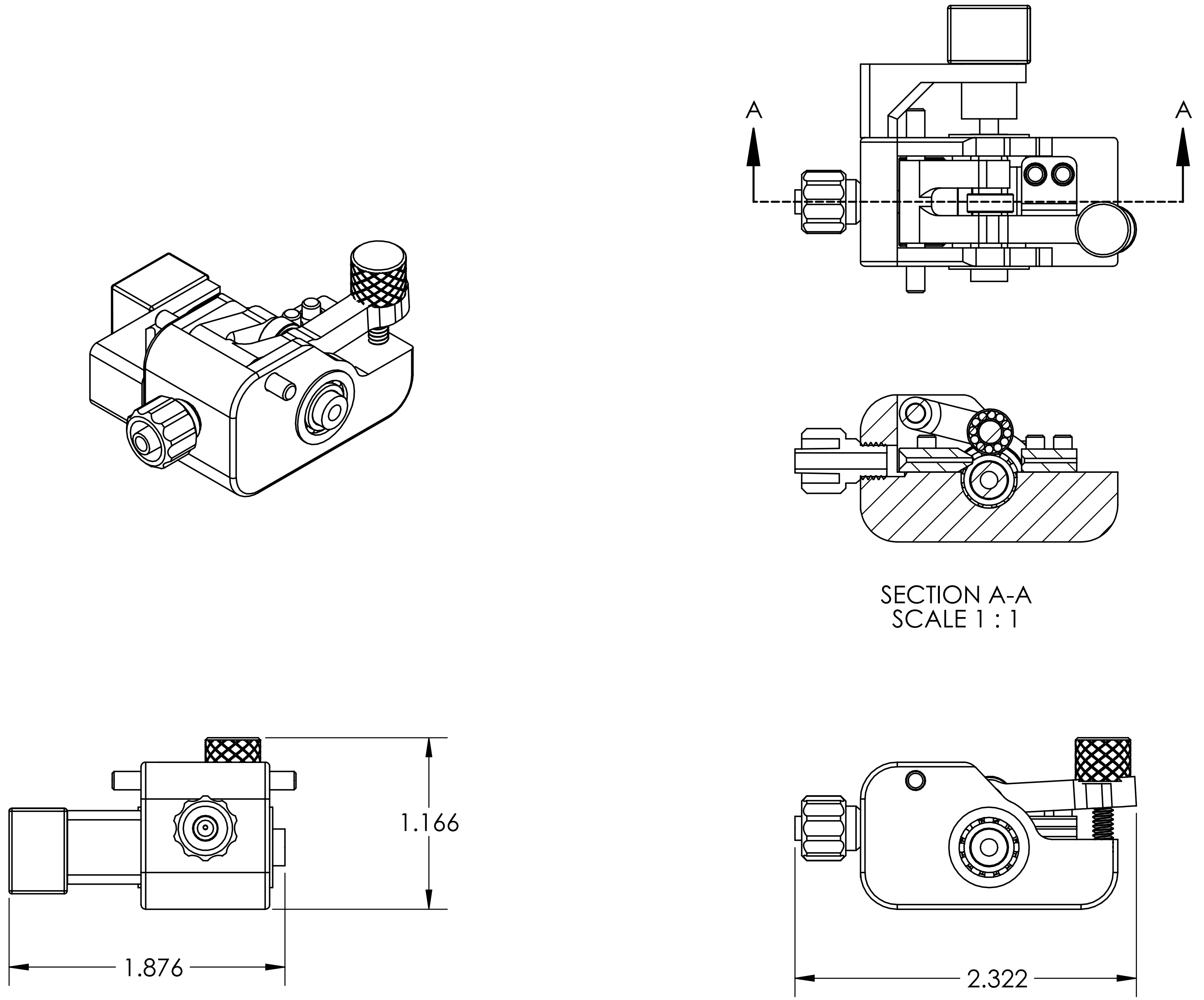

Cal Poly Biomedical Engineering Catheter Localization Thesis Project			Title: ASSEMBLY		Drwn. By: A. EVARD
			Date: 5/14/18	Scale: 1:1	

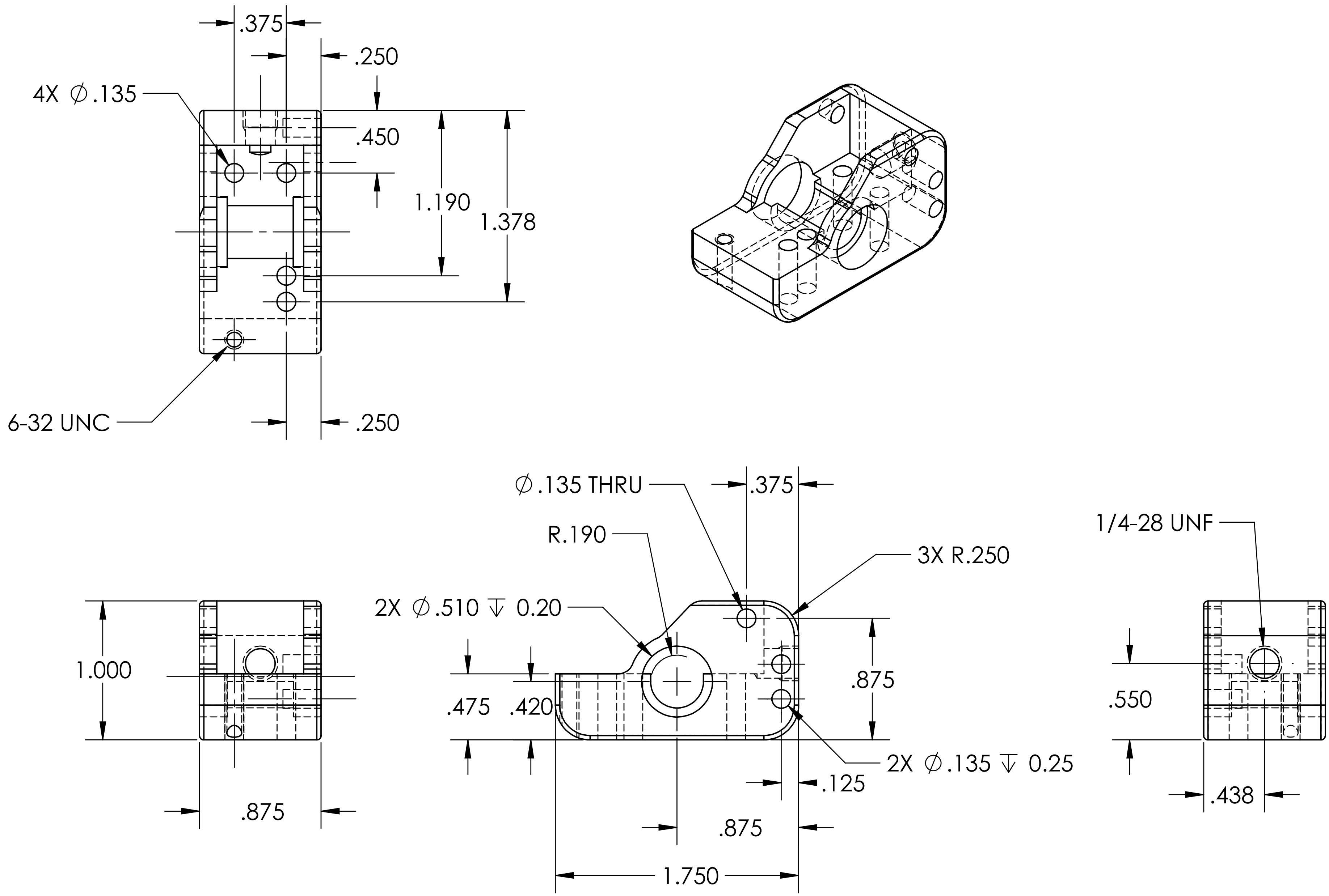

Cal Poly Biomedical Engineering Catheter Localization Thesis Project			Title: BOTTOM	Drwn. By: A. EVARD
			Date: 5/14/18 — Scale: 1:1	

ENTRY ALIGNMENT BLOCK

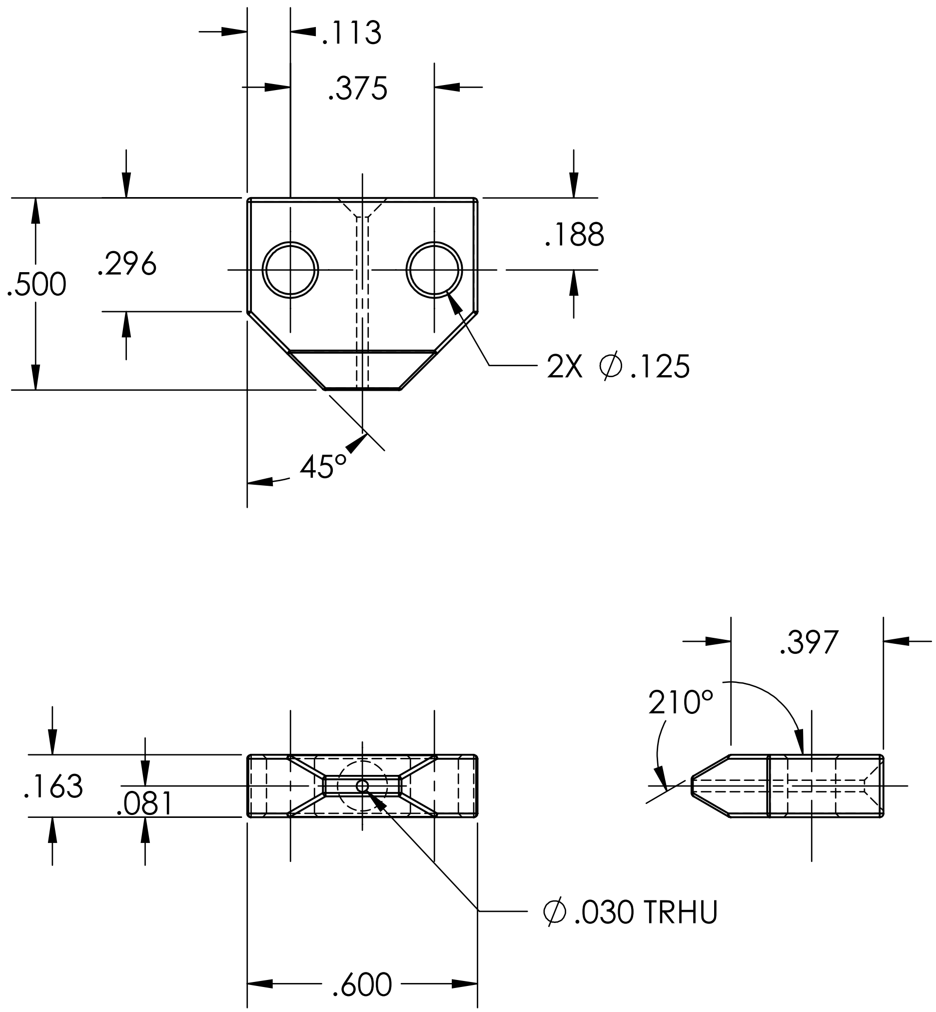

EXIT ALIGNMENT BLOCK

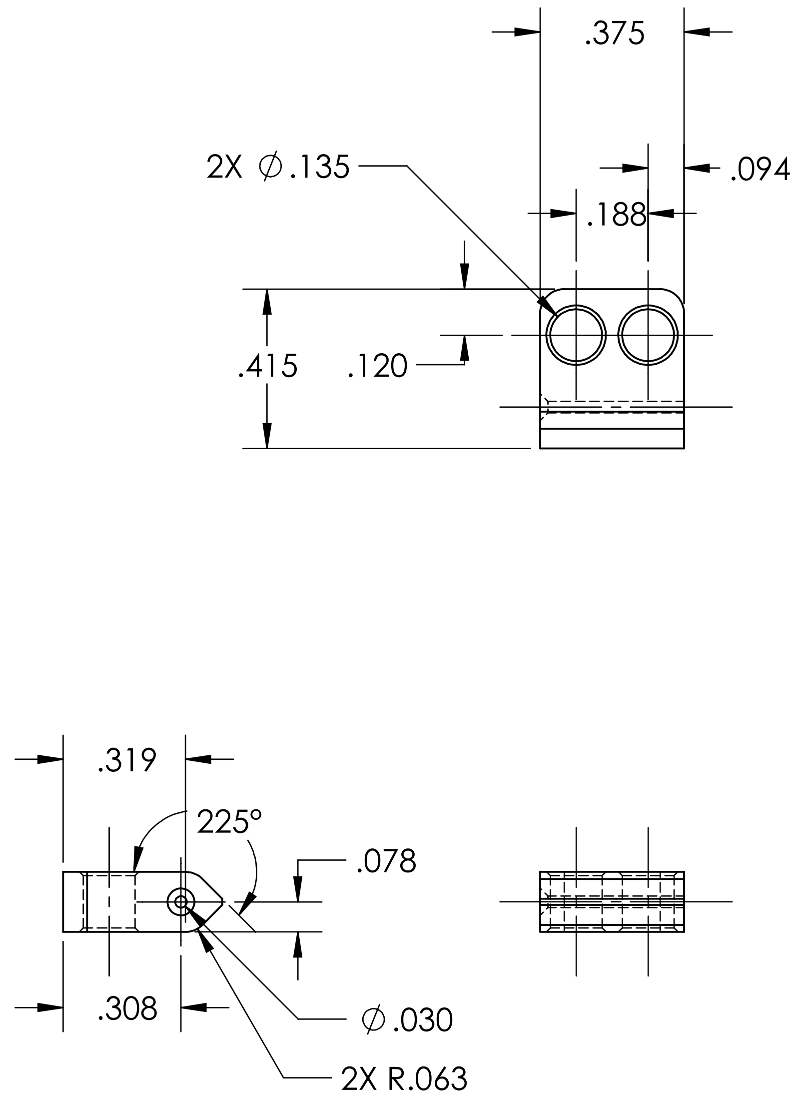

Cal Poly Biomedical Engineering Catheter Localization Thesis Project			Title: ALIGNMENT BLOCKS	Drwn. By: A. EVARD
			Date: 5/14/18 / Scale: 2:1	

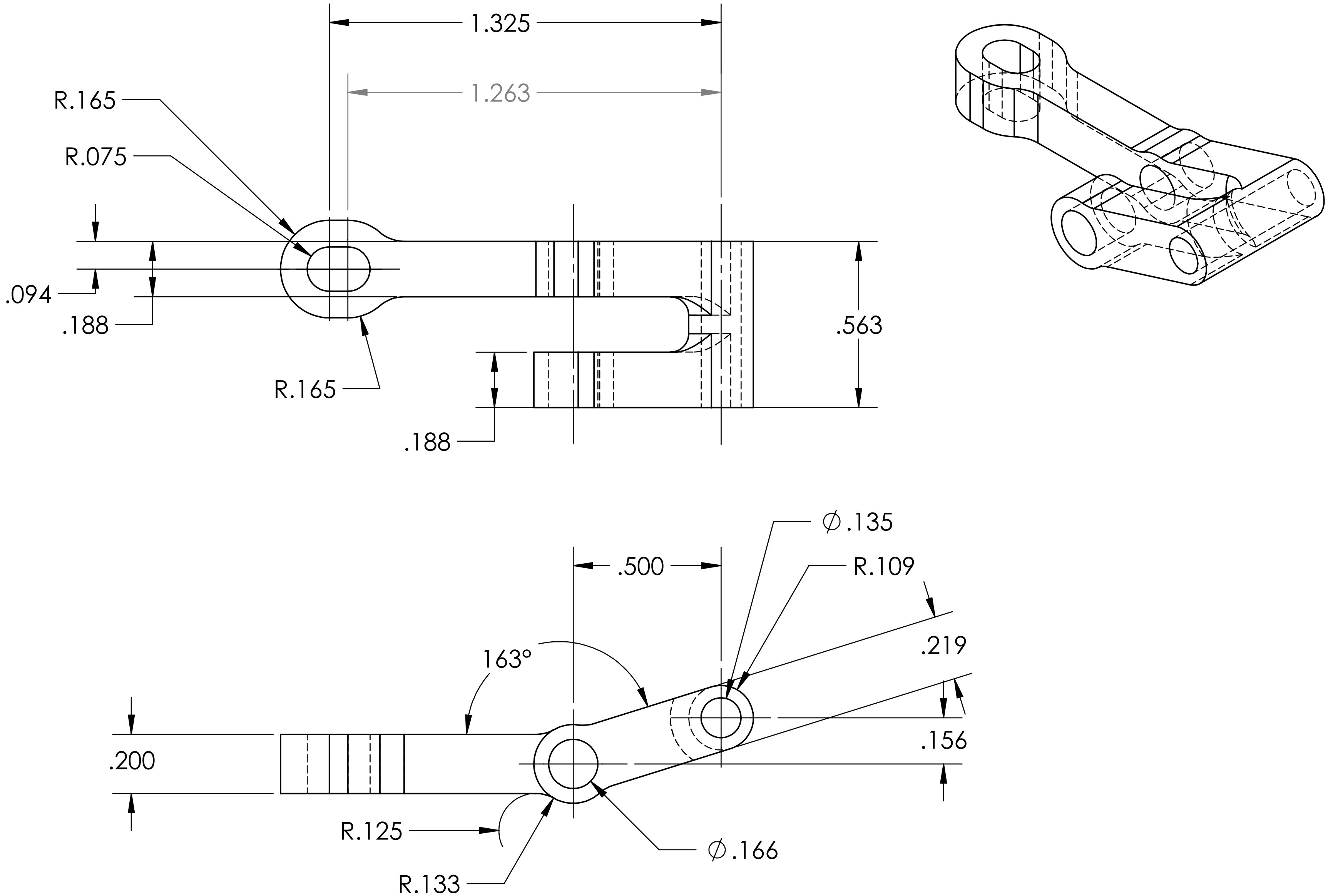

Cal Poly Biomedical Engineering Catheter Localization Thesis Project			Title: CLAMP ARM	Drwn. By: A. EVARD
			Date: 5/14/18 / Scale: 2:1	

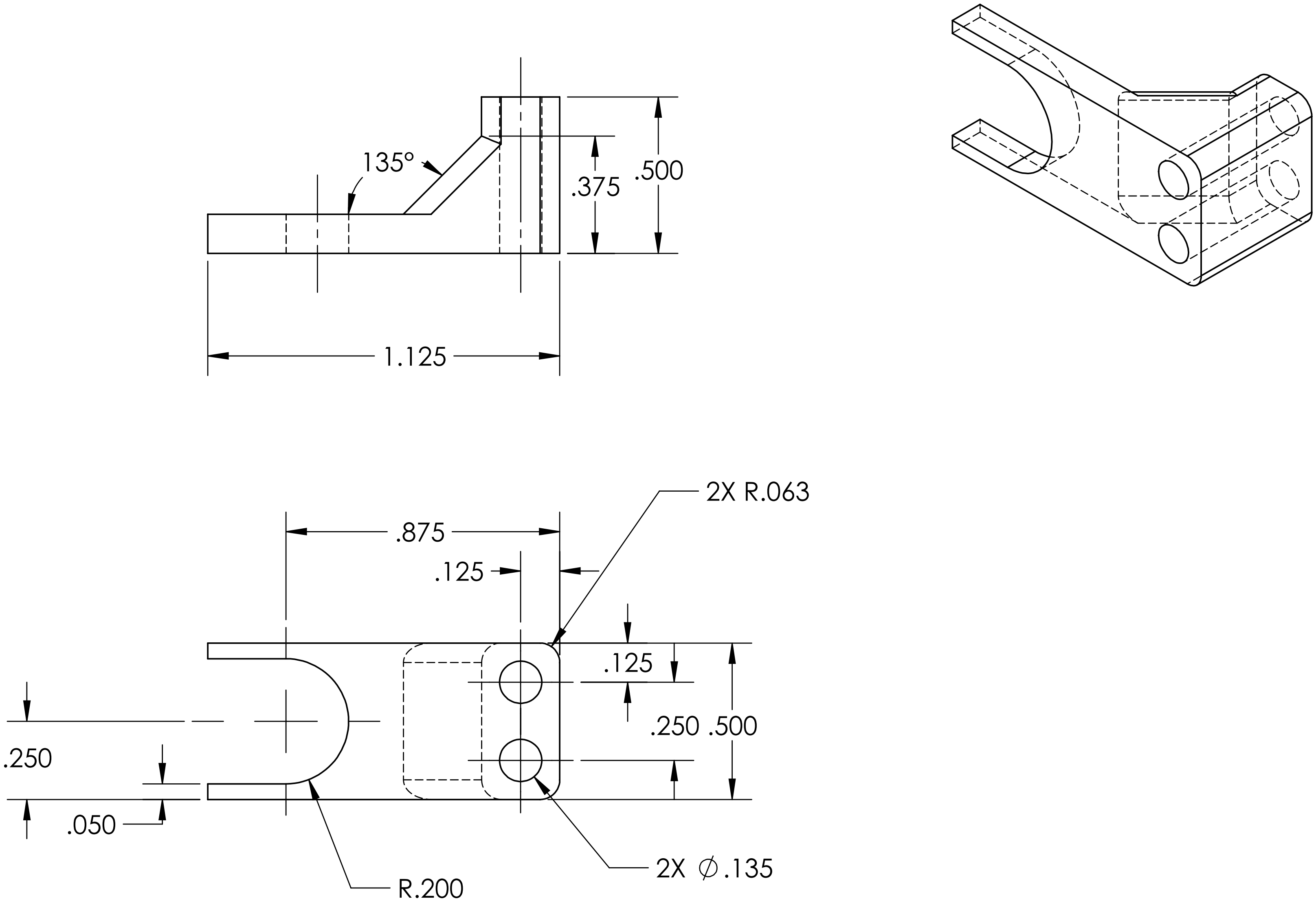

Cal Poly Biomedical Engineering Catheter Localization Thesis Project			Title: ENCODER MOUNT	Drwn. By: A. EVARD
			Date: 5/14/18 | Scale: 2:1	

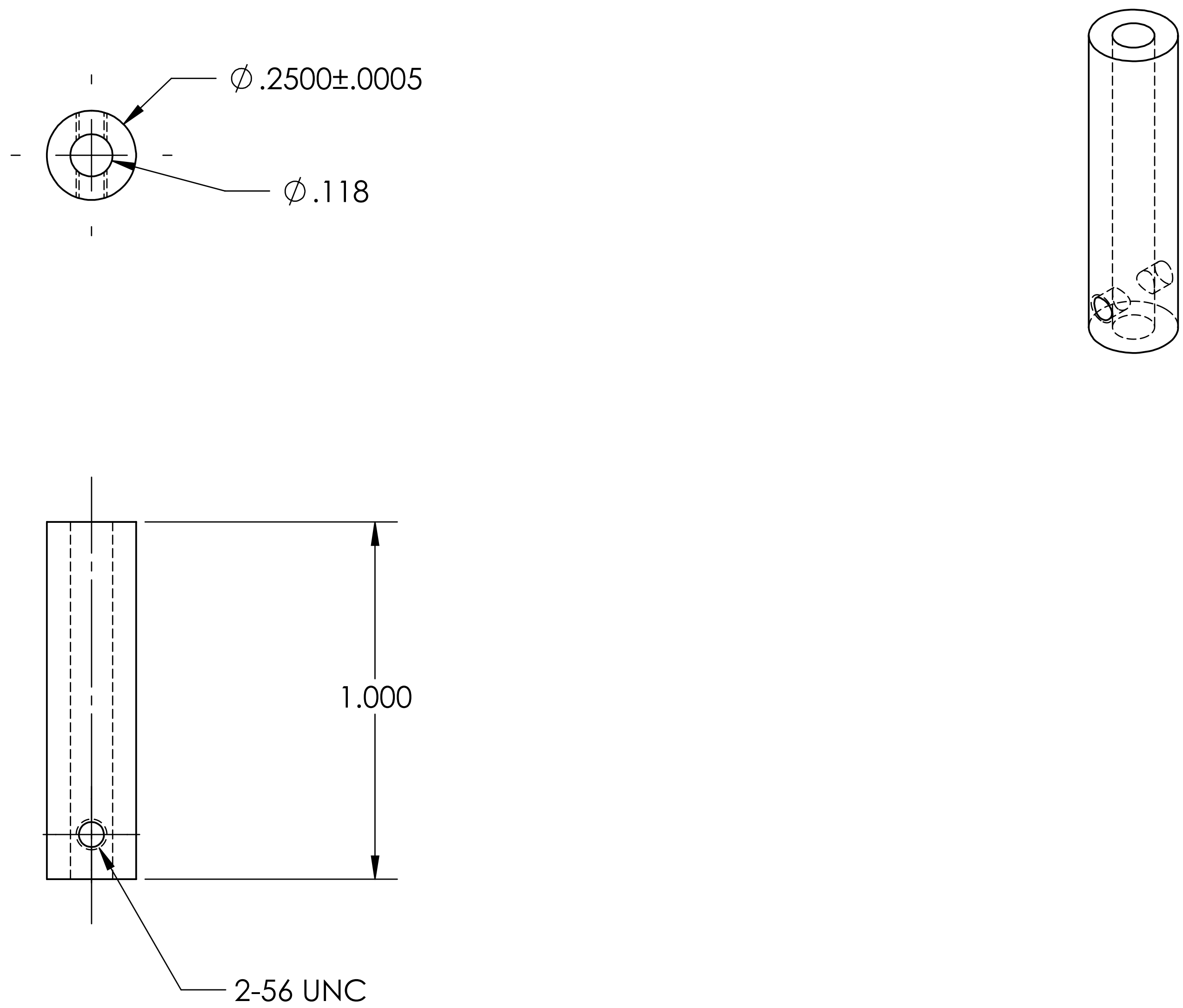

Cal Poly Biomedical Engineering Catheter Localization Thesis Project			Title: ENCODER SHAFT	Drwn. By: A. EVARD
			Date: 5/14/18 | Scale: 2:1	

ITEM NO.	PART NUMBER	DESCRIPTION	QTY.
1	57155K304	1/2 X 1/4 FLANGE BEARING R188	2
2	AlignmentBlock	CATHETER ENTRY ALIGNMENT GUIDE	1
3	ES14	BOURNES ES14 ROTARY ENCODER	1
4	EncoderShaft	ENCODER SHAFT	1
5	Bottom	PRIMARY COMPONENT OF DEVICE	1
6	90145A477	5/32 18-8 DOWEL PIN	1
7	AlignmentBlockExit	CATHETER EXIT ALIGNMENT GUIDE	1
8	ClampArm	IDLER BEARING CLAMPING ARM	1
9	57155K371	5/32 BEARING R155-2Z	1
10	90145A490	5/32 18-8 DOWEL PIN	1
11	93585A016	KNURLED KNOB 6-32 X 1/2	2
12	EncoderMount	ENCODER MOUNT	1
13	90145A471	1/8 X 1/2 18-8 DOWEL PIN	6

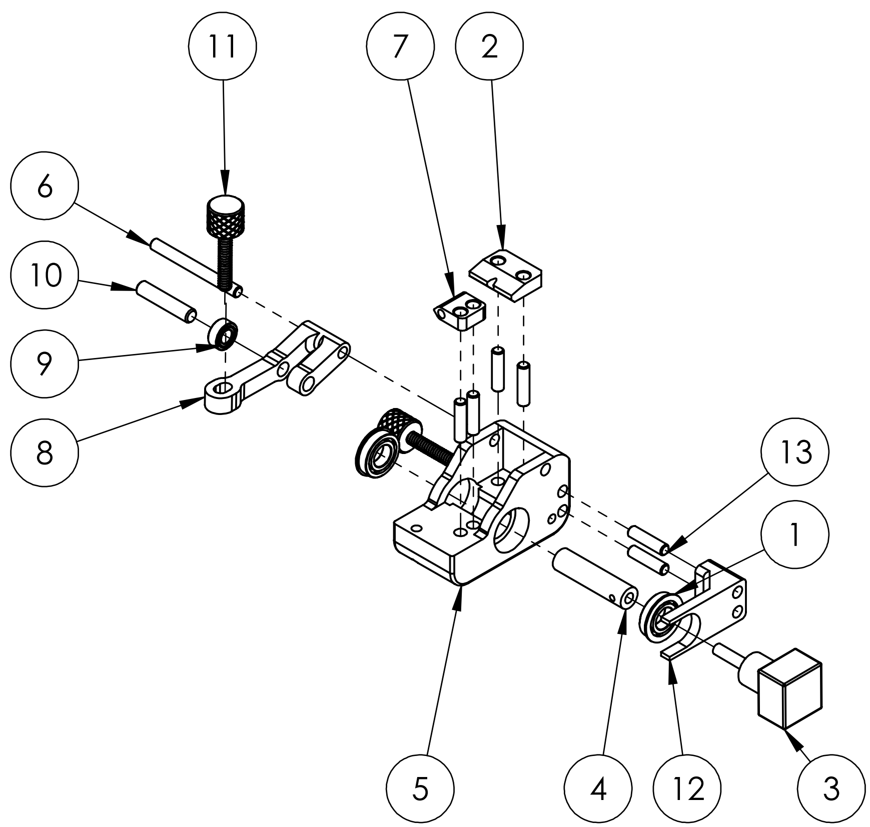

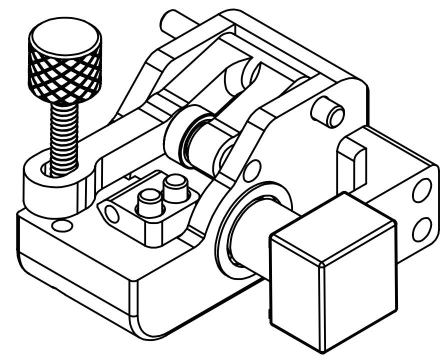

SCALE: 1:1

Cal Poly Biomedical Engineering Catheter Localization Thesis Project			Title: RAPID EXCHANGE DEVICE	Drwn. By: A. EVARD
			Date: 5/14/18 / Scale: 1:2	

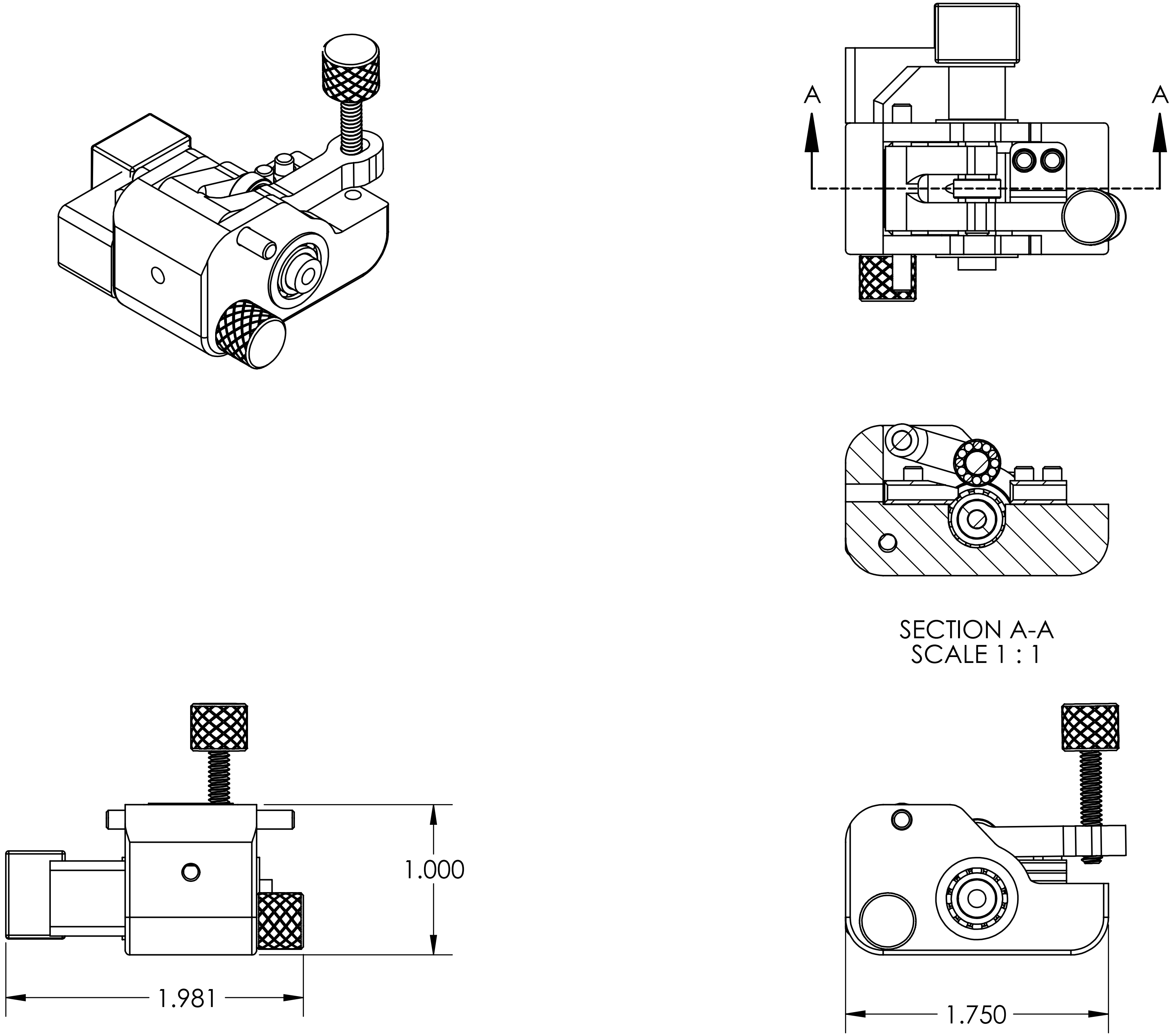

Cal Poly Biomedical Engineering Catheter Localization Thesis Project			Title: ASSEMBLY	Drwn. By: A. EVARD
			Date: 5/14/18 / Scale: 1:1	

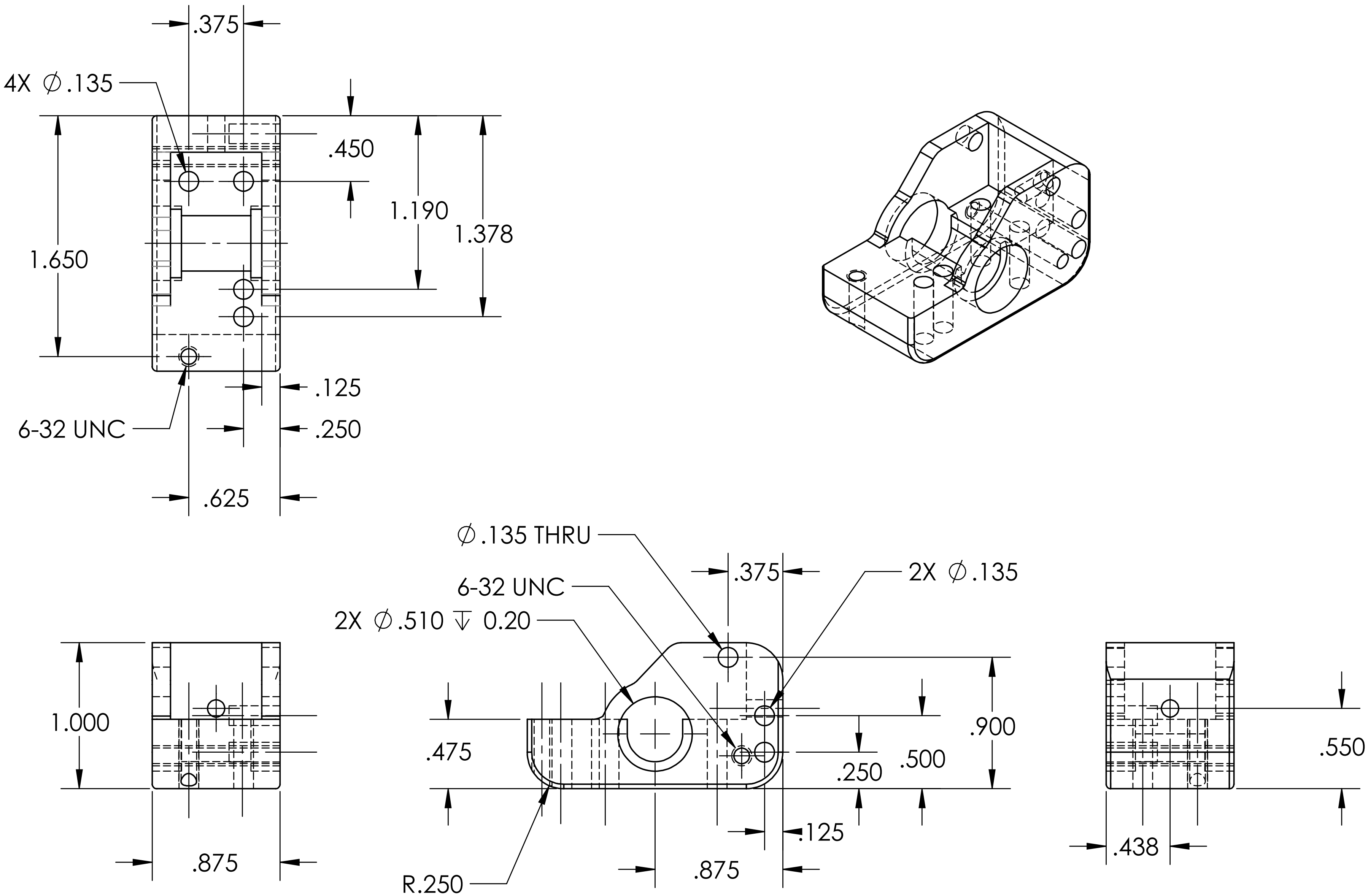

Cal Poly Biomedical Engineering Catheter Localization Thesis Project			Title: BOTTOM	Drwn. By: A. EVARD
			Date: 5/14/18 / Scale: 1:1	

ENTRY ALIGNMENT BLOCK

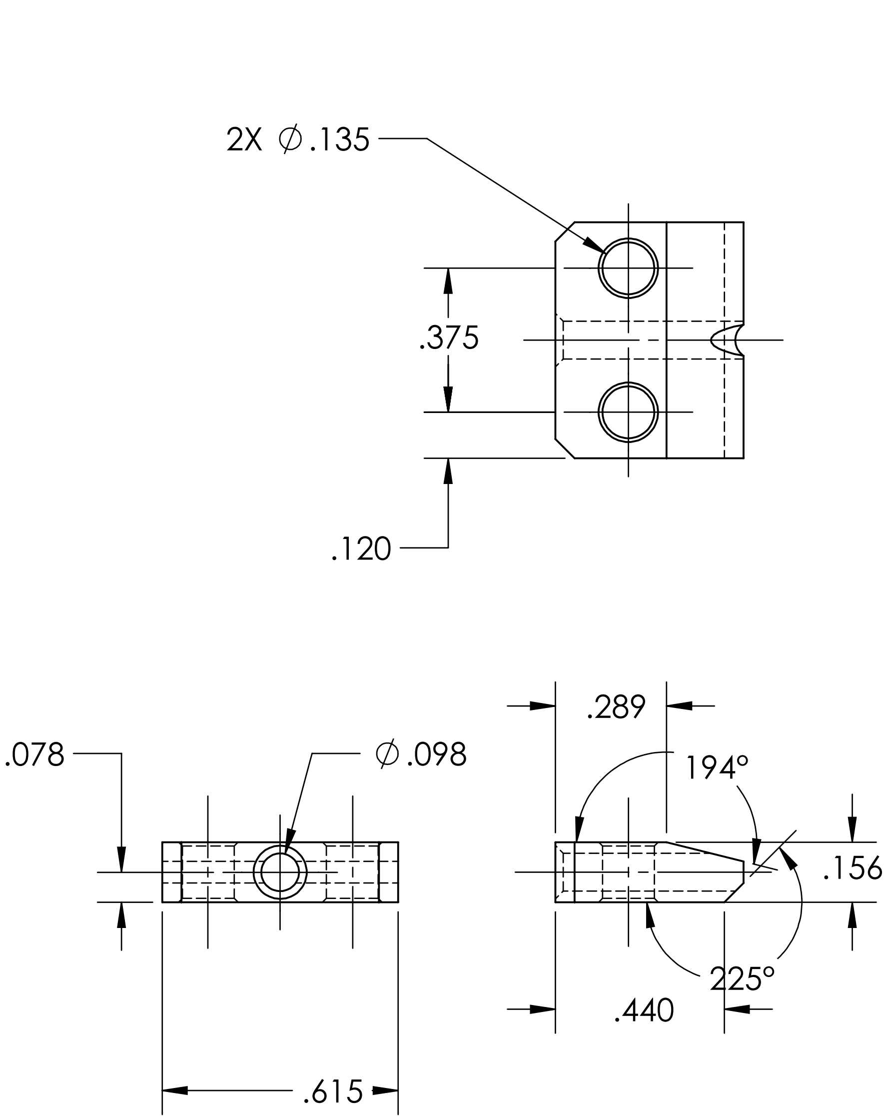

EXIT ALIGNMENT BLOCK

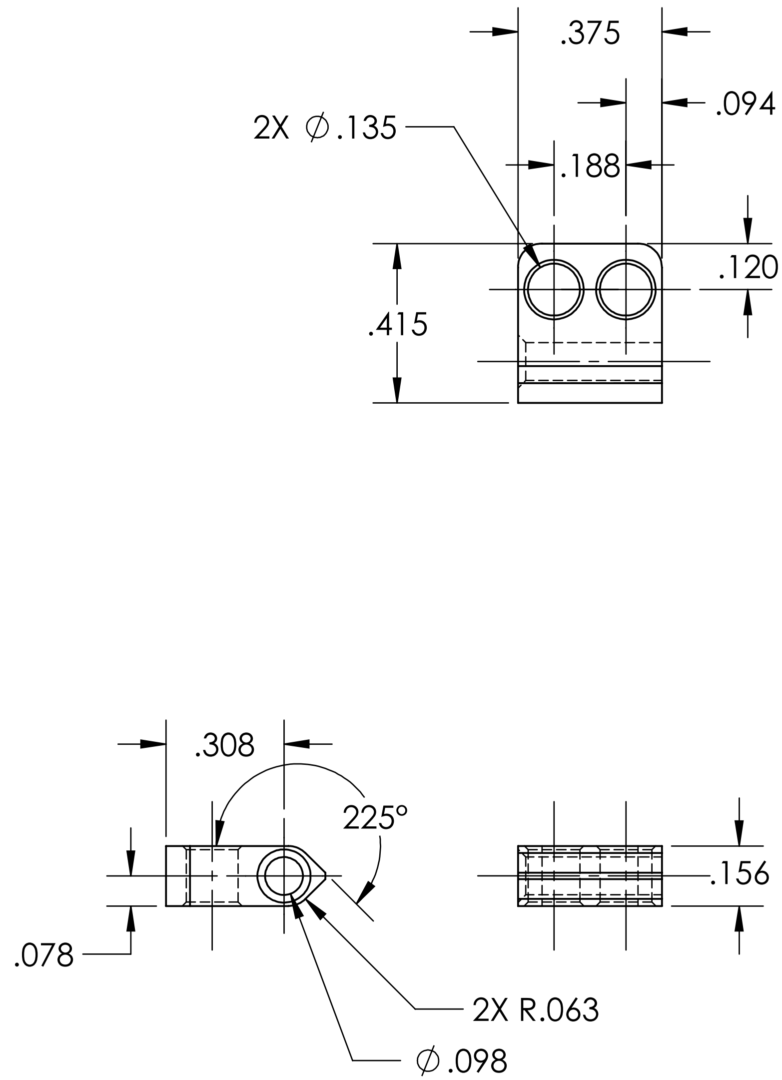

Cal Poly Biomedical Engineering Catheter Localization Thesis Project			Title: ALIGNMENT BLOCKS	Drwn. By: A. EVARD
			Date: 5/14/18 / Scale: 2:1	

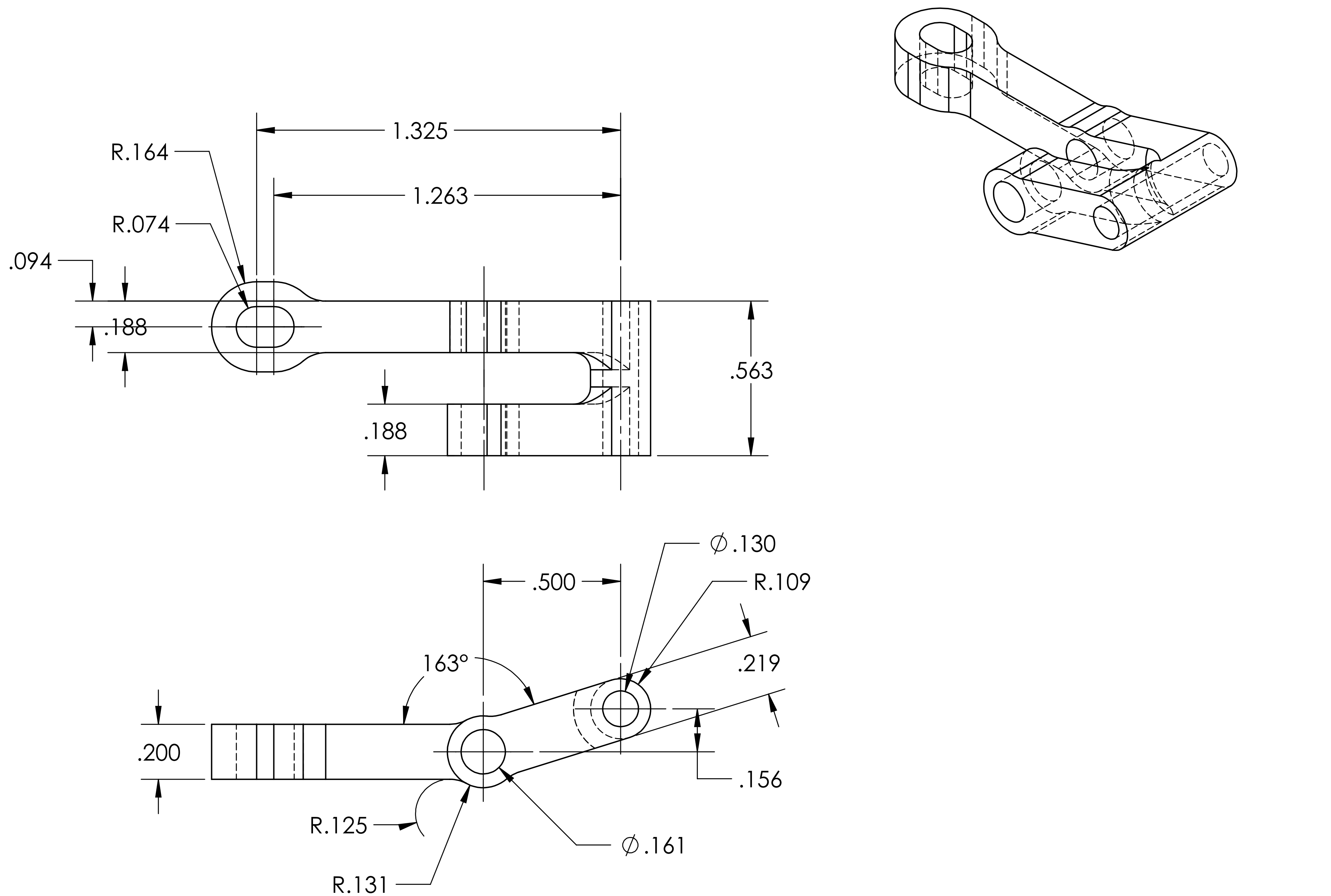

Cal Poly Biomedical Engineering Catheter Localization Thesis Project			Title: CLAMP ARM	Drwn. By: A. EVARD
			Date: 5/14/18 / Scale: 2:1	

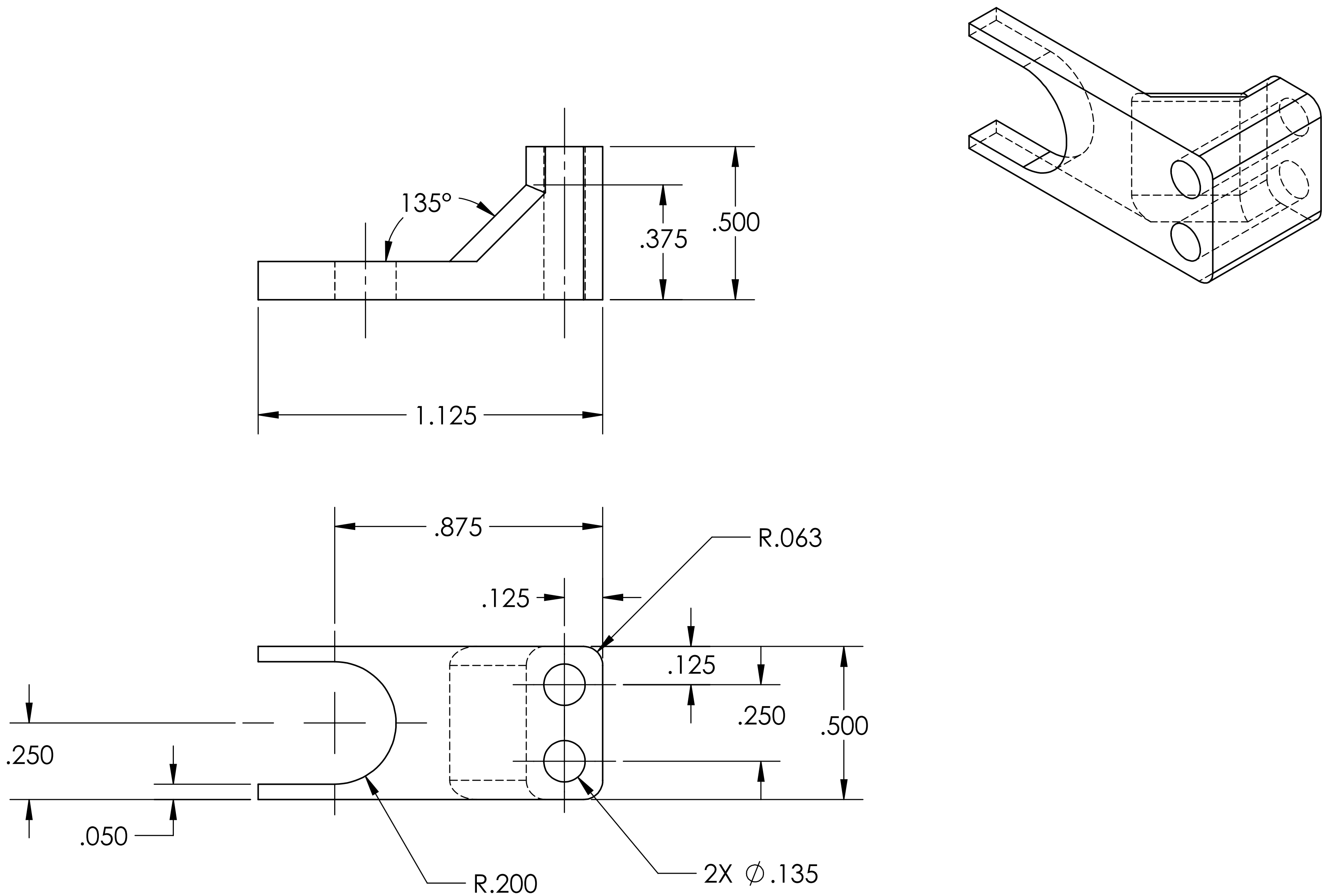

Cal Poly Biomedical Engineering Catheter Localization Thesis Project			Title: ENCODER MOUNT		Drwn. By: A. EVARD
			Date: 5/14/18	Scale: 2:1	

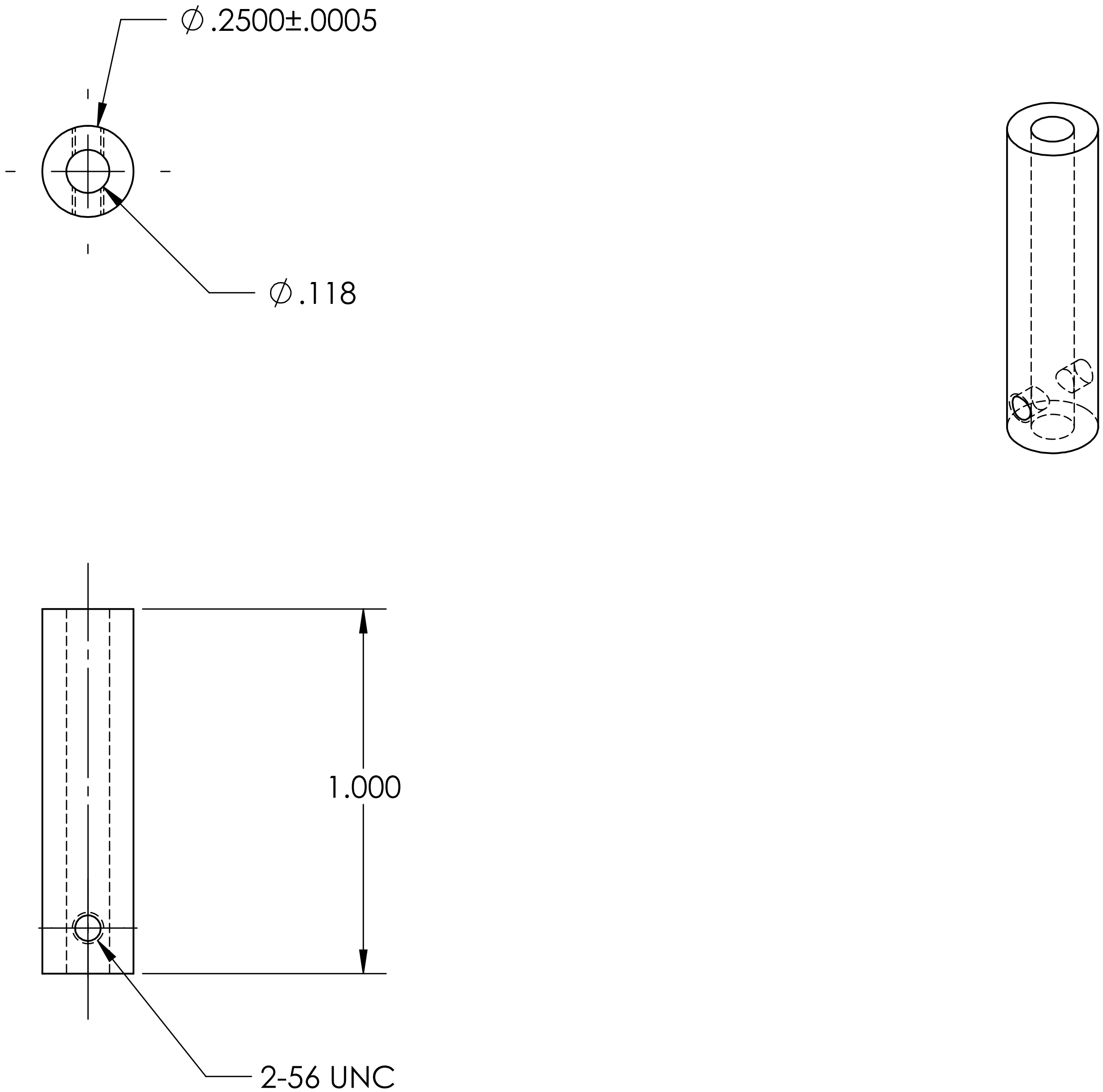

Cal Poly Biomedical Engineering Catheter Localization Thesis Project			Title: ENCODER SHAFT	Drwn. By: A. EVARD
			Date: 5/14/18 / Scale: 2:1	

Appendix F: CPH Test Data

This appendix contains the measured data from the MediGuide equipped catheter laboratory at the Abbott CPH facility. Additionally included are the results of the statistical calculations and analysis.

Attempt #	Measured Distance [in]	Measured Distance [mm]	Device Measured Distance [mm]	Difference [mm]	Normalized [mm]
1	0.070	1.8	0.2	-1.58	-0.19
2	0.045	1.1	0.0	-1.14	0.25
3	0.137	3.5	1.1	-2.38	-0.99
4	0.030	0.8	0.3	-0.46	0.93
5	0.203	5.2	3.4	-1.76	-0.37
6	0.064	1.6	0.7	-0.93	0.46
7	0.122	3.1	1.8	-1.30	0.09
8	0.175	4.4	0.4	-4.05	-2.65
9	0.050	1.3	1.0	-0.27	1.12
10	0.185	4.7	0.6	-4.10	-2.71
11	0.069	1.8	1.5	-0.25	1.14
12	0.057	1.4	1.2	-0.25	1.14
13	0.111	2.8	2.3	-0.52	0.87
14	0.085	2.2	1.3	-0.86	0.53
15	0.115	2.9	1.9	-1.02	0.37

Statistic	Variable	Value	Units
Standard Deviation of difference	s	1.245	mm
Number of measurements	n	15	-
Sample Mean	$\overline{x}$	-1.39	mm
Two-tail T-Value at 95%	t_{95}	1.67	-
Two tail T-Value at 99%	t_{99}	2.39	-
95% confidence band		0.537	mm
99% confidence band		0.768	mm

Appendix G: Instron Tensile Displacement Test Data

This appendix contains the measured data from the Instron displacement controlled testing of the over-the-wire device prototype. Additionally included are the results of the statistical calculations and analysis.

Constant Distance Variable Rate

	100mm/min			500mm/min			1000mm/min		
	Encoder [mm]	Instron [mm]	Difference [mm]	Encoder [mm]	Instron [mm]	Difference [mm]	Encoder [mm]	Instron [mm]	Difference [mm]
	100.00	100.7	0.7	100.02	100.7	0.68	100.03	100.8	0.77
	100.00	100.4	0.4	100.02	100.7	0.68	100.00	100.8	0.80
	100.00	100.4	0.4	100.00	100.7	0.70	100.03	100.8	0.77
	100.00	100.4	0.4	100.02	100.6	0.58	100.00	100.8	0.80
	100.00	100.5	0.5	100.00	100.7	0.70	100.03	100.8	0.77
	100.00	100.5	0.5	100.00	100.6	0.60	100.00	100.8	0.80
	100.00	100.5	0.5	100.00	100.6	0.60	100.03	100.8	0.77
	100.00	100.5	0.5	100.02	100.6	0.58	100.00	100.7	0.70
	100.00	100.4	0.4	100.00	100.8	0.80	100.03	100.8	0.77
	100.00	100.4	0.4	100.02	100.7	0.68	100.00	100.8	0.80
	100.00	100.5	0.5	100.00	100.8	0.80	100.00	100.8	0.80
	100.00	100.5	0.5	100.02	100.8	0.78	100.03	100.8	0.77
	100.00	100.4	0.4	100.02	100.7	0.68	100.00	100.8	0.80
	100.00	100.5	0.5	100.02	100.8	0.78	100.00	100.8	0.80
	100.00	100.5	0.5	100.00	100.7	0.70	100.00	100.8	0.80
Avg	**100.00**	**100.47**	**0.47**	**100.01**	**100.70**	**0.69**	**100.01**	**100.79**	**0.78**
Std Dev	**0.00**	**0.08**	**0.08**	**0.01**	**0.08**	**0.08**	**0.02**	**0.03**	**0.03**

Constant Rate Variable Distance

	100mm			175mm			250mm		
	Encoder [mm]	Instron [mm]	Difference [mm]	Encoder [mm]	Instron [mm]	Difference	Encoder [mm]	Instron [mm]	Difference [mm]
	100.02	100.7	0.68	175.00	176.3	1.3	250.00	251.8	1.8
	100.02	100.7	0.68	175.00	176.3	1.3	250.02	251.7	1.68
	100.00	100.7	0.7	175.02	176.3	1.28	250.02	251.7	1.68
	100.02	100.6	0.58	175.00	176.1	1.1	250.00	251.5	1.5
	100.00	100.7	0.7	175.02	175.9	0.88	250.00	251.7	1.7
	100.00	100.6	0.6	175.00	176	1			
	100.00	100.6	0.6						
	100.02	100.6	0.58						
	100.00	100.8	0.8						
	100.02	100.7	0.68						
	100.00	100.8	0.8						
	100.02	100.8	0.78						
	100.02	100.7	0.68						
	100.02	100.8	0.78						
	100.00	100.7	0.7						
Avg	**100.01**	**100.70**	**0.69**	**175.01**	**176.15**	**1.14**	**250.01**	**251.68**	**1.67**
Std Dev	**0.01**	**0.08**	**0.08**	**0.01**	**0.18**	**0.18**	**0.01**	**0.11**	**0.11**

Statistic	Variable	Value	Units
Standard Deviation of Difference/Length	s	0.00134	mm/mm
Number of measurements	n	56	-
Sample Mean	$\bar{x}$	0.0065	mm/mm
Two-tail T-Value at 95%	t_{95}	1.67	-
Two tail T-Value at 99%	t_{99}	2.39	-
95% confidence band		0.0003	mm/mm
99% confidence band		0.0004	mm/mm

Appendix H: Guidewire Fit DOE Data

This appendix contains the results of the guidewire fit analysis testing. The raw data is included as well as a description of the blocking parameters for the different datasets used.

Test File Used	Block	Description
1	1	RCA
2a	2	LAD
2b	3	LAD to Circumflex
3	4	Curve
4	5	Spiral
5a	6	Coronary Model long
5b	7	Coronary Model short

		Factors						Response	
Test File	BLOCK	Iterations [-]	minGap [cm]	BetweenPlane [cm]	ClosePoint [cm]	nPlanes [-]	nPoints [-]	Fit	Runtime [s]
1	1	3	0.48	3.23	2.59	13	4	10.27	6.67
1	1	3	0.48	3.23	2.59	13	8	9.45	6.43
1	1	3	0.48	3.23	2.59	27	4	11.32	9.80
1	1	3	0.48	3.23	2.59	27	8	10.47	10.34
1	1	3	0.48	3.23	5.41	13	4	12.32	8.72
1	1	3	0.48	3.23	5.41	13	8	11.37	8.69
1	1	3	0.48	3.23	5.41	27	4	13.01	12.26
1	1	3	0.48	3.23	5.41	27	8	13.49	14.28
1	1	3	0.48	6.77	2.59	13	4	10.27	6.53
1	1	3	0.48	6.77	2.59	13	8	9.45	6.34
1	1	3	0.48	6.77	2.59	27	4	11.32	9.47
1	1	3	0.48	6.77	2.59	27	8	10.47	9.56
1	1	3	0.48	6.77	5.41	13	4	0.00	0.00
1	1	3	0.48	6.77	5.41	13	8	0.00	0.00
1	1	3	0.48	6.77	5.41	27	4	8.79	11.91
1	1	3	0.48	6.77	5.41	27	8	7.89	11.67
1	1	3	1.02	3.23	2.59	13	4	10.27	6.13
1	1	3	1.02	3.23	2.59	13	8	9.45	6.16
1	1	3	1.02	3.23	2.59	27	4	11.32	9.12
1	1	3	1.02	3.23	2.59	27	8	10.47	9.35
1	1	3	1.02	3.23	5.41	13	4	10.77	7.97
1	1	3	1.02	3.23	5.41	13	8	10.34	8.05
1	1	3	1.02	3.23	5.41	27	4	14.96	11.17
1	1	3	1.02	3.23	5.41	27	8	13.63	11.11
1	1	3	1.02	6.77	2.59	13	4	10.27	6.25
1	1	3	1.02	6.77	2.59	13	8	9.45	6.22
1	1	3	1.02	6.77	2.59	27	4	11.32	9.34
1	1	3	1.02	6.77	2.59	27	8	10.47	9.70
1	1	3	1.02	6.77	5.41	13	4	12.21	11.31
1	1	3	1.02	6.77	5.41	13	8	11.75	11.29
1	1	3	1.02	6.77	5.41	27	4	8.92	14.83
1	1	3	1.02	6.77	5.41	27	8	8.52	15.08
1	1	5	0.48	3.23	2.59	13	4	10.27	8.97
1	1	5	0.48	3.23	2.59	13	8	9.45	9.10

1	1	5	0.48	3.23	2.59	27	4	11.32	13.94
1	1	5	0.48	3.23	2.59	27	8	10.47	13.13
1	1	5	0.48	3.23	5.41	13	4	9.61	12.49
1	1	5	0.48	3.23	5.41	13	8	10.25	12.60
1	1	5	0.48	3.23	5.41	27	4	14.33	17.05
1	1	5	0.48	3.23	5.41	27	8	14.36	16.84
1	1	5	0.48	6.77	2.59	13	4	10.27	9.17
1	1	5	0.48	6.77	2.59	13	8	9.45	9.29
1	1	5	0.48	6.77	2.59	27	4	11.32	13.53
1	1	5	0.48	6.77	2.59	27	8	10.47	14.13
1	1	5	0.48	6.77	5.41	13	4	9.45	19.23
1	1	5	0.48	6.77	5.41	13	8	8.88	16.83
1	1	5	0.48	6.77	5.41	27	4	9.10	18.16
1	1	5	0.48	6.77	5.41	27	8	8.38	18.00
1	1	5	1.02	3.23	2.59	13	4	10.27	6.80
1	1	5	1.02	3.23	2.59	13	8	9.45	6.92
1	1	5	1.02	3.23	2.59	27	4	11.32	9.98
1	1	5	1.02	3.23	2.59	27	8	10.47	10.58
1	1	5	1.02	3.23	5.41	13	4	10.99	9.23
1	1	5	1.02	3.23	5.41	13	8	10.75	9.15
1	1	5	1.02	3.23	5.41	27	4	14.94	12.57
1	1	5	1.02	3.23	5.41	27	8	14.98	13.08
1	1	5	1.02	6.77	2.59	13	4	10.27	7.20
1	1	5	1.02	6.77	2.59	13	8	9.45	7.25
1	1	5	1.02	6.77	2.59	27	4	11.32	10.16
1	1	5	1.02	6.77	2.59	27	8	10.47	10.24
1	1	5	1.02	6.77	5.41	13	4	12.83	10.24
1	1	5	1.02	6.77	5.41	13	8	12.05	10.43
1	1	5	1.02	6.77	5.41	27	4	9.42	13.41
1	1	5	1.02	6.77	5.41	27	8	8.92	13.74
1	1	1	0.75	5.00	4.00	20	6	11.23	5.68
1	1	8	0.75	5.00	4.00	20	6	11.87	13.03
1	1	4	1.00	5.00	4.00	20	6	11.73	10.40
1	1	4	1.50	5.00	4.00	20	6	11.38	12.35
1	1	4	0.75	1.00	4.00	20	6	8.64	15.26
1	1	4	0.75	10.00	4.00	20	6	10.69	14.84
1	1	4	0.75	5.00	1.00	20	6	18.97	11.35
1	1	4	0.75	5.00	8.00	20	6	9.56	16.45
1	1	4	0.75	5.00	4.00	5	6	15.96	10.40
1	1	4	0.75	5.00	4.00	40	6	13.72	21.40
1	1	4	0.75	5.00	4.00	20	3	11.07	13.95
1	1	4	0.75	5.00	4.00	20	12	10.83	14.57
1	1	4	0.75	5.00	4.00	20	6	11.87	14.22
3	4	3	0.48	3.23	2.59	13	4	1.66	1.89
3	4	3	0.48	3.23	2.59	13	8	1.65	2.00
3	4	3	0.48	3.23	2.59	27	4	1.42	3.03
3	4	3	0.48	3.23	2.59	27	8	1.42	3.28
3	4	3	0.48	3.23	5.41	13	4	1.56	1.84
3	4	3	0.48	3.23	5.41	13	8	1.54	1.92
3	4	3	0.48	3.23	5.41	27	4	1.39	3.12
3	4	3	0.48	3.23	5.41	27	8	1.38	3.31
3	4	3	0.48	6.77	2.59	13	4	1.66	1.75
3	4	3	0.48	6.77	2.59	13	8	1.65	1.97
3	4	3	0.48	6.77	2.59	27	4	1.42	3.10
3	4	3	0.48	6.77	2.59	27	8	1.42	3.37
3	4	3	0.48	6.77	5.41	13	4	1.56	1.84
3	4	3	0.48	6.77	5.41	13	8	1.54	1.83
3	4	3	0.48	6.77	5.41	27	4	1.39	3.14
3	4	3	0.48	6.77	5.41	27	8	1.38	3.36
3	4	3	1.02	3.23	2.59	13	4	1.63	1.62
3	4	3	1.02	3.23	2.59	13	8	1.63	1.69
3	4	3	1.02	3.23	2.59	27	4	1.82	2.82
3	4	3	1.02	3.23	2.59	27	8	1.82	2.87
3	4	3	1.02	3.23	5.41	13	4	1.43	1.59
3	4	3	1.02	3.23	5.41	13	8	1.44	1.61
3	4	3	1.02	3.23	5.41	27	4	1.68	2.84
3	4	3	1.02	3.23	5.41	27	8	1.68	3.06

3	4	3	1.02	6.77	2.59	13	4	1.63	1.60
3	4	3	1.02	6.77	2.59	13	8	1.63	1.64
3	4	3	1.02	6.77	2.59	27	4	1.82	2.76
3	4	3	1.02	6.77	2.59	27	8	1.82	2.90
3	4	3	1.02	6.77	5.41	13	4	1.43	1.53
3	4	3	1.02	6.77	5.41	13	8	1.44	1.63
3	4	3	1.02	6.77	5.41	27	4	1.68	2.82
3	4	3	1.02	6.77	5.41	27	8	1.68	3.16
3	4	5	0.48	3.23	2.59	13	4	1.69	2.45
3	4	5	0.48	3.23	2.59	13	8	1.82	2.52
3	4	5	0.48	3.23	2.59	27	4	2.18	3.45
3	4	5	0.48	3.23	2.59	27	8	2.15	3.99
3	4	5	0.48	3.23	5.41	13	4	1.53	2.34
3	4	5	0.48	3.23	5.41	13	8	1.70	2.42
3	4	5	0.48	3.23	5.41	27	4	2.00	3.45
3	4	5	0.48	3.23	5.41	27	8	1.99	3.65
3	4	5	0.48	6.77	2.59	13	4	1.69	2.42
3	4	5	0.48	6.77	2.59	13	8	1.82	2.46
3	4	5	0.48	6.77	2.59	27	4	2.18	3.45
3	4	5	0.48	6.77	2.59	27	8	2.15	3.64
3	4	5	0.48	6.77	5.41	13	4	1.53	2.27
3	4	5	0.48	6.77	5.41	13	8	1.70	2.40
3	4	5	0.48	6.77	5.41	27	4	2.00	3.37
3	4	5	0.48	6.77	5.41	27	8	1.99	3.66
3	4	5	1.02	3.23	2.59	13	4	1.63	1.58
3	4	5	1.02	3.23	2.59	13	8	1.63	1.59
3	4	5	1.02	3.23	2.59	27	4	1.82	2.76
3	4	5	1.02	3.23	2.59	27	8	1.82	2.94
3	4	5	1.02	3.23	5.41	13	4	1.43	1.50
3	4	5	1.02	3.23	5.41	13	8	1.44	1.60
3	4	5	1.02	3.23	5.41	27	4	1.68	2.69
3	4	5	1.02	3.23	5.41	27	8	1.68	3.00
3	4	5	1.02	6.77	2.59	13	4	1.63	1.49
3	4	5	1.02	6.77	2.59	13	8	1.63	1.69
3	4	5	1.02	6.77	2.59	27	4	1.82	2.63
3	4	5	1.02	6.77	2.59	27	8	1.82	2.94
3	4	5	1.02	6.77	5.41	13	4	1.43	1.52
3	4	5	1.02	6.77	5.41	13	8	1.44	1.74
3	4	5	1.02	6.77	5.41	27	4	1.68	2.63
3	4	5	1.02	6.77	5.41	27	8	1.68	2.94
3	4	1	0.75	5.00	4.00	20	6	2.51	1.59
3	4	8	0.75	5.00	4.00	20	6	2.58	2.84
3	4	4	1.00	5.00	4.00	20	6	1.56	2.11
3	4	4	1.50	5.00	4.00	20	6	2.47	2.27
3	4	4	0.75	1.00	4.00	20	6	2.58	2.78
3	4	4	0.75	10.00	4.00	20	6	2.58	2.98
3	4	4	0.75	5.00	1.00	20	6	3.72	1.81
3	4	4	0.75	5.00	8.00	20	6	2.58	2.73
3	4	4	0.75	5.00	4.00	5	6	1.98	1.62
3	4	4	0.75	5.00	4.00	40	6	1.40	4.49
3	4	4	0.75	5.00	4.00	20	3	2.57	2.97
3	4	4	0.75	5.00	4.00	20	12	2.58	3.36
3	4	4	0.75	5.00	4.00	20	6	2.58	2.72
5a	6	3	0.48	3.23	2.59	13	4	6.43	1.77
5a	6	3	0.48	3.23	2.59	13	8	6.41	2.07
5a	6	3	0.48	3.23	2.59	27	4	6.55	3.02
5a	6	3	0.48	3.23	2.59	27	8	6.55	3.33
5a	6	3	0.48	3.23	5.41	13	4	5.92	2.56
5a	6	3	0.48	3.23	5.41	13	8	5.63	2.64
5a	6	3	0.48	3.23	5.41	27	4	6.51	3.78
5a	6	3	0.48	3.23	5.41	27	8	6.88	4.09
5a	6	3	0.48	6.77	2.59	13	4	6.35	1.90
5a	6	3	0.48	6.77	2.59	13	8	6.59	1.89
5a	6	3	0.48	6.77	2.59	27	4	8.36	3.16
5a	6	3	0.48	6.77	2.59	27	8	8.36	3.25
5a	6	3	0.48	6.77	5.41	13	4	6.34	2.19
5a	6	3	0.48	6.77	5.41	13	8	6.13	2.33

5a	6	3	0.48	6.77	5.41	27	4	4.83	3.26
5a	6	3	0.48	6.77	5.41	27	8	4.81	3.43
5a	6	3	1.02	3.23	2.59	13	4	6.43	1.76
5a	6	3	1.02	3.23	2.59	13	8	6.41	1.96
5a	6	3	1.02	3.23	2.59	27	4	6.55	3.04
5a	6	3	1.02	3.23	2.59	27	8	6.55	3.28
5a	6	3	1.02	3.23	5.41	13	4	5.91	2.47
5a	6	3	1.02	3.23	5.41	13	8	5.59	2.62
5a	6	3	1.02	3.23	5.41	27	4	5.27	3.84
5a	6	3	1.02	3.23	5.41	27	8	5.29	3.92
5a	6	3	1.02	6.77	2.59	13	4	6.35	1.80
5a	6	3	1.02	6.77	2.59	13	8	6.59	1.97
5a	6	3	1.02	6.77	2.59	27	4	8.36	3.06
5a	6	3	1.02	6.77	2.59	27	8	8.36	3.39
5a	6	3	1.02	6.77	5.41	13	4	6.34	2.25
5a	6	3	1.02	6.77	5.41	13	8	6.13	2.34
5a	6	3	1.02	6.77	5.41	27	4	4.83	3.18
5a	6	3	1.02	6.77	5.41	27	8	4.81	3.53
5a	6	5	0.48	3.23	2.59	13	4	6.43	1.99
5a	6	5	0.48	3.23	2.59	13	8	6.41	2.01
5a	6	5	0.48	3.23	2.59	27	4	6.55	3.30
5a	6	5	0.48	3.23	2.59	27	8	6.55	3.55
5a	6	5	0.48	3.23	5.41	13	4	6.68	5.05
5a	6	5	0.48	3.23	5.41	13	8	6.23	5.05
5a	6	5	0.48	3.23	5.41	27	4	6.24	6.18
5a	6	5	0.48	3.23	5.41	27	8	7.15	6.35
5a	6	5	0.48	6.77	2.59	13	4	7.54	2.06
5a	6	5	0.48	6.77	2.59	13	8	6.16	2.20
5a	6	5	0.48	6.77	2.59	27	4	7.29	3.52
5a	6	5	0.48	6.77	2.59	27	8	7.59	3.81
5a	6	5	0.48	6.77	5.41	13	4	6.97	4.33
5a	6	5	0.48	6.77	5.41	13	8	7.08	5.01
5a	6	5	0.48	6.77	5.41	27	4	6.34	5.47
5a	6	5	0.48	6.77	5.41	27	8	6.58	5.72
5a	6	5	1.02	3.23	2.59	13	4	6.43	1.92
5a	6	5	1.02	3.23	2.59	13	8	6.41	2.12
5a	6	5	1.02	3.23	2.59	27	4	6.55	3.31
5a	6	5	1.02	3.23	2.59	27	8	6.55	3.42
5a	6	5	1.02	3.23	5.41	13	4	7.73	3.08
5a	6	5	1.02	3.23	5.41	13	8	7.63	3.07
5a	6	5	1.02	3.23	5.41	27	4	5.87	4.40
5a	6	5	1.02	3.23	5.41	27	8	5.87	4.52
5a	6	5	1.02	6.77	2.59	13	4	7.54	2.17
5a	6	5	1.02	6.77	2.59	13	8	6.16	2.29
5a	6	5	1.02	6.77	2.59	27	4	7.29	3.52
5a	6	5	1.02	6.77	2.59	27	8	7.59	3.84
5a	6	5	1.02	6.77	5.41	13	4	6.72	3.16
5a	6	5	1.02	6.77	5.41	13	8	6.56	3.29
5a	6	5	1.02	6.77	5.41	27	4	6.29	4.31
5a	6	5	1.02	6.77	5.41	27	8	6.31	4.55
5a	6	1	0.75	5.00	4.00	20	6	10.45	2.02
5a	6	8	0.75	5.00	4.00	20	6	8.30	4.55
5a	6	4	1.00	5.00	4.00	20	6	7.32	3.46
5a	6	4	1.50	5.00	4.00	20	6	8.24	2.63
5a	6	4	0.75	1.00	4.00	20	6	7.27	3.80
5a	6	4	0.75	10.00	4.00	20	6	10.78	2.92
5a	6	4	0.75	5.00	1.00	20	6	13.64	2.56
5a	6	4	0.75	5.00	8.00	20	6	7.27	3.83
5a	6	4	0.75	5.00	4.00	5	6	9.05	2.80
5a	6	4	0.75	5.00	4.00	40	6	6.76	5.53
5a	6	4	0.75	5.00	4.00	20	3	7.63	3.80
5a	6	4	0.75	5.00	4.00	20	12	7.76	4.38
5a	6	4	0.75	5.00	4.00	20	6	7.78	4.16
5b	7	3	0.48	3.23	2.59	13	4	6.25	1.47
5b	7	3	0.48	3.23	2.59	13	8	5.74	1.46
5b	7	3	0.48	3.23	2.59	27	4	6.11	3.12
5b	7	3	0.48	3.23	2.59	27	8	6.14	3.19

5b	7	3	0.48	3.23	5.41	13	4	4.84	2.11
5b	7	3	0.48	3.23	5.41	13	8	4.68	2.20
5b	7	3	0.48	3.23	5.41	27	4	3.66	3.51
5b	7	3	0.48	3.23	5.41	27	8	3.61	3.61
5b	7	3	0.48	6.77	2.59	13	4	6.07	1.41
5b	7	3	0.48	6.77	2.59	13	8	6.38	1.50
5b	7	3	0.48	6.77	2.59	27	4	5.08	2.99
5b	7	3	0.48	6.77	2.59	27	8	5.12	3.35
5b	7	3	0.48	6.77	5.41	13	4	5.47	1.72
5b	7	3	0.48	6.77	5.41	13	8	5.71	1.91
5b	7	3	0.48	6.77	5.41	27	4	4.62	2.98
5b	7	3	0.48	6.77	5.41	27	8	4.54	3.36
5b	7	3	1.02	3.23	2.59	13	4	6.25	1.39
5b	7	3	1.02	3.23	2.59	13	8	5.74	1.50
5b	7	3	1.02	3.23	2.59	27	4	6.11	3.15
5b	7	3	1.02	3.23	2.59	27	8	6.14	3.27
5b	7	3	1.02	3.23	5.41	13	4	4.43	1.83
5b	7	3	1.02	3.23	5.41	13	8	4.50	1.79
5b	7	3	1.02	3.23	5.41	27	4	4.49	3.13
5b	7	3	1.02	3.23	5.41	27	8	4.46	3.28
5b	7	3	1.02	6.77	2.59	13	4	6.07	1.42
5b	7	3	1.02	6.77	2.59	13	8	6.38	1.47
5b	7	3	1.02	6.77	2.59	27	4	5.08	3.00
5b	7	3	1.02	6.77	2.59	27	8	5.12	3.23
5b	7	3	1.02	6.77	5.41	13	4	5.64	1.70
5b	7	3	1.02	6.77	5.41	13	8	5.10	1.76
5b	7	3	1.02	6.77	5.41	27	4	4.45	3.07
5b	7	3	1.02	6.77	5.41	27	8	4.57	3.14
5b	7	5	0.48	3.23	2.59	13	4	6.25	1.64
5b	7	5	0.48	3.23	2.59	13	8	5.74	1.62
5b	7	5	0.48	3.23	2.59	27	4	6.11	3.14
5b	7	5	0.48	3.23	2.59	27	8	6.14	3.36
5b	7	5	0.48	3.23	5.41	13	4	4.27	3.15
5b	7	5	0.48	3.23	5.41	13	8	3.90	3.16
5b	7	5	0.48	3.23	5.41	27	4	3.65	4.57
5b	7	5	0.48	3.23	5.41	27	8	3.62	4.78
5b	7	5	0.48	6.77	2.59	13	4	6.07	1.52
5b	7	5	0.48	6.77	2.59	13	8	6.38	1.62
5b	7	5	0.48	6.77	2.59	27	4	5.08	3.24
5b	7	5	0.48	6.77	2.59	27	8	5.12	3.39
5b	7	5	0.48	6.77	5.41	13	4	5.03	3.31
5b	7	5	0.48	6.77	5.41	13	8	4.88	3.60
5b	7	5	0.48	6.77	5.41	27	4	4.16	4.69
5b	7	5	0.48	6.77	5.41	27	8	4.09	4.68
5b	7	5	1.02	3.23	2.59	13	4	6.25	1.51
5b	7	5	1.02	3.23	2.59	13	8	5.74	1.59
5b	7	5	1.02	3.23	2.59	27	4	6.11	3.14
5b	7	5	1.02	3.23	2.59	27	8	6.14	3.49
5b	7	5	1.02	3.23	5.41	13	4	4.03	2.03
5b	7	5	1.02	3.23	5.41	13	8	4.10	2.21
5b	7	5	1.02	3.23	5.41	27	4	3.88	3.45
5b	7	5	1.02	3.23	5.41	27	8	3.88	3.70
5b	7	5	1.02	6.77	2.59	13	4	6.07	1.52
5b	7	5	1.02	6.77	2.59	13	8	6.38	1.63
5b	7	5	1.02	6.77	2.59	27	4	5.08	3.28
5b	7	5	1.02	6.77	2.59	27	8	5.12	3.44
5b	7	5	1.02	6.77	5.41	13	4	4.21	2.23
5b	7	5	1.02	6.77	5.41	13	8	4.17	2.30
5b	7	5	1.02	6.77	5.41	27	4	4.21	3.72
5b	7	5	1.02	6.77	5.41	27	8	4.34	3.87
5b	7	1	0.75	5.00	4.00	20	6	5.69	1.79
5b	7	8	0.75	5.00	4.00	20	6	3.95	3.42
5b	7	4	1.00	5.00	4.00	20	6	4.66	2.74
5b	7	4	1.50	5.00	4.00	20	6	4.00	2.48
5b	7	4	0.75	1.00	4.00	20	6	4.55	2.95
5b	7	4	0.75	10.00	4.00	20	6	8.14	2.21
5b	7	4	0.75	5.00	1.00	20	6	8.86	2.30

5b	7	4	0.75	5.00	8.00	20	6	4.55	3.00
5b	7	4	0.75	5.00	4.00	5	6	4.40	1.90
5b	7	4	0.75	5.00	4.00	40	6	4.65	5.11
5b	7	4	0.75	5.00	4.00	20	3	4.46	2.92
5b	7	4	0.75	5.00	4.00	20	12	4.59	3.54
5b	7	4	0.75	5.00	4.00	20	6	4.49	3.00
1	1	3	0.48	3.23	2.59	13	4	9.56	8.24
1	1	3	0.48	3.23	2.59	13	8	9.38	8.38
1	1	3	0.48	3.23	2.59	27	4	11.14	12.69
1	1	3	0.48	3.23	2.59	27	8	10.55	12.76
1	1	3	0.48	3.23	5.41	13	4	12.04	10.67
1	1	3	0.48	3.23	5.41	13	8	11.13	10.77
1	1	3	0.48	3.23	5.41	27	4	14.38	15.07
1	1	3	0.48	3.23	5.41	27	8	13.50	15.11
1	1	3	0.48	6.77	2.59	13	4	9.56	8.34
1	1	3	0.48	6.77	2.59	13	8	9.38	8.68
1	1	3	0.48	6.77	2.59	27	4	11.14	12.93
1	1	3	0.48	6.77	2.59	27	8	10.55	12.90
1	1	3	0.48	6.77	5.41	13	4	0.00	0.00
1	1	3	0.48	6.77	5.41	13	8	0.00	0.00
1	1	3	0.48	6.77	5.41	27	4	8.05	15.27
1	1	3	0.48	6.77	5.41	27	8	7.63	15.32
1	1	3	1.02	3.23	2.59	13	4	9.56	8.23
1	1	3	1.02	3.23	2.59	13	8	9.38	8.94
1	1	3	1.02	3.23	2.59	27	4	11.14	12.67
1	1	3	1.02	3.23	2.59	27	8	10.55	13.12
1	1	3	1.02	3.23	5.41	13	4	12.73	10.42
1	1	3	1.02	3.23	5.41	13	8	11.94	10.68
1	1	3	1.02	3.23	5.41	27	4	15.07	14.18
1	1	3	1.02	3.23	5.41	27	8	15.02	14.57
1	1	3	1.02	6.77	2.59	13	4	9.56	8.37
1	1	3	1.02	6.77	2.59	13	8	9.38	8.53
1	1	3	1.02	6.77	2.59	27	4	11.14	12.72
1	1	3	1.02	6.77	2.59	27	8	10.55	13.49
1	1	3	1.02	6.77	5.41	13	4	11.95	11.62
1	1	3	1.02	6.77	5.41	13	8	11.60	11.34
1	1	3	1.02	6.77	5.41	27	4	8.26	14.99
1	1	3	1.02	6.77	5.41	27	8	7.76	15.29
1	1	5	0.48	3.23	2.59	13	4	9.56	9.30
1	1	5	0.48	3.23	2.59	13	8	9.38	9.24
1	1	5	0.48	3.23	2.59	27	4	11.14	13.71
1	1	5	0.48	3.23	2.59	27	8	10.55	13.87
1	1	5	0.48	3.23	5.41	13	4	15.68	12.72
1	1	5	0.48	3.23	5.41	13	8	14.91	12.77
1	1	5	0.48	3.23	5.41	27	4	13.80	17.18
1	1	5	0.48	3.23	5.41	27	8	11.61	17.81
1	1	5	0.48	6.77	2.59	13	4	9.56	9.47
1	1	5	0.48	6.77	2.59	13	8	9.38	9.58
1	1	5	0.48	6.77	2.59	27	4	11.14	14.35
1	1	5	0.48	6.77	2.59	27	8	10.55	14.25
1	1	5	0.48	6.77	5.41	13	4	10.31	19.77
1	1	5	0.48	6.77	5.41	13	8	9.90	19.90
1	1	5	0.48	6.77	5.41	27	4	0.00	0.00
1	1	5	0.48	6.77	5.41	27	8	0.00	0.00
1	1	5	1.02	3.23	2.59	13	4	9.56	9.13
1	1	5	1.02	3.23	2.59	13	8	9.38	9.47
1	1	5	1.02	3.23	2.59	27	4	11.14	13.96
1	1	5	1.02	3.23	2.59	27	8	10.55	13.83
1	1	5	1.02	3.23	5.41	13	4	10.03	12.45
1	1	5	1.02	3.23	5.41	13	8	9.75	12.84
1	1	5	1.02	3.23	5.41	27	4	15.08	17.01
1	1	5	1.02	3.23	5.41	27	8	12.00	17.97
1	1	5	1.02	6.77	2.59	13	4	9.56	9.52
1	1	5	1.02	6.77	2.59	13	8	9.38	9.56
1	1	5	1.02	6.77	2.59	27	4	11.14	14.09
1	1	5	1.02	6.77	2.59	27	8	10.55	14.16
1	1	5	1.02	6.77	5.41	13	4	12.71	13.27

1	1	5	1.02	6.77	5.41	13	8	12.00	13.54
1	1	5	1.02	6.77	5.41	27	4	9.83	18.19
1	1	5	1.02	6.77	5.41	27	8	9.39	18.42
1	1	1	0.75	5.00	4.00	20	6	12.37	7.51
1	1	8	0.75	5.00	4.00	20	6	12.62	17.77
1	1	4	1.00	5.00	4.00	20	6	11.38	13.54
1	1	4	1.50	5.00	4.00	20	6	11.46	11.61
1	1	4	0.75	1.00	4.00	20	6	8.43	15.77
1	1	4	0.75	10.00	4.00	20	6	10.94	15.26
1	1	4	0.75	5.00	1.00	20	6	16.54	11.79
1	1	4	0.75	5.00	8.00	20	6	8.85	16.76
1	1	4	0.75	5.00	4.00	5	6	15.26	10.71
1	1	4	0.75	5.00	4.00	40	6	14.61	22.55
1	1	4	0.75	5.00	4.00	20	3	11.80	14.97
1	1	4	0.75	5.00	4.00	20	12	12.46	15.31
1	1	4	0.75	5.00	4.00	20	6	12.62	15.19
3	4	3	0.48	3.23	2.59	13	4	1.38	1.96
3	4	3	0.48	3.23	2.59	13	8	1.38	2.03
3	4	3	0.48	3.23	2.59	27	4	1.67	3.18
3	4	3	0.48	3.23	2.59	27	8	1.69	3.39
3	4	3	0.48	3.23	5.41	13	4	1.44	1.77
3	4	3	0.48	3.23	5.41	13	8	1.44	2.04
3	4	3	0.48	3.23	5.41	27	4	1.68	3.15
3	4	3	0.48	3.23	5.41	27	8	1.70	3.38
3	4	3	0.48	6.77	2.59	13	4	1.38	1.87
3	4	3	0.48	6.77	2.59	13	8	1.38	1.86
3	4	3	0.48	6.77	2.59	27	4	1.67	3.09
3	4	3	0.48	6.77	2.59	27	8	1.69	3.39
3	4	3	0.48	6.77	5.41	13	4	1.44	1.87
3	4	3	0.48	6.77	5.41	13	8	1.44	2.06
3	4	3	0.48	6.77	5.41	27	4	1.68	3.25
3	4	3	0.48	6.77	5.41	27	8	1.70	3.31
3	4	3	1.02	3.23	2.59	13	4	1.43	1.56
3	4	3	1.02	3.23	2.59	13	8	1.43	1.77
3	4	3	1.02	3.23	2.59	27	4	1.81	2.71
3	4	3	1.02	3.23	2.59	27	8	1.86	3.03
3	4	3	1.02	3.23	5.41	13	4	1.26	1.52
3	4	3	1.02	3.23	5.41	13	8	1.29	1.77
3	4	3	1.02	3.23	5.41	27	4	1.46	2.73
3	4	3	1.02	3.23	5.41	27	8	1.51	3.04
3	4	3	1.02	6.77	2.59	13	4	1.43	1.52
3	4	3	1.02	6.77	2.59	13	8	1.43	1.76
3	4	3	1.02	6.77	2.59	27	4	1.81	2.74
3	4	3	1.02	6.77	2.59	27	8	1.86	3.06
3	4	3	1.02	6.77	5.41	13	4	1.26	1.53
3	4	3	1.02	6.77	5.41	13	8	1.29	1.80
3	4	3	1.02	6.77	5.41	27	4	1.46	3.00
3	4	3	1.02	6.77	5.41	27	8	1.51	3.19
3	4	5	0.48	3.23	2.59	13	4	1.52	2.73
3	4	5	0.48	3.23	2.59	13	8	1.52	2.82
3	4	5	0.48	3.23	2.59	27	4	1.45	4.11
3	4	5	0.48	3.23	2.59	27	8	1.46	4.16
3	4	5	0.48	3.23	5.41	13	4	1.69	2.66
3	4	5	0.48	3.23	5.41	13	8	1.71	2.79
3	4	5	0.48	3.23	5.41	27	4	1.57	4.05
3	4	5	0.48	3.23	5.41	27	8	1.57	4.49
3	4	5	0.48	6.77	2.59	13	4	1.52	2.85
3	4	5	0.48	6.77	2.59	13	8	1.52	2.98
3	4	5	0.48	6.77	2.59	27	4	1.45	4.36
3	4	5	0.48	6.77	2.59	27	8	1.46	4.21
3	4	5	0.48	6.77	5.41	13	4	1.69	2.88
3	4	5	0.48	6.77	5.41	13	8	1.71	2.83
3	4	5	0.48	6.77	5.41	27	4	1.57	4.09
3	4	5	0.48	6.77	5.41	27	8	1.57	4.17
3	4	5	1.02	3.23	2.59	13	4	2.08	1.75
3	4	5	1.02	3.23	2.59	13	8	2.07	1.94
3	4	5	1.02	3.23	2.59	27	4	1.44	2.88

3	4	5	1.02	3.23	2.59	27	8	1.44	3.09
3	4	5	1.02	3.23	5.41	13	4	1.26	1.70
3	4	5	1.02	3.23	5.41	13	8	1.29	1.64
3	4	5	1.02	3.23	5.41	27	4	1.46	2.83
3	4	5	1.02	3.23	5.41	27	8	1.51	2.96
3	4	5	1.02	6.77	2.59	13	4	2.08	1.88
3	4	5	1.02	6.77	2.59	13	8	2.07	1.95
3	4	5	1.02	6.77	2.59	27	4	1.44	2.95
3	4	5	1.02	6.77	2.59	27	8	1.44	3.26
3	4	5	1.02	6.77	5.41	13	4	1.26	1.67
3	4	5	1.02	6.77	5.41	13	8	1.29	1.73
3	4	5	1.02	6.77	5.41	27	4	1.46	2.91
3	4	5	1.02	6.77	5.41	27	8	1.51	2.95
3	4	1	0.75	5.00	4.00	20	6	2.51	1.77
3	4	8	0.75	5.00	4.00	20	6	1.70	2.69
3	4	4	1.00	5.00	4.00	20	6	1.80	2.15
3	4	4	1.50	5.00	4.00	20	6	2.89	2.23
3	4	4	0.75	1.00	4.00	20	6	1.70	2.71
3	4	4	0.75	10.00	4.00	20	6	1.70	2.72
3	4	4	0.75	5.00	1.00	20	6	3.90	1.88
3	4	4	0.75	5.00	8.00	20	6	1.70	3.00
3	4	4	0.75	5.00	4.00	5	6	1.86	1.75
3	4	4	0.75	5.00	4.00	40	6	1.89	4.62
3	4	4	0.75	5.00	4.00	20	3	1.70	2.63
3	4	4	0.75	5.00	4.00	20	12	1.70	3.29
3	4	4	0.75	5.00	4.00	20	6	1.70	2.68
5a	6	3	0.48	3.23	2.59	13	4	10.63	1.64
5a	6	3	0.48	3.23	2.59	13	8	10.38	1.82
5a	6	3	0.48	3.23	2.59	27	4	8.86	2.76
5a	6	3	0.48	3.23	2.59	27	8	8.88	3.42
5a	6	3	0.48	3.23	5.41	13	4	6.96	2.55
5a	6	3	0.48	3.23	5.41	13	8	7.56	2.61
5a	6	3	0.48	3.23	5.41	27	4	4.69	3.59
5a	6	3	0.48	3.23	5.41	27	8	4.84	3.79
5a	6	3	0.48	6.77	2.59	13	4	0.00	0.00
5a	6	3	0.48	6.77	2.59	13	8	0.00	0.00
5a	6	3	0.48	6.77	2.59	27	4	6.28	2.92
5a	6	3	0.48	6.77	2.59	27	8	6.81	3.29
5a	6	3	0.48	6.77	5.41	13	4	7.49	2.09
5a	6	3	0.48	6.77	5.41	13	8	7.77	2.17
5a	6	3	0.48	6.77	5.41	27	4	5.94	3.75
5a	6	3	0.48	6.77	5.41	27	8	6.77	3.94
5a	6	3	1.02	3.23	2.59	13	4	10.63	1.84
5a	6	3	1.02	3.23	2.59	13	8	10.38	1.79
5a	6	3	1.02	3.23	2.59	27	4	8.86	2.77
5a	6	3	1.02	3.23	2.59	27	8	8.88	3.12
5a	6	3	1.02	3.23	5.41	13	4	6.58	2.48
5a	6	3	1.02	3.23	5.41	13	8	6.56	2.55
5a	6	3	1.02	3.23	5.41	27	4	6.23	3.45
5a	6	3	1.02	3.23	5.41	27	8	6.25	3.66
5a	6	3	1.02	6.77	2.59	13	4	0.00	0.00
5a	6	3	1.02	6.77	2.59	13	8	0.00	0.00
5a	6	3	1.02	6.77	2.59	27	4	6.28	2.92
5a	6	3	1.02	6.77	2.59	27	8	6.81	3.21
5a	6	3	1.02	6.77	5.41	13	4	7.49	2.08
5a	6	3	1.02	6.77	5.41	13	8	7.77	2.32
5a	6	3	1.02	6.77	5.41	27	4	5.94	3.75
5a	6	3	1.02	6.77	5.41	27	8	6.77	4.11
5a	6	5	0.48	3.23	2.59	13	4	10.63	1.93
5a	6	5	0.48	3.23	2.59	13	8	10.38	2.01
5a	6	5	0.48	3.23	2.59	27	4	8.86	3.07
5a	6	5	0.48	3.23	2.59	27	8	8.88	3.14
5a	6	5	0.48	3.23	5.41	13	4	6.49	5.27
5a	6	5	0.48	3.23	5.41	13	8	6.75	5.38
5a	6	5	0.48	3.23	5.41	27	4	7.02	6.95
5a	6	5	0.48	3.23	5.41	27	8	7.19	6.70
5a	6	5	0.48	6.77	2.59	13	4	8.41	1.96

5a	6	5	0.48	6.77	2.59	13	8	8.82	2.20
5a	6	5	0.48	6.77	2.59	27	4	8.47	3.29
5a	6	5	0.48	6.77	2.59	27	8	9.33	3.51
5a	6	5	0.48	6.77	5.41	13	4	6.25	3.37
5a	6	5	0.48	6.77	5.41	13	8	6.44	3.30
5a	6	5	0.48	6.77	5.41	27	4	6.92	4.56
5a	6	5	0.48	6.77	5.41	27	8	6.93	4.84
5a	6	5	1.02	3.23	2.59	13	4	10.63	1.83
5a	6	5	1.02	3.23	2.59	13	8	10.38	1.89
5a	6	5	1.02	3.23	2.59	27	4	8.86	2.93
5a	6	5	1.02	3.23	2.59	27	8	8.88	3.25
5a	6	5	1.02	3.23	5.41	13	4	7.65	3.18
5a	6	5	1.02	3.23	5.41	13	8	7.57	3.36
5a	6	5	1.02	3.23	5.41	27	4	4.99	4.67
5a	6	5	1.02	3.23	5.41	27	8	5.07	4.84
5a	6	5	1.02	6.77	2.59	13	4	8.41	2.08
5a	6	5	1.02	6.77	2.59	13	8	8.82	2.19
5a	6	5	1.02	6.77	2.59	27	4	8.47	3.28
5a	6	5	1.02	6.77	2.59	27	8	9.33	3.63
5a	6	5	1.02	6.77	5.41	13	4	7.00	5033.50
5a	6	5	1.02	6.77	5.41	13	8	7.73	3.11
5a	6	5	1.02	6.77	5.41	27	4	6.65	4.03
5a	6	5	1.02	6.77	5.41	27	8	6.33	3.84
5a	6	1	0.75	5.00	4.00	20	6	8.69	2.14
5a	6	8	0.75	5.00	4.00	20	6	9.10	4.03
5a	6	4	1.00	5.00	4.00	20	6	8.30	3.11
5a	6	4	1.50	5.00	4.00	20	6	10.01	2.30
5a	6	4	0.75	1.00	4.00	20	6	7.93	3.19
5a	6	4	0.75	10.00	4.00	20	6	11.41	2.34
5a	6	4	0.75	5.00	1.00	20	6	15.68	2.15
5a	6	4	0.75	5.00	8.00	20	6	7.93	3.35
5a	6	4	0.75	5.00	4.00	5	6	0.00	0.00
5a	6	4	0.75	5.00	4.00	40	6	6.04	4.79
5a	6	4	0.75	5.00	4.00	20	3	6.86	3.21
5a	6	4	0.75	5.00	4.00	20	12	7.20	3.85
5a	6	4	0.75	5.00	4.00	20	6	7.84	3.32
5b	7	3	0.48	3.23	2.59	13	4	7.58	1.19
5b	7	3	0.48	3.23	2.59	13	8	7.42	1.28
5b	7	3	0.48	3.23	2.59	27	4	6.63	2.45
5b	7	3	0.48	3.23	2.59	27	8	6.69	2.63
5b	7	3	0.48	3.23	5.41	13	4	4.70	1.74
5b	7	3	0.48	3.23	5.41	13	8	4.84	1.88
5b	7	3	0.48	3.23	5.41	27	4	3.35	3.04
5b	7	3	0.48	3.23	5.41	27	8	3.34	3.03
5b	7	3	0.48	6.77	2.59	13	4	7.49	1.21
5b	7	3	0.48	6.77	2.59	13	8	7.67	1.26
5b	7	3	0.48	6.77	2.59	27	4	6.95	2.08
5b	7	3	0.48	6.77	2.59	27	8	6.99	2.25
5b	7	3	0.48	6.77	5.41	13	4	4.75	1.61
5b	7	3	0.48	6.77	5.41	13	8	5.07	1.55
5b	7	3	0.48	6.77	5.41	27	4	4.16	2.66
5b	7	3	0.48	6.77	5.41	27	8	4.15	2.85
5b	7	3	1.02	3.23	2.59	13	4	7.58	1.16
5b	7	3	1.02	3.23	2.59	13	8	7.42	1.22
5b	7	3	1.02	3.23	2.59	27	4	6.63	2.52
5b	7	3	1.02	3.23	2.59	27	8	6.69	2.78
5b	7	3	1.02	3.23	5.41	13	4	4.39	1.49
5b	7	3	1.02	3.23	5.41	13	8	4.50	1.58
5b	7	3	1.02	3.23	5.41	27	4	3.17	2.69
5b	7	3	1.02	3.23	5.41	27	8	3.22	2.75
5b	7	3	1.02	6.77	2.59	13	4	7.49	1.19
5b	7	3	1.02	6.77	2.59	13	8	7.67	1.26
5b	7	3	1.02	6.77	2.59	27	4	6.95	2.11
5b	7	3	1.02	6.77	2.59	27	8	6.99	2.27
5b	7	3	1.02	6.77	5.41	13	4	4.73	1.45
5b	7	3	1.02	6.77	5.41	13	8	4.78	1.52
5b	7	3	1.02	6.77	5.41	27	4	4.38	2.49

5b	7	3	1.02	6.77	5.41	27	8	4.41	2.65
5b	7	5	0.48	3.23	2.59	13	4	7.58	1.24
5b	7	5	0.48	3.23	2.59	13	8	7.42	1.44
5b	7	5	0.48	3.23	2.59	27	4	6.63	2.64
5b	7	5	0.48	3.23	2.59	27	8	6.69	2.92
5b	7	5	0.48	3.23	5.41	13	4	4.44	2.52
5b	7	5	0.48	3.23	5.41	13	8	4.06	2.68
5b	7	5	0.48	3.23	5.41	27	4	3.66	3.80
5b	7	5	0.48	3.23	5.41	27	8	3.67	3.79
5b	7	5	0.48	6.77	2.59	13	4	7.49	1.41
5b	7	5	0.48	6.77	2.59	13	8	7.67	1.38
5b	7	5	0.48	6.77	2.59	27	4	6.95	2.20
5b	7	5	0.48	6.77	2.59	27	8	6.99	2.37
5b	7	5	0.48	6.77	5.41	13	4	4.22	2.01
5b	7	5	0.48	6.77	5.41	13	8	4.74	2.10
5b	7	5	0.48	6.77	5.41	27	4	0.00	0.00
5b	7	5	0.48	6.77	5.41	27	8	0.00	0.00
5b	7	5	1.02	3.23	2.59	13	4	7.58	1.26
5b	7	5	1.02	3.23	2.59	13	8	7.42	1.35
5b	7	5	1.02	3.23	2.59	27	4	6.63	2.74
5b	7	5	1.02	3.23	2.59	27	8	6.69	2.86
5b	7	5	1.02	3.23	5.41	13	4	3.94	1.72
5b	7	5	1.02	3.23	5.41	13	8	4.31	1.89
5b	7	5	1.02	3.23	5.41	27	4	3.71	2.91
5b	7	5	1.02	3.23	5.41	27	8	3.59	3.08
5b	7	5	1.02	6.77	2.59	13	4	7.49	1.31
5b	7	5	1.02	6.77	2.59	13	8	7.67	1.53
5b	7	5	1.02	6.77	2.59	27	4	6.95	2.19
5b	7	5	1.02	6.77	2.59	27	8	6.99	2.37
5b	7	5	1.02	6.77	5.41	13	4	4.27	1.86
5b	7	5	1.02	6.77	5.41	13	8	4.16	1.93
5b	7	5	1.02	6.77	5.41	27	4	4.13	2.91
5b	7	5	1.02	6.77	5.41	27	8	4.11	3.04
5b	7	1	0.75	5.00	4.00	20	6	5.61	1.48
5b	7	8	0.75	5.00	4.00	20	6	4.58	2.83
5b	7	4	1.00	5.00	4.00	20	6	4.62	2.17
5b	7	4	1.50	5.00	4.00	20	6	3.85	2.00
5b	7	4	0.75	1.00	4.00	20	6	4.48	2.43
5b	7	4	0.75	10.00	4.00	20	6	7.89	1.81
5b	7	4	0.75	5.00	1.00	20	6	7.38	1.94
5b	7	4	0.75	5.00	8.00	20	6	4.48	2.54
5b	7	4	0.75	5.00	4.00	5	6	5.25	1.60
5b	7	4	0.75	5.00	4.00	40	6	3.49	4.44
5b	7	4	0.75	5.00	4.00	20	3	4.19	2.46
5b	7	4	0.75	5.00	4.00	20	12	4.42	2.81
5b	7	4	0.75	5.00	4.00	20	6	4.32	2.48
2a	2	3	0.48	3.23	2.59	13	4	20.97	19.95
2a	2	3	0.48	3.23	2.59	13	8	21.42	10.17
2a	2	3	0.48	3.23	2.59	27	4	12.17	13.92
2a	2	3	0.48	3.23	2.59	27	8	12.25	13.78
2a	2	3	0.48	3.23	5.41	13	4	20.98	9.08
2a	2	3	0.48	3.23	5.41	13	8	21.42	9.20
2a	2	3	0.48	3.23	5.41	27	4	12.18	13.45
2a	2	3	0.48	3.23	5.41	27	8	12.25	13.77
2a	2	3	0.48	6.77	2.59	13	4	20.97	12.67
2a	2	3	0.48	6.77	2.59	13	8	21.42	12.76
2a	2	3	0.48	6.77	2.59	27	4	12.17	18.98
2a	2	3	0.48	6.77	2.59	27	8	12.25	18.81
2a	2	3	0.48	6.77	5.41	13	4	20.98	12.92
2a	2	3	0.48	6.77	5.41	13	8	21.42	12.85
2a	2	3	0.48	6.77	5.41	27	4	12.18	19.31
2a	2	3	0.48	6.77	5.41	27	8	12.25	19.20
2a	2	3	1.02	3.23	2.59	13	4	20.97	11.83
2a	2	3	1.02	3.23	2.59	13	8	21.42	11.95
2a	2	3	1.02	3.23	2.59	27	4	12.17	14.20
2a	2	3	1.02	3.23	2.59	27	8	12.25	13.70
2a	2	3	1.02	3.23	5.41	13	4	20.98	9.03

2a	2	3	1.02	3.23	5.41	13	8	21.42	8.80
2a	2	3	1.02	3.23	5.41	27	4	12.18	17.50
2a	2	3	1.02	3.23	5.41	27	8	12.25	17.75
2a	2	3	1.02	6.77	2.59	13	4	20.97	12.73
2a	2	3	1.02	6.77	2.59	13	8	21.42	12.70
2a	2	3	1.02	6.77	2.59	27	4	12.17	18.44
2a	2	3	1.02	6.77	2.59	27	8	12.25	18.83
2a	2	3	1.02	6.77	5.41	13	4	20.98	13.15
2a	2	3	1.02	6.77	5.41	13	8	21.42	10.76
2a	2	3	1.02	6.77	5.41	27	4	12.18	13.90
2a	2	3	1.02	6.77	5.41	27	8	12.25	14.21
2a	2	5	0.48	3.23	2.59	13	4	20.97	10.71
2a	2	5	0.48	3.23	2.59	13	8	21.42	10.86
2a	2	5	0.48	3.23	2.59	27	4	12.17	16.63
2a	2	5	0.48	3.23	2.59	27	8	12.25	20.74
2a	2	5	0.48	3.23	5.41	13	4	20.98	14.18
2a	2	5	0.48	3.23	5.41	13	8	21.42	14.04
2a	2	5	0.48	3.23	5.41	27	4	12.18	20.47
2a	2	5	0.48	3.23	5.41	27	8	12.25	20.13
2a	2	5	0.48	6.77	2.59	13	4	20.97	16.05
2a	2	5	0.48	6.77	2.59	13	8	21.42	15.81
2a	2	5	0.48	6.77	2.59	27	4	12.17	22.03
2a	2	5	0.48	6.77	2.59	27	8	12.25	22.13
2a	2	5	0.48	6.77	5.41	13	4	20.98	15.52
2a	2	5	0.48	6.77	5.41	13	8	21.42	15.67
2a	2	5	0.48	6.77	5.41	27	4	12.18	21.74
2a	2	5	0.48	6.77	5.41	27	8	12.25	20.95
2a	2	5	1.02	3.23	2.59	13	4	20.97	10.81
2a	2	5	1.02	3.23	2.59	13	8	21.42	10.57
2a	2	5	1.02	3.23	2.59	27	4	12.17	15.04
2a	2	5	1.02	3.23	2.59	27	8	12.25	15.22
2a	2	5	1.02	3.23	5.41	13	4	20.98	10.62
2a	2	5	1.02	3.23	5.41	13	8	21.42	10.96
2a	2	5	1.02	3.23	5.41	27	4	12.18	14.99
2a	2	5	1.02	3.23	5.41	27	8	12.25	15.23
2a	2	5	1.02	6.77	2.59	13	4	20.97	17.89
2a	2	5	1.02	6.77	2.59	13	8	21.42	16.59
2a	2	5	1.02	6.77	2.59	27	4	12.17	21.57
2a	2	5	1.02	6.77	2.59	27	8	12.25	22.08
2a	2	5	1.02	6.77	5.41	13	4	20.98	15.88
2a	2	5	1.02	6.77	5.41	13	8	21.42	16.50
2a	2	5	1.02	6.77	5.41	27	4	12.18	22.22
2a	2	5	1.02	6.77	5.41	27	8	12.25	22.16
2a	2	1	0.75	5.00	4.00	20	6	12.00	12.59
2a	2	8	0.75	5.00	4.00	20	6	12.00	23.35
2a	2	4	1.00	5.00	4.00	20	6	12.00	16.89
2a	2	4	1.50	5.00	4.00	20	6	12.00	16.97
2a	2	4	0.75	1.00	4.00	20	6	12.00	15.61
2a	2	4	0.75	10.00	4.00	20	6	12.00	19.06
2a	2	4	0.75	5.00	1.00	20	6	11.09	19.16
2a	2	4	0.75	5.00	8.00	20	6	12.00	13.69
2a	2	4	0.75	5.00	4.00	5	6	21.28	7.93
2a	2	4	0.75	5.00	4.00	40	6	15.64	24.09
2a	2	4	0.75	5.00	4.00	20	3	11.39	13.02
2a	2	4	0.75	5.00	4.00	20	12	12.85	13.19
2a	2	4	0.75	5.00	4.00	20	6	12.00	12.86
2b	3	3	0.48	3.23	2.59	13	4	11.75	9.82
2b	3	3	0.48	3.23	2.59	13	8	12.46	10.04
2b	3	3	0.48	3.23	2.59	27	4	10.79	15.35
2b	3	3	0.48	3.23	2.59	27	8	10.77	15.78
2b	3	3	0.48	3.23	5.41	13	4	11.87	10.28
2b	3	3	0.48	3.23	5.41	13	8	12.87	10.19
2b	3	3	0.48	3.23	5.41	27	4	10.78	15.59
2b	3	3	0.48	3.23	5.41	27	8	11.02	15.76
2b	3	3	0.48	6.77	2.59	13	4	11.47	10.11
2b	3	3	0.48	6.77	2.59	13	8	11.35	10.35
2b	3	3	0.48	6.77	2.59	27	4	10.69	15.36

2b	3	3	0.48	6.77	2.59	27	8	10.79	15.21
2b	3	3	0.48	6.77	5.41	13	4	11.87	10.43
2b	3	3	0.48	6.77	5.41	13	8	12.87	10.64
2b	3	3	0.48	6.77	5.41	27	4	10.78	15.48
2b	3	3	0.48	6.77	5.41	27	8	11.02	19.39
2b	3	3	1.02	3.23	2.59	13	4	11.75	13.30
2b	3	3	1.02	3.23	2.59	13	8	12.46	13.10
2b	3	3	1.02	3.23	2.59	27	4	10.79	19.82
2b	3	3	1.02	3.23	2.59	27	8	10.77	20.11
2b	3	3	1.02	3.23	5.41	13	4	11.87	13.47
2b	3	3	1.02	3.23	5.41	13	8	12.87	13.45
2b	3	3	1.02	3.23	5.41	27	4	10.78	20.24
2b	3	3	1.02	3.23	5.41	27	8	11.02	20.47
2b	3	3	1.02	6.77	2.59	13	4	11.47	13.05
2b	3	3	1.02	6.77	2.59	13	8	11.35	13.00
2b	3	3	1.02	6.77	2.59	27	4	10.69	20.42
2b	3	3	1.02	6.77	2.59	27	8	10.79	20.54
2b	3	3	1.02	6.77	5.41	13	4	11.87	13.54
2b	3	3	1.02	6.77	5.41	13	8	12.87	13.91
2b	3	3	1.02	6.77	5.41	27	4	10.78	20.57
2b	3	3	1.02	6.77	5.41	27	8	11.02	21.19
2b	3	5	0.48	3.23	2.59	13	4	11.75	15.64
2b	3	5	0.48	3.23	2.59	13	8	12.46	16.75
2b	3	5	0.48	3.23	2.59	27	4	10.79	22.75
2b	3	5	0.48	3.23	2.59	27	8	10.77	23.37
2b	3	5	0.48	3.23	5.41	13	4	11.87	14.74
2b	3	5	0.48	3.23	5.41	13	8	12.87	15.11
2b	3	5	0.48	3.23	5.41	27	4	10.78	21.81
2b	3	5	0.48	3.23	5.41	27	8	11.02	21.99
2b	3	5	0.48	6.77	2.59	13	4	11.47	16.28
2b	3	5	0.48	6.77	2.59	13	8	11.35	15.97
2b	3	5	0.48	6.77	2.59	27	4	10.69	23.77
2b	3	5	0.48	6.77	2.59	27	8	10.79	23.24
2b	3	5	0.48	6.77	5.41	13	4	11.87	15.18
2b	3	5	0.48	6.77	5.41	13	8	12.87	12.70
2b	3	5	0.48	6.77	5.41	27	4	10.78	17.14
2b	3	5	0.48	6.77	5.41	27	8	11.02	17.09
2b	3	5	1.02	3.23	2.59	13	4	11.75	12.06
2b	3	5	1.02	3.23	2.59	13	8	12.46	12.60
2b	3	5	1.02	3.23	2.59	27	4	10.79	17.27
2b	3	5	1.02	3.23	2.59	27	8	10.77	17.80
2b	3	5	1.02	3.23	5.41	13	4	11.87	11.55
2b	3	5	1.02	3.23	5.41	13	8	12.87	11.89
2b	3	5	1.02	3.23	5.41	27	4	10.78	16.82
2b	3	5	1.02	3.23	5.41	27	8	11.02	17.39
2b	3	5	1.02	6.77	2.59	13	4	11.47	12.53
2b	3	5	1.02	6.77	2.59	13	8	11.35	12.54
2b	3	5	1.02	6.77	2.59	27	4	10.69	17.61
2b	3	5	1.02	6.77	2.59	27	8	10.79	17.67
2b	3	5	1.02	6.77	5.41	13	4	11.87	11.66
2b	3	5	1.02	6.77	5.41	13	8	12.87	11.63
2b	3	5	1.02	6.77	5.41	27	4	10.78	16.96
2b	3	5	1.02	6.77	5.41	27	8	11.02	22.83
2b	3	1	0.75	5.00	4.00	20	6	12.05	12.77
2b	3	8	0.75	5.00	4.00	20	6	13.52	20.80
2b	3	4	1.00	5.00	4.00	20	6	13.52	17.70
2b	3	4	1.50	5.00	4.00	20	6	13.52	17.03
2b	3	4	0.75	1.00	4.00	20	6	14.22	31.16
2b	3	4	0.75	10.00	4.00	20	6	12.48	20.26
2b	3	4	0.75	5.00	1.00	20	6	13.26	20.84
2b	3	4	0.75	5.00	8.00	20	6	17.17	21.62
2b	3	4	0.75	5.00	4.00	5	6	14.42	11.44
2b	3	4	0.75	5.00	4.00	40	6	9.98	25.19
2b	3	4	0.75	5.00	4.00	20	3	12.77	17.04
2b	3	4	0.75	5.00	4.00	20	12	13.16	17.99
2b	3	4	0.75	5.00	4.00	20	6	13.52	17.06
2a	2	3	0.48	3.23	2.59	13	4	32.03	11.08

2a	2	3	0.48	3.23	2.59	13	8	28.69	10.91
2a	2	3	0.48	3.23	2.59	27	4	19.56	16.40
2a	2	3	0.48	3.23	2.59	27	8	19.58	16.93
2a	2	3	0.48	3.23	5.41	13	4	31.20	10.97
2a	2	3	0.48	3.23	5.41	13	8	28.50	11.01
2a	2	3	0.48	3.23	5.41	27	4	19.47	16.45
2a	2	3	0.48	3.23	5.41	27	8	19.46	14.01
2a	2	3	0.48	6.77	2.59	13	4	32.03	9.33
2a	2	3	0.48	6.77	2.59	13	8	28.69	9.37
2a	2	3	0.48	6.77	2.59	27	4	19.56	13.59
2a	2	3	0.48	6.77	2.59	27	8	19.58	14.41
2a	2	3	0.48	6.77	5.41	13	4	31.20	9.71
2a	2	3	0.48	6.77	5.41	13	8	28.50	9.98
2a	2	3	0.48	6.77	5.41	27	4	19.47	13.38
2a	2	3	0.48	6.77	5.41	27	8	19.46	13.86
2a	2	3	1.02	3.23	2.59	13	4	32.03	8.33
2a	2	3	1.02	3.23	2.59	13	8	28.69	8.42
2a	2	3	1.02	3.23	2.59	27	4	19.56	12.96
2a	2	3	1.02	3.23	2.59	27	8	19.58	12.75
2a	2	3	1.02	3.23	5.41	13	4	31.20	12.39
2a	2	3	1.02	3.23	5.41	13	8	28.50	13.27
2a	2	3	1.02	3.23	5.41	27	4	19.47	16.97
2a	2	3	1.02	3.23	5.41	27	8	19.46	16.77
2a	2	3	1.02	6.77	2.59	13	4	32.03	12.00
2a	2	3	1.02	6.77	2.59	13	8	28.69	12.17
2a	2	3	1.02	6.77	2.59	27	4	19.56	18.31
2a	2	3	1.02	6.77	2.59	27	8	19.58	18.16
2a	2	3	1.02	6.77	5.41	13	4	31.20	13.10
2a	2	3	1.02	6.77	5.41	13	8	28.50	12.88
2a	2	3	1.02	6.77	5.41	27	4	19.47	17.97
2a	2	3	1.02	6.77	5.41	27	8	19.46	19.46
2a	2	5	0.48	3.23	2.59	13	4	32.03	16.35
2a	2	5	0.48	3.23	2.59	13	8	28.69	15.81
2a	2	5	0.48	3.23	2.59	27	4	19.56	19.64
2a	2	5	0.48	3.23	2.59	27	8	19.58	19.58
2a	2	5	0.48	3.23	5.41	13	4	31.20	14.20
2a	2	5	0.48	3.23	5.41	13	8	28.50	13.77
2a	2	5	0.48	3.23	5.41	27	4	19.47	19.80
2a	2	5	0.48	3.23	5.41	27	8	19.46	21.65
2a	2	5	0.48	6.77	2.59	13	4	32.03	17.35
2a	2	5	0.48	6.77	2.59	13	8	28.69	16.42
2a	2	5	0.48	6.77	2.59	27	4	19.56	22.56
2a	2	5	0.48	6.77	2.59	27	8	19.58	22.96
2a	2	5	0.48	6.77	5.41	13	4	31.20	15.47
2a	2	5	0.48	6.77	5.41	13	8	28.50	15.36
2a	2	5	0.48	6.77	5.41	27	4	19.47	21.08
2a	2	5	0.48	6.77	5.41	27	8	19.46	21.17
2a	2	5	1.02	3.23	2.59	13	4	32.03	14.34
2a	2	5	1.02	3.23	2.59	13	8	28.69	15.27
2a	2	5	1.02	3.23	2.59	27	4	19.56	19.30
2a	2	5	1.02	3.23	2.59	27	8	19.58	19.72
2a	2	5	1.02	3.23	5.41	13	4	31.20	14.57
2a	2	5	1.02	3.23	5.41	13	8	28.50	13.68
2a	2	5	1.02	3.23	5.41	27	4	19.47	19.67
2a	2	5	1.02	3.23	5.41	27	8	19.46	19.69
2a	2	5	1.02	6.77	2.59	13	4	32.03	15.22
2a	2	5	1.02	6.77	2.59	13	8	28.69	15.42
2a	2	5	1.02	6.77	2.59	27	4	19.56	21.08
2a	2	5	1.02	6.77	2.59	27	8	19.58	21.92
2a	2	5	1.02	6.77	5.41	13	4	31.20	15.44
2a	2	5	1.02	6.77	5.41	13	8	28.50	15.40
2a	2	5	1.02	6.77	5.41	27	4	19.47	20.71
2a	2	5	1.02	6.77	5.41	27	8	19.46	21.42
2a	2	1	0.75	5.00	4.00	20	6	29.59	12.61
2a	2	8	0.75	5.00	4.00	20	6	29.59	17.85
2a	2	4	1.00	5.00	4.00	20	6	29.59	13.62
2a	2	4	1.50	5.00	4.00	20	6	29.59	13.54

2a	2	4	0.75	1.00	4.00	20	6	29.59	10.06
2a	2	4	0.75	10.00	4.00	20	6	29.59	13.77
2a	2	4	0.75	5.00	1.00	20	6	30.02	12.92
2a	2	4	0.75	5.00	8.00	20	6	29.59	12.83
2a	2	4	0.75	5.00	4.00	5	6	22.07	7.60
2a	2	4	0.75	5.00	4.00	40	6	19.40	22.99
2a	2	4	0.75	5.00	4.00	20	3	29.98	12.92
2a	2	4	0.75	5.00	4.00	20	12	28.73	13.19
2a	2	4	0.75	5.00	4.00	20	6	29.59	12.86
2b	3	3	0.48	3.23	2.59	13	4	0.00	0.00
2b	3	3	0.48	3.23	2.59	13	8	0.00	0.00
2b	3	3	0.48	3.23	2.59	27	4	12.18	13.44
2b	3	3	0.48	3.23	2.59	27	8	12.17	13.70
2b	3	3	0.48	3.23	5.41	13	4	0.00	0.00
2b	3	3	0.48	3.23	5.41	13	8	0.00	0.00
2b	3	3	0.48	3.23	5.41	27	4	12.39	13.21
2b	3	3	0.48	3.23	5.41	27	8	12.49	13.60
2b	3	3	0.48	6.77	2.59	13	4	11.47	11.10
2b	3	3	0.48	6.77	2.59	13	8	14.44	12.65
2b	3	3	0.48	6.77	2.59	27	4	12.81	18.39
2b	3	3	0.48	6.77	2.59	27	8	12.41	18.66
2b	3	3	0.48	6.77	5.41	13	4	13.75	13.41
2b	3	3	0.48	6.77	5.41	13	8	14.41	15.06
2b	3	3	0.48	6.77	5.41	27	4	11.56	19.29
2b	3	3	0.48	6.77	5.41	27	8	11.00	20.21
2b	3	3	1.02	3.23	2.59	13	4	0.00	0.00
2b	3	3	1.02	3.23	2.59	13	8	0.00	0.00
2b	3	3	1.02	3.23	2.59	27	4	12.18	17.53
2b	3	3	1.02	3.23	2.59	27	8	12.17	17.73
2b	3	3	1.02	3.23	5.41	13	4	0.00	0.00
2b	3	3	1.02	3.23	5.41	13	8	0.00	0.00
2b	3	3	1.02	3.23	5.41	27	4	12.39	18.24
2b	3	3	1.02	3.23	5.41	27	8	12.49	18.17
2b	3	3	1.02	6.77	2.59	13	4	11.47	12.60
2b	3	3	1.02	6.77	2.59	13	8	14.44	13.28
2b	3	3	1.02	6.77	2.59	27	4	12.81	18.95
2b	3	3	1.02	6.77	2.59	27	8	12.41	18.42
2b	3	3	1.02	6.77	5.41	13	4	13.75	14.52
2b	3	3	1.02	6.77	5.41	13	8	14.41	14.33
2b	3	3	1.02	6.77	5.41	27	4	11.56	20.19
2b	3	3	1.02	6.77	5.41	27	8	11.00	19.76
2b	3	5	0.48	3.23	2.59	13	4	0.00	0.00
2b	3	5	0.48	3.23	2.59	13	8	0.00	0.00
2b	3	5	0.48	3.23	2.59	27	4	12.18	18.57
2b	3	5	0.48	3.23	2.59	27	8	12.17	18.90
2b	3	5	0.48	3.23	5.41	13	4	0.00	0.00
2b	3	5	0.48	3.23	5.41	13	8	0.00	0.00
2b	3	5	0.48	3.23	5.41	27	4	12.39	18.42
2b	3	5	0.48	3.23	5.41	27	8	12.49	19.72
2b	3	5	0.48	6.77	2.59	13	4	11.47	15.89
2b	3	5	0.48	6.77	2.59	13	8	14.44	16.71
2b	3	5	0.48	6.77	2.59	27	4	12.81	20.97
2b	3	5	0.48	6.77	2.59	27	8	12.41	21.46
2b	3	5	0.48	6.77	5.41	13	4	13.75	14.55
2b	3	5	0.48	6.77	5.41	13	8	14.41	12.20
2b	3	5	0.48	6.77	5.41	27	4	11.56	16.66
2b	3	5	0.48	6.77	5.41	27	8	11.00	22.28
2b	3	5	1.02	3.23	2.59	13	4	0.00	0.00
2b	3	5	1.02	3.23	2.59	13	8	0.00	0.00
2b	3	5	1.02	3.23	2.59	27	4	12.18	18.39
2b	3	5	1.02	3.23	2.59	27	8	12.17	18.86
2b	3	5	1.02	3.23	5.41	13	4	0.00	0.00
2b	3	5	1.02	3.23	5.41	13	8	0.00	0.00
2b	3	5	1.02	3.23	5.41	27	4	12.39	18.37
2b	3	5	1.02	3.23	5.41	27	8	12.49	18.54
2b	3	5	1.02	6.77	2.59	13	4	11.47	15.21
2b	3	5	1.02	6.77	2.59	13	8	14.44	15.29

2b	3	5	1.02	6.77	2.59	27	4	12.81	21.03
2b	3	5	1.02	6.77	2.59	27	8	12.41	21.42
2b	3	5	1.02	6.77	5.41	13	4	13.75	16.20
2b	3	5	1.02	6.77	5.41	13	8	14.41	16.22
2b	3	5	1.02	6.77	5.41	27	4	11.56	17.65
2b	3	5	1.02	6.77	5.41	27	8	11.00	16.79
2b	3	1	0.75	5.00	4.00	20	6	13.28	9.76
2b	3	8	0.75	5.00	4.00	20	6	15.68	13.85
2b	3	4	1.00	5.00	4.00	20	6	15.68	11.95
2b	3	4	1.50	5.00	4.00	20	6	15.68	11.94
2b	3	4	0.75	1.00	4.00	20	6	15.68	12.76
2b	3	4	0.75	10.00	4.00	20	6	12.08	19.73
2b	3	4	0.75	5.00	1.00	20	6	12.06	19.54
2b	3	4	0.75	5.00	8.00	20	6	15.68	16.58
2b	3	4	0.75	5.00	4.00	5	6	16.39	8.57
2b	3	4	0.75	5.00	4.00	40	6	15.44	31.12
2b	3	4	0.75	5.00	4.00	20	3	16.47	15.85
2b	3	4	0.75	5.00	4.00	20	12	16.53	16.50
2b	3	4	0.75	5.00	4.00	20	6	15.68	16.16